

**INTERACTION OF NANOPARTICLES (ZNO & CEO₂) AND COEXISTENCE
OF HEAVY METALS/ METALLOIDS (CD, PB & AS) WITH DIETARY
PLANTS, A FOOD SAFETY PERSPECTIVE**

A Dissertation

by

HAMIDREZA SHARIFAN

Submitted to the Office of Graduate and Professional Studies of
Texas A&M University
in partial fulfillment of the requirements for the degree of

DOCTOR OF PHILOSOPHY

Chair of Committee,	Janie Moore
Co-Chair of Committee,	Xingmao Ma
Committee Members,	Sandun Fernando
	Maria King
Head of Department,	Steve Searcy

December 2019

Major Subject: Biological and Agricultural Engineering

Copyright 2019 Hamidreza Sharifan

ABSTRACT

Crops and leafy vegetables are a rich source of protein, essential minerals, and fibers for the human diet, which may turn to toxic plants if exposed to heavy metals or metalloids contamination. Cadmium (Cd), Lead (Pb) and Arsenic (III/V) are extremely toxic elements to humans even at trace concentrations. Elevated levels of such compounds in agricultural soil due to various industrial activities lead to their hyper accumulation in a variety of dietary plant tissues and food products, which raise food safety concerns for consumers. Due to advances in nanotechnology-facilitated agrichemicals, engineered nanoparticles (ENPs) are substantially entering into agricultural systems. Exposure of edible plants with the coexistence of ENPs and heavy metals can alter their uptake and localization of essential minerals such as Fe through different mechanisms. However, the change of this uptake pattern is very critical for the leafy vegetable compared to crops, because of their direct consumption by humans. The goal of this research is to understand the mutual effects of metallic oxide nanoparticles (CeO_2 & ZnO) and coexisting divalent heavy metals Pb^{2+} and Cd^{2+} and metalloids (As(III/V)) on their uptake and accumulation as well localization of essential minerals in biological systems of a grain plants, Soybean (*Glycine max (L.) Merr.*), and four leafy vegetables including Spinach (*Spinacia oleracea*), Parsley (*Petroselinum sativum*), Romaine lettuce (*Lactuca sativa L. var. Longifolia*), cilantro (*Coriandrum sativum*) by Romaine lettuce (*Lactuca sativa L. var. Longifolia*) in soil and hydroponic systems in both pre-harvesting and post-harvesting stages of plant life. At termination, shoots were gently separated from the roots, and the concentrations of Pb, Cd, Fe, Cu, Ce and Zn in all plant tissues were quantified by

inductively coupled plasma-mass spectrometry (ICP-MS). In addition, microbial density analysis in the growth media was performed for the treatments in some studies. The last chapter focused on the role of ZnO nanoparticles on the shelf life of tomato (*Solanum Lycopersicum*). The results will shed light on the role of ENPs on governing the essential elements translocation as well as their key role in alleviating the bioavailability of heavy metals to leafy vegetables and crops which are produced in hydroponics and soil.

DEDICATION

I dedicate my dissertation work to God, my source of inspiration, wisdom, knowledge and understanding, to children whose parents have divorced, and they are affected in many ways through their entire life. To my Mom who sacrificed her life, health and young age to raise me alone. To my wife Melina that without her support, I may have given up, who loves me unconditionally and supports me in all situations. To my grandmother and grandfather for all their support. To my American parents, Jalaldin and Fay Martin Mansourzadeh, for all their love and support. Also, to my many friends including Fahad Asiri and Dr. Ali Ardalan and church family, especially Doug and Dian Chandler who have supported me throughout this journey.

ACKNOWLEDGEMENTS

I would like to thank my committee chair, Dr. Moore and co-chair Dr. Ma, and my committee members, Dr. Fernando and Dr. King, for their guidance and support throughout the course of this research.

Thanks also go to my friends and colleagues and the department faculty and staff for making my time at Texas A&M University a great experience.

CONTRIBUTORS AND FUNDING SOURCES

Contributors

This work was supervised by a dissertation committee consisting of Dr. Moore advisor from Department of Biological and Agricultural Engineering and co-advisor Dr. Ma from the Department of Environment and Civil Engineering of Texas A & M University.

All other work conducted for the dissertation was completed by the student independently.

Funding Sources

Graduate study was supported by a fellowship from Texas A&M University and Rollins Family and Harold J. "Bill" Haynes Fellowship, Texas A & M University

This work was also made possible in part by the Texas A&M Engineering Experiment Station, the Texas A&M University College of Engineering, and the Texas A&M University Division of Research Strategic Areas Interdisciplinary Research Seed Grants.

TABLE OF CONTENTS

	Page
ABSTRACT	ii
DEDICATION	iv
ACKNOWLEDGEMENTS	v
CONTRIBUTORS AND FUNDING SOURCES	vi
TABLE OF CONTENTS	vii
LIST OF FIGURES	x
LIST OF TABLES	xiv
CHAPTER I. INTRODUCTION AND LITERATURE REVIEW	1
1.1. Application of nanotechnology in food safety	1
1.2. Nanofertilizers	3
1.3. Nanopesticides.....	4
1.4. Nanosensors.....	9
1.5. Nanoparticle interaction with plants.....	11
1.6. Nanoparticle interaction with amino acids is root exudates.....	12
1.7. Cerium oxide Nanoparticles	16
1.8. Zinc Oxide Nanoparticles	18
1.9. Inhibitors of the biological processes.....	20
1.10. Research Hypothesis and Goals	23
1.11. References	31
CHAPTER II. INVESTIGATION ON THE PLANT ROOT EXUDATE EFFECTS ON THE MODIFICATION OF PHYSICOCHEMICAL PROPERTIES OF CERIUM OXIDE NANOPARTICLES THROUGH ADSORPTION OF Cd AND As(III)/As(V).....	48
2.1. Summary.....	48
2.2. Introduction	49
2.3. Material and Methods.....	51

2.4. Results	55
2.5. Discussion.....	62
2.6. Conclusion.....	66
2.7. References	67
CHAPTER III. IMPACT OF NANOPARTICLE SURFACE CHARGE AND PHOSPHATE ON THE UPTAKE OF COEXISTING CERIUM OXIDE NANOPARTICLES AND CADMIUM BY SOYBEAN (GLYCINE MAX. (L.) MERR.)	71
3.1. Summary.....	71
3.2. Introduction	73
3.3. Material and Methods.....	75
3.4. Results and Discussion	78
3.5. Conclusion.....	85
3.6. References	85
CHAPTER IV. MUTUAL EFFECTS AND IN-PLANTA UPTAKE OF CERIUM OXIDE NANOPARTICLES AND CADMIUM IN HYDROPONICALLY GROWN SOYBEAN (GLYCINE MAX (L.) MERR.)	90
4.1. Summary.....	90
4.2. Introduction	91
4.3. Material and Methods.....	93
4.4. Results	97
4.5. Discussion.....	103
4.6. Conclusion.....	106
4.7. References	107
CHAPTER V. ZINC OXIDE NANOPARTICLES ALLEVIATED THE BIOAVAILABILITY OF CADMIUM AND LEAD AND CHANGED THE UPTAKE OF IRON IN HYDROPONICALLY GROWN LETTUCE (<i>LACTUCA SATIVA L.</i> <i>VAR. LONGIFOLIA</i>)	114
5.1. Summary.....	114
5.2. Introduction	115
5.3. Material and Methods.....	117
5.4. Results	120
5.5. Discussion.....	125
5.6. Conclusion.....	129
5.7. References	130
CHAPTER VI. IMPACTS OF ZNO NANOPARTICLES ON THE MOBILIZATION OF ESSENTIAL MICRONUTRIENT (IRON AND COPPER) AND	

BIOAVAILABILITY OF HEAVY METALS (LEAD AND CADMIUM) IN VEGETABLES	137
6.1. Summary.....	137
6.2. Introduction	138
6.3. Material and Methods	140
6.4. Results	144
6.5. Discussion.....	151
6.6. Conclusion.....	157
6.7. References	157
CHAPTER VII. INVESTIGATION OF FOLIAR APPLICATION OF ZNO- NANOPARTICLES FOR ENHANCING SHELF-LIFE OF TOMATO (<i>SOLANUM LYCOPERSICUM</i>)	163
7.1. Summary.....	163
7.2. Introduction	164
7.3. Material and Methods.....	166
7.4. Results and Discussion	170
7.6. Conclusion.....	176
7.7. References	176
CHAPTER VIII. CONCLUSION AND RESEARCH PERSPECTIVE.....	181
8.1. Challenge and Research Needs	181
8.2. Research Perspective	182
8.3. References	185

LIST OF FIGURES

	Page
Figure 1.1 A comparison of the levels of repulsion energy between a metallic ENPs and a carbon-ENPs (CNPs) based on reported data from Tian et al. (2010).	9
Figure 1.2 Potential impacts of coating with the assumption of increasing the size of the nanoparticles on their interaction energies.	10
Figure 1.3 The schematic diagram for the CeO ₂ NPs and possible binding between synthetic root exudate molecules and Cd ²⁺ on the surface of CeO ₂ NPs during adsorption.	17
Figure 1.4 Proposed model by Liu et al. 2008[101] for the uncoupling effects of DNP which induces metabolic stress through interruption of the hydrogen ion shuttling across the inner membrane.	24
Figure 2.1 The adsorption isotherms of A) Cd, B) As (III) and C) As (V) onto CeO ₂ NPs. q _e (mg g ⁻¹) is the amount of Cd or As adsorbed per unit weight of CeO ₂ NPs at equilibrium, and C _e (mg L ⁻¹) is the adsorbate concentration in solution at equilibrium.	55
Figure 2.2 Average concentrations of Ce ³⁺ (mg L ⁻¹) in solution after CeO ₂ NPs were mixed with A) Cd B) As (III) and C) As (V), alone or in combination with the synthetic root exudates (SRE).	56
Figure 2.3 Zeta potential of CeO ₂ NPs as a function of the adsorbate doses in the presence and absence of SRE.	57
Figure 2.4 Distribution of the hydrodynamic sizes of CeO ₂ NPs after exposure to different concentrations of A) Cd; B) As (III) and C) As (V) in DI water. The reported curves are representative of three replicates at each concentration.	58
Figure 2.5 Distribution of the hydrodynamic sizes of CeO ₂ NPs after exposure to A) Cd; B) As (III) and C) As (V) concurrently with SRE. The reported curves are representative of three replicates at each concentration.	59
Figure 2.6 Liquid concentration of Ce ³⁺ (mg L ⁻¹) and solid concentration of Cd on CeO ₂ NPs in three different treatments with an initial concentration of 4 mg L ⁻¹ of Cd.	63

Figure 2.7 High resolution of Transmission electron microscopy TEM (JEOL JEM-1200EX, JEOL Ltd., Tokyo, Japan) studies of 100 mg/L CeO ₂ ENP (A) the TEM image of intact CeO ₂ ENPs. (B)	66
Figure 3.1 Dry weight (g) of soybean roots (A) and shoots (B) grown in 1.0 mg L ⁻¹ Cd and 100 mg L ⁻¹ CeO ₂ NPs ⁽⁺⁾ or CeO ₂ NPs ⁽⁻⁾ separately.....	79
Figure 3.2 Cerium concentrations in soybean roots (A) and shoots (B) grown in 1.0 mg L ⁻¹ Cd and 100 mg L ⁻¹ CeO ₂ NPs ⁽⁺⁾ or CeO ₂ NPs ⁽⁻⁾ separately or in combination.....	80
Figure 3.3 Cadmium concentrations in soybean roots (A) and shoots (B) grown in 1.0 mg L ⁻¹ Cd and 100 mg L ⁻¹ CeO ₂ NPs ⁽⁺⁾ or CeO ₂ NPs ⁽⁻⁾ separately or in combination.....	83
Figure 3.4 Accumulative transpiration of soybean seedlings exposed to 1.0 mg L ⁻¹ Cd and 100 mg L ⁻¹ CeO ₂ NPs ⁽⁺⁾ or CeO ₂ NPs ⁽⁻⁾ separately or in combination.	84
Figure 4.1 Dry weight of Glycine max grown in the presence of 100 mg L ⁻¹ CeO ₂ NPs and 1 mg L ⁻¹ Cd..	98
Figure 4.2 Total cerium concentration in roots (A) and shoots (B) of Glycine max grown in the presence of 100 mg L ⁻¹ CeO ₂ NPs and 1 mg L ⁻¹ Cd.....	99
Figure 4.3 Cadmium concentration (mg/kg) in root (A) and leaves (B) of Glycine max grew in the presence of 100 mg L ⁻¹ CeO ₂ NPs and 1 mg L ⁻¹ Cd.	99
Figure 4.4 Total organic carbon (TOC) in Glycine max grown in the presence of 100 mg L ⁻¹ CeO ₂ NPs and 1 mg L ⁻¹ Cd.	100
Figure 4.5 The XPS spectrum of the presence of cadmium (30 mg/L) on the surface of CeO ₂ NPs (75 mg/L).	102
Figure 4.6 illustrates the Ce 3d _{3/2} , 5/2 spectra obtained for the CeO ₂ compound and dissociated ions.	106
Figure 5.1 Dry biomass of lettuce tissues under different treatments including combinations of 1 mg/L of Cd, 100 mg/L Pb and/or 100 mg/L ZnONPs.	121
Figure 5.2 (A) Phenotype of <i>Lactuca sativa</i> L. var. <i>Longifolia</i> plants grown in hydroponic systems after exposure to different combinations of 1 mg/L of Cd+100 mg/L Pb and 100 mg/L ZnONPs,	122
Figure 5.3 Concentrations of heavy metals (Cd and Pb) in A) lettuce shoot and B) lettuce root tissues from different treatments.	123

Figure 5.4 The mean concentrations of total Zn in (A) shoots (B) roots of lettuce exposed to four different treatments of heavy metals (Pb and Cd) and nanoparticles (ZnO). Error bars indicate standard deviation (n = 3).	124
Figure 5.5 Concentrations of Fe in A) lettuce shoots and B) roots exposed to 100 mg/L of ZnONPs alone or in combination with 1 mg/L Cd+ 100 mg/L Pb (. Reported values indicate mean \pm SD (n = 3)	125
Figure 5.6 Correlation between concentrations of Fe and Zn in <i>L. sativa</i> upon exposure to 100 mg/L of ZnONPs alone or in combination with 1 mg/L Cd+ 100 mg/L Pb. Each bar represents the mean (n = 3).	127
Figure 5.7 A relationship between the log of the colony forming units (CFU) in the growth media and the log of total Zn in shoots. Letters indicate significant differences. Error bars represent the standard deviation between treatments. 128	
Figure 5.8 pH in the growth media of lettuce grown in the presence of 100 mg/L ZnONPs and/or 1 mg/L Cd +100 mg/L Pb. The reported values are mean \pm SD (n = 3). Different letters reflect significant differences as analyzed by ANOVA followed by Tukey's test (p < 0.05).	129
Figure 6.1 Impact of dry biomass of shoot tissues in three species in response to four treatments (ZnONPs, Cd&Pb+ZnONPs, Cd&Pb, Control A) cilantro (<i>Coriandrum sativum</i>) B) parsley (<i>Petroselinum sativum</i>), and C) spinach (<i>Spinaciae oleracea</i>). Each column indicates the mean of the dataset and the error bars represent standard deviation (n = 3 or 4). Different letters differentiate the significance level (p \leq 0.05)..	145
Figure 6.2 Dry biomass of root tissues in three leafy greens under different treatments on the mean basis	145
Figure 6.3 Detected level of heavy metals (Cd and Pb) in shoot tissues A) cilantro (<i>Coriandrum sativum</i>) B) parsley (<i>Petroselinum sativum</i>), and C) spinach (<i>Spinaciae oleracea</i>) exposed to different treatments.	146
Figure 6.4 Concentration of cadmium and lead in roots of three species A) cilantro (<i>Coriandrum sativum</i>) B) parsley (<i>Petroselinum sativum</i>), and C) spinach (<i>Spinaciae oleracea</i>) exposed to different treatments	147
Figure 6.5 Concentrations of essential minerals (Fe and Cu) in edible biomass (shoots) of A) cilantro (<i>Coriandrum sativum</i>) B) parsley (<i>Petroselinum sativum</i>), and C) spinach (<i>Spinaciae oleracea</i>) subjected to different treatments (100 mg/L of ZnONPs alone or in combination with 1 mg/L Cd+ 100 mg/L Pb)..	149

Figure 6.6 Total Zn concentration on a mean basis in roots and shoots A) cilantro (Coriandrum sativum) B) parsley (Petroselinum sativum), and C) spinach (Spinaciae oleracea) exposed to four different treatments of heavy metals (Pb and Cd) and nanoparticles (ZnO).	150
Figure 6.7 The relocation rate of the essential minerals Fe and Cu on a mean basis in three species of cilantro (Coriandrum sativum), parsley (Petroselinum sativum), and spinach (Spinaciae oleracea) during two weeks of exposure time.....	154
Figure 7.1 The Colony Forming Units (CFU) formed after 100 mg L ⁻¹ foliar application of ZnO ENPs in potato dextrose agar medium to monitor the susceptibility of existing microbial community on tomato skins to presence of ENPs..	171
Figure 7.2 . Inhibition of microbial growth in presence of the 100 mg L ⁻¹ foliar application of ZnO ENPs or Zn ²⁺ on outer surface of tomato	171
Figure 7.3 Water loss profile of tomato: the mean data set of control, ZnO ENPs and Zn ²⁺ treatments under three storage temperatures were examined by measuring the biomass change over five days of exposure.	173
Figure 7.4 The black curves represent the relationship between the a/b color factor of tomatoes under each treatment (control, 100 mg L ⁻¹ foliar application of ZnO ENPs or Zn ²⁺) and storage time.	174
Figure 7.5 Projected concentration of lycopene antioxidant under three different treatments.	175
Figure 7.5 Illustration of the total Zn contents after washing the tomato at termination stage. The letters indicate the significance level using one-way ANNOVA (p<0.05, n=3).	176
Figure 8.1 Potential interaction of between plant and nanoparticles and heavy metals in a hydroponic system.been reported up to now to substantiate the assumption that ENPs are actively transported into plant roots through proteinous channels.....	183

LIST OF TABLES

	Page
Table 1.1 Frequently implemented Engineering nanoparticles in nanosensors structures for the monitor, detect and qualify the certain compounds in agricultural products..	13
Table 2.1 Freundlich isotherm fitting parameters for the adsorption of Cd and As (III)/As(V) onto cerium oxide nanoparticles (CeO ₂ NPs) with and without presence of SRE.	60
Table 4.1 Root surface and growth medium pH values of Glycine max grown in the presence of 100 mg L ⁻¹ CeO ₂ NPs and 1 mg L ⁻¹ Cd. Means ± SD (n = 3) labeled by different letters are significantly different by Tukey's post-hoc test (p < 0.05).	101
Table 6.1 Measured pH values from the hydroponic system after the uptake experiment.....	151

CHAPTER I

INTRODUCTION AND LITERATURE REVIEW

1.1. Application of nanotechnology in food safety

Due to the rapid advancement of nanotechnology in industrial areas, engineering nanoparticles have established their role as an engineered indicator for many fundamental implications including medicine, nutrition, agriculture, personal care, electronics, energy, transport, and communications. The global investment in nanotechnologies market was estimated up to \$10 billion by 2005 [1], the growth of this market led to an annual rate of \$1 trillion from 2011 to 2015 [2].

The massive growth of this sector is due to the novel physicochemical properties of nanomaterials, which characterize their applicability in different fields [3]. Chemically, nanomaterials are provided from organic sources (i.e., quantum dots, nanotubes, and fullerene) or inorganic (i.e., zero-valent metals and metal oxides/salts). Physical properties include size range (<100 nm), shape, surface area, aggregation state, zeta potential, density and color [4, 5]. The combination of both physical and chemical properties put nanomaterials in three fundamental classes: i) nanoparticulates; ii) nanoplatelets; and iii) nanofibers [6].

Engineered nanoparticles (ENPs) represents a class of manufactured based materials with especial physicochemical characteristics and coatings; unique mechanical, electrical, thermal, and imaging

characteristics, which make them highly suitable for a variety of applications within the agriculture, medical and environmental engineering [7].

Presence of nanoparticles in foods can naturally occur through the environmental contamination or intentionally through different engineering applications. The properties of the engineering nanoparticles (ENPs) offer many new opportunities for food industries, such as more efficient coloring of the foods, adding a variety of flavors and nutritional elements[8]. Nanoparticles can also apply as antimicrobial ingredients for food packaging, anti-fungal for post harvested agro-commodities and controlled release of pesticides and fertilizers[9, 10].

There are many nanoparticles designed and implemented for diverse food applications at industrial scale. For example, titanium dioxide and zinc oxide nanoparticles have been widely used as food additive and antimicrobial agents for food packaging and in storage vessels[8, 11]. Some studies, reported the applications of silver (Ag) nanoparticles as antimicrobial agents for the food storage packaging, and in coating of the chopping boards and refrigerators[8, 12].

Providing the direct use of safe irrigation and healthy crops during the flooding events is one of the innovative applications of the nanoparticles in food safety prospective. It can economically and environmentally benefit the Texas State Water Plan and further reduce the load of wastewater treatment for urban planning. ENPs possess special properties, such as high surface area and adsorption capacity, easy operation, and cost-effective production [9, 13, 14]. To increase the food safety during the flood events as well as many other environmental incidents, there is high interest in the use of ENPs for the removal of heavy metals in aqueous systems such as flooded condition and immobilizing them into soil composite or retain their uptake by dietary plants[14, 15]. ENPs can change the hazardous state of the toxic metal ions into a stable or safe state and reduce the need for the treatment of flooding water for agriculture and immobilize the heavy metals in the

soil [16, 17]. Further, ENPs have demonstrated to increase crops tolerance to the water stress [18, 19]. In addition, large-scale applications of ENPs in crop lands to reduce the uptake of heavy metals is economically feasible.

Several studies indicated the high adsorption capacity of heavy metals and organic compounds onto ENPs surfaces, and strong attachment of ENPs on the sediment properties [10, 20]. For example, CeO₂-ENPs display high adsorption capacity for hazardous heavy metals such as arsenic (As), lead (Pb) and cadmium (Cd) [13, 16]. The CeO₂-ENPs surface by immobilizing the Cd²⁺ can reduce its uptake into plant tissues or retain Cd²⁺ in plant rhizosphere when and hold them in soil composite [14, 21]. In such a biological matrix, sediment morphology and composition of soil play a critical role in adsorption efficiency of heavy metals on ENPs.

In food safety prospective, metal-ENPs (Au, Ag, Ni, Zn, Cu, and Fe) and metal oxides-ENPs (TiO₂, SiO₂, CeO₂, Fe₃O₄, and Al₂O) are the most frequently used in agriculture as nano-pesticide, nano-fertilizers, and nano-sensors[3, 22, 23].

Many research studies and critical reviews have been focused on behavior, effects and environmental fate of ENPs in different media including water and soil. Studies on the application of ENPs in agricultural fields is missing. This chapter aims to discuss the application of the ENPs in the most recent revolutionary use of nanotechnology in increasing the agricultural food safety and security.

1.2. Nano-fertilizers

Agriculture plays a critical role in the economy of developing countries where the increasing global population growth calls for efficient agriculture products. Conversely, climate and environmental

changes are affecting agriculture production. As a result, the agriculture system of any country is a point of concern to deal with sustainable development. In this regard, nanotechnology is a promising tool for sustainable agriculture by providing of slow and controlled release fertilizers [24].

The natural composition of soil consists of organic and inorganic nanomaterials including aluminosilicate minerals; oxides and hydroxides of iron (Fe), aluminum (Al), and manganese (Mn); humic substances and mobile colloids [25]. The hydrodynamic diameters of most ENPs fall inside the range of these natural nanoparticles. Therefore, ENPS exhibit high natural compatibility within the soil structure [26]. Several researchers have suggested that the presence of ENPs can be beneficial to soil matrix by adding the meta-pedogenetic factors [27]. In fact, metallic ENPs in soil increase wettability of agricultural formulations, and positively impact the soil microbial structure and function via influencing nutrient turnover in soil over long time exposure [28]. Also, metallic ENPs may directly or indirectly alter the formation of symbiotic associations with root fungi and bacteria; influencing nutrient availability, uptake and plant growth [28]. For example, Zhang et al. 2017 reported the ENPs-CeO₂ increased the growth of radish storage roots [29].

Several studies indicated the beneficial application of ENPs in the germination phase of an agricultural process. In this process, the main critical factor in the stimulation of seed germination to grow faster is the diffusion of ENPS into the seed [30]. Zheng et al. 2005, reported a 73% more dry weight of spinach seeds when treated by ENPs-TiO₂ (at an optimum dose of 2.5‰). In addition, the photosynthetic rate increased three times higher than control, and an increase of 45% in chlorophyll *a*, and 28% chlorophyll *b* were observed in comparison to the control seeds (with no TiO₂) during 30 days of germination [31].

A different study demonstrated the carbon nanotubes/materials (CNMS) improve the water uptake in seeds of the tomato (*Solanum lycopersicum*). As a result, the multi-walled carbon nanotubes (MWCNTs) at a concentration range of 10-40 ug/ml increased the moisture uptake (which was three times greater than control) leading to an increase up to 90% of the germination rate within 20 days [32]. In the same way, applying fullerol [C₆₀ (OH)₂₀] at a productive dose of (47 nM) through a CNMS- seed treatment increased the biomass yield of bitter melon (*Momordica charantia*) more than 50% over 85 days of harvesting. [33]. The productivity of this nanoparticle resulted in significant increases in fruit number (60%) and weight (70%), which raised the total fruit yield of bitter melon up to 128%[33]. Due to this beneficial role, the fullerol has been suggested as a potential candidate for drought resistance in sugar beets (*Beta vulgaris* L.) via foliar application (20 full pump amplitudes) during three months of drought condition for the four months aged plants. This approach potentially increases the intercellular water supply, which enables ENPs to bind with available water in cell compartments and easily absorb onto the plant leaf and root tissues [34]. Moreover, the foliar spray application assists in avoiding the toxicity effects of soil for certain ENPS. For example, foliar spray of the of zinc (Zn) and boron (B) nanofertilizers on pomegranate (*Punica granatum* L. cv. Ardestani) resulted in promoting the quality of the fruit yield by increasing the number of fruits per tree while conserving its physical and nutritional characteristics [35].

In addition to the utilization of ENPS as fertilizer, porous nanostructure media such as prepared nanocomposite (*i.e.*, zeolite and silica-based) were proposed as an efficient low-release of nutrients for soil enrichment, plant growth and controlled delivery of pesticides, guaranteeing long-term bioavailability of macronutrients and micronutrients to plants [24, 36]. Development of such nanostructure composition can bloom agro-economic by saving more water and land and dealing

with drought condition. However, the research on a hybrid complex between nanostructured porous media and the implication of known ENPS as fertilizer elements can open a new research horizon in AgroSciences. Research in this area can overcome the deficiency of this nano-matrices (i.e., Loading cations). Due to the low mobility of ENPs and their stimulating properties onto the cells of the root, an empirical ratio of organic components can enhance the efficiency of such nanostructure, which has not been researched yet.

1.3. Nano-Pesticides

One of the main concerns in agricultural food production is the applications of efficient pesticides and antibacterial agents with no contamination of water or soil environment. Conventional pesticides sometimes leave their byproducts, which stay in the environment as persistent organic pollutants (POPs) and cause serious risks. For instance, by-products of a organochlorines pesticides (including DDT, methoxychlor, lindane, chlordane, dieldrin, and benzene hexachloride), which are frequently used in agriculture to control insects are associated with endocrine disruption impacts on human health, the high annual rate of 1 million cases has been reported [37, 38]. ENPs (*i.e.*, TiO₂, zero-valent Fe and carbon nanotubes) were introduced in agricultural practice as an effective tool in the removal of such POPs through photocatalytic degradation [37, 39]. In addition, metallic ENPs are demonstrated as a promising solution for sustainable agriculture due to their effective pesticide characteristics [28].

Also, metallic ENPs can alleviate the toxicity of biotoxins by changing the bioavailability of nutrient or toxic substances or acts as an antioxidant through the elimination of free radical before

oxidative damage to the living organisms[40, 41]. This underlying mechanism is a key concept behind their application as antimicrobial, antifungal or pesticides. In addition, in the context of sustainable agriculture metallic ENPs are capable to effectively enhance the nutrient diffusion and wettability of agricultural soils [28]. As an example, silver nanoparticle (ENPs-Ag) was proposed as antifungal due to the release of Ag^+ ions to the medium [5, 41].

In addition, several types of research on gold nanoparticle (ENPs-Au) indicated the antibacterial characteristics of this nanoparticle, which significantly reduce the growth rate of gram-positive and negative bacteria (*i.e.*, *Escherichia coli* and *Staphylococcus aureus*) [42]. Arokiyaraj et al., 2013, showed about %50 enhancement of antibacterial activity on *Argemone mexicana* (planted for medical purposes) when it was treated with iron oxide ENPs (50 $\mu\text{g}/\text{disc}$) against a widely distributed bacteria (*Proteus mirabilis*) in the environmental matrices, including soil and contaminated water [43]. In a similar study, a high dose of iron oxide ENPs (3 mg/mL) considerably inhibited, the growth rate of *Staphylococcus aureus* compared to the control samples [44].

Recently, nanosilica application was successfully developed for controlling a wide range of agricultural pest insects for a variety of horticultural and crop plants [45]. This nonmetallic ENPs are capable of being absorbed onto the cuticular cell lipids, and effectively through a biological mechanism that kills the pest insects. The advantage of this nano-bio technique is the conservation of physical and biological properties of photosynthesis or respiration from the leaf and stem surface of the plants [45].

Stadler et al. 2010, for the first time, proved the applicability of nanostructured alumina (250 mg kg^{-1}) on two worldwide predominant pest insects' species (*Sitophilus oryzae* L. and *Rhyzopertha*

dominica) in food supplies including wheat. Their results illustrated a substantial mortality rate as high as %80 between the adult population of both species within nine days of exposure to treated wheat; the mortality rate could reach up to 95% within three days at a higher dose at 1000 mg kg^{-1} concentration level [46].

However, despite many research aimed to understand the positive implication of certain ENPs as antibacterial or pesticide, but due to the thermodynamic behavior of such ENPs will influence by the composition of soil matrices (i.e., NOM and other ionic and cationic elements). For example, Grillo et al. (2015) explained in detail the possible confounding behavior of ENPs in the presence of NOM. As the soil profile is a mixture of different trace and macro elements (i.e., Cu^{+2} , Mg^{+2} , etc.) and comprise a variety of naturally deposited ENPs as well as those that have been introduced in the soil as nano-fertilizers, there is a question mark, whether a chemical interaction between ENPs fertilizers (i.e., CeO_2) and antibacterial nanoparticles (i.e., ZnO) exist due to changing the electrophoretic mobility in soil. For example, the repulsion force between two nano-metal particles as well as CNPs may incorporate in their bioavailability and mobility into a receiving porous media. This is a new field of research that has not been seriously addressed. In order to illustrate the potential affecting the energy of the nanoparticles, figure 1 compares the levels of repulsion energy between a metallic ENPs and a carbon-ENPs (CNPs) based on reported data from Tian et al. (2010). This comparison is an identical comparison between different ENPs, in this case, the Ionic Strength and Zeta Potential were considered constant for both ENPs. As it can be interpreted the interaction energy is considerable in affecting the collision of two ENPs and their affinity with NOM. This remarkable difference can be explained by different effective diameter, variable surface potential, and other corresponding parameters.

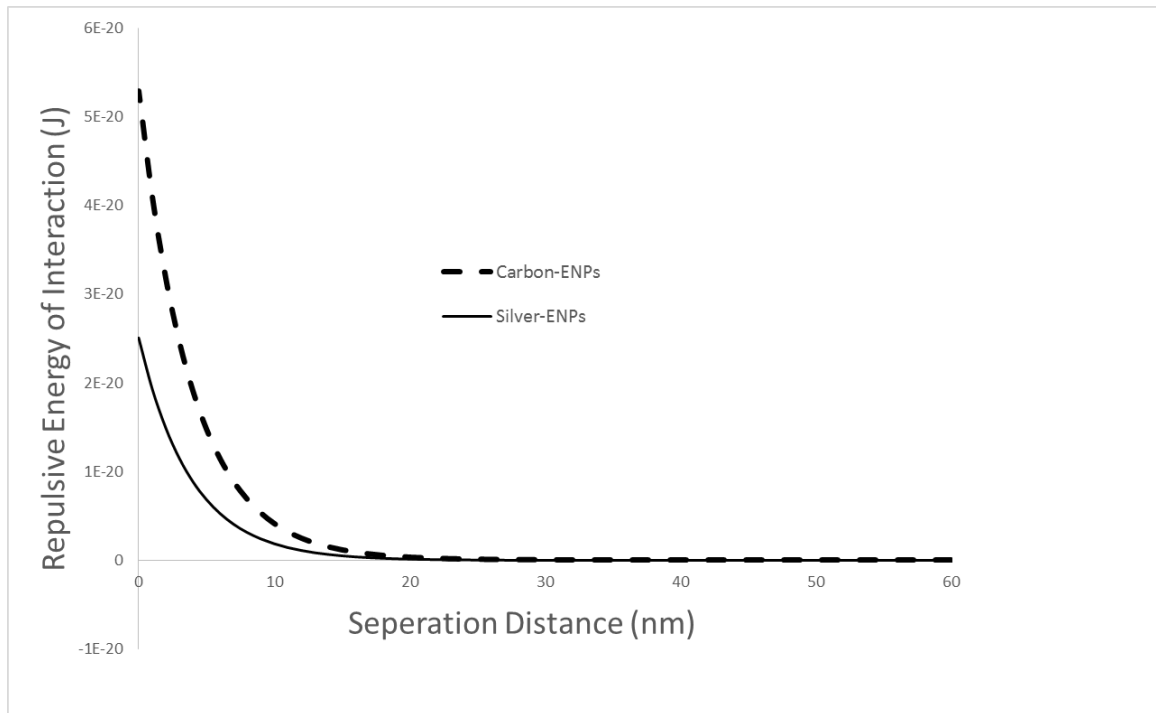


Figure 1.1. A comparison of the levels of repulsion energy between a metallic ENPs and a carbon-ENPs (CNPs) based on reported data from Tian et al. (2010).

The ENPs have a high susceptibility to environmental factors (i.e., chemical stability, dispersion, and surface functionalization) through their implication as pesticide or fertilizer as discussed earlier. It may most likely occur due to unique surface-to-volume ratio, which made them prone to be attacked by oxidative or corrosive environmental matrices including soil, leading to deformation of their nanostructure properties[47].

In order to improve the quality of ENPs implication in soil composition, several techniques have been developed to create protective coating materials around nanoparticles[47]. Wang et al. (2016) deliberately summarized a list of most frequently used coating materials including fluorescein and citrate[48].

However, this coating is beneficial for the functionality of ENPs, but it may considerably change the thermodynamic behavior of the particles as the size may increase as high as 15 to 45 folds (sphere particle) according to reported data from Wang et al. (2015). The matter of coating seems to be very critical instability of attraction force of the ENPs as well as their EPM characteristics. Figure 1-2 represents an example of an ENPs with potential impacts of coating with the assumption of increasing the size of the ENPs. This graph was calculated on the basis of classic DLVO theory specified for the behavior of ENPs in soil matrices. The detail about this model is out of the scope of this literature review (detail presented by [49, 50]). However, regardless of Ionic strength and chemical composition of the soil matrices, this figure is a clear picture of coating effect (i.e., Fe^{+2}) on increasing the energy barrier of an ENPs to target the porous media. This energy barrier will decrease upon to type of coating and redox condition in the soil.

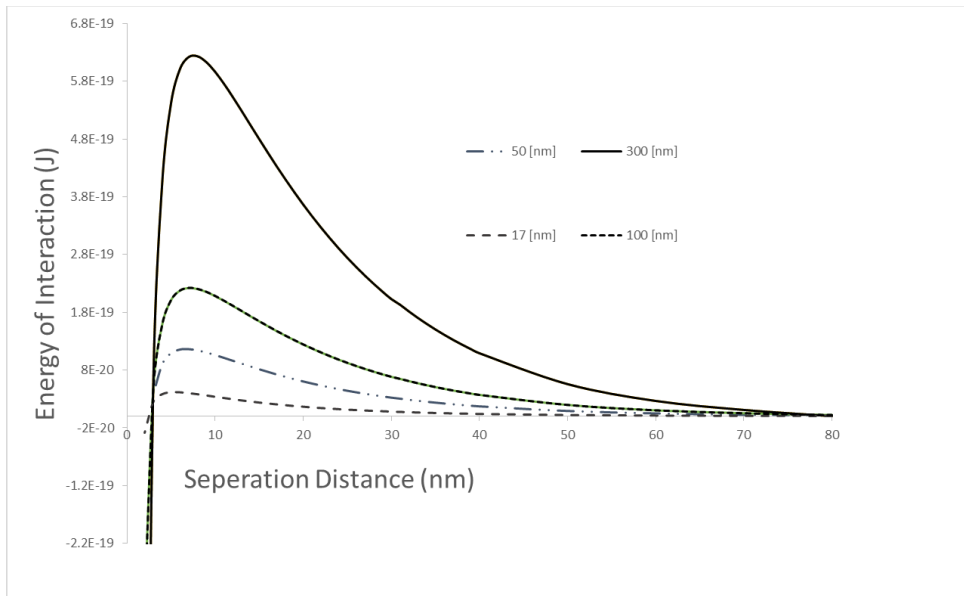


Figure 1.2. Potential impacts of coating with the assumption of increasing the size of the nanoparticles on their interaction energies. This graphs were calculated on the basis of classic DLVO theory specified for the behavior of engineered nanoparticles in soil matrices.

1.4. Nano-Sensors

In the context of agriculture and its direct relation to human health, it is essential to protect the quality and safety of water resources and food supplies from their production points. In this regard, there are increasing demands for reliable field-deployable devices for on-site monitoring of various contaminants in the environment particularly for agriculture and food supplies [30, 51]. For example, the residue of organophosphorus chemicals as derivatives of used pesticides or chemical weapons can contaminate the water and soil and put human and animal life at risk [52]. Sensing such a chemical by conventional microbiological techniques, analytical methods, and in some cases live animal tests are costly, time-consuming, require more complicated instrumentation and substantial scientific expertise [53, 54].

Development of nanotechnology into sensing science can effectively overcome these shortcomings in precise nanoscale levels. The selected ENPs including nanowire (proficiency of very high detection sensitivity), carbon nanotubes (large surface area) or magnetic nanoparticle-based are promising novel approaches to detect such contaminants as a nano-biosensor element [55]. The applications of ENPS as nanosensors can be defined by their roles in three fundamental principles; i) as receptors that explicitly bind to the target analyte, ii) to provide a physical interface for biological activities, and iii) amplifying the received signal from a nano-transducer element [56]. Due to high sensitivity, simplicity, capture efficiency, low price, and nanosize, ENPs have been widely used in nano-biosensors [52].

For example, a combination of nanowires and metallic nanoparticles (i.e., Au, Ag) represent identical biosensor elements in electrochemical labels to sense the DNA [56, 57], which ultimately can incorporate in genetically modified agricultural plant species.

The nanosensors based on ENPs-TiO₂ has been successfully applied for detecting the redox state on a variety of herbals including chamomile (*Matricaria chamomilla*), green/black tea, mint (*Lamiaceae*), sage (*Salvia*) and fennel (*F. Vulgare*) [58].

For the first time, Wang et al. 2015 developed a nanosensor using a conjugate form of graphene quantum dots (GQDs) and ENPS-Au for sensing the highly toxic element of Cyanide (CN⁻) in the plants such as cassava roots [59]. In another study, Chaiyo et al. 2015, successfully applied a nanosensor designed on ENPS-Au application for highly sensitive and selective detection of Cu²⁺ over 15 of most available macro and micro-nutritional elements in a variety of agricultural and food products including rice, tomato, groundwater and mineral water [60].

The pyrophosphate is an additive to agricultural products, with potential health threat at high doses, ENPs-Au and Ag have been applied for monitoring of this compounds in a wide variety of products including white flour, sugar, vegetable fat, soya flour and dry wheat gluten [61]. Table 1.1 represents some of the frequently implemented ENPs in nanosensors structures for the monitor, detect and qualify the certain compounds in agricultural products.

Table 1.1. Frequently implemented Engineering nanoparticles in nanosensors structures for the monitor, detect and qualify the certain compounds in agricultural products.

ENPs	Detection Technique	Sensing element	Agricultural benefits	Ref
Carbon dots coated with vitamin B₁₂	fluorescence resonance	N-methyl carbamates	Detecting a highly toxic residue of pesticide *	[62]
Cellulose nanofibers (CNFs) with silver ENPs-Ag	surface-enhanced Raman spectroscopy (SERS)	thiabendazole	thiabendazole (TBZ) pesticides in various food products (i.e., apples)	[63]
Graphene quantum dots (QDs)	fluorescence	fenoxycarb carbamate i	Detecting toxic residue of pesticide	[64]
ENPs-Au/Ag	graphene-enhanced Raman spectroscopy (GERS)	Direct GERS response	Assessment of the freshness of fruits and vegetables (Wax apple, Lemon, Tomato, Red Pepper, and Carrot)	[65]

*Carbofuran is considered as a toxic pesticide by FAO (Food Agriculture Organization)

1.5. More insight into the interaction of nanoparticles with plants

Proteins consist of a chain of amino acids, in which through a different sequence of the amino acids the physical shape, structure, and function of proteins form. The primary compartments of protein secondary structure are known as α -helices and β -sheets, which their three-dimensional arrangement forms the tertiary structure[66].

The functional conformation of a protein is strictly governed by the shape of the hydrophobic compartments. The intrusion of the nanoparticles into a biosystem is associated with the interruption of the protein established conformation and, therefore, the protein is prone to dysfunction[67]. This event corresponds to one of the primary biological impacts of nanoparticles.

The effect of the surface chemistry of nanoparticle on its interaction with the protein is a very complex process which incorporated many factors including the electrostatic and hydrophobic interactions, as well as specific chemical interactions between the protein and the nanoparticle surface charges [67, 68].

It is highly possible that the surface charge of nanoparticles will be partially or entirely affected by the presence of root exudate and associated amino acids in rhizosphere zones of the plants before plant uptake [13]. Because the pathways of the nanoparticle to the root cells are entrapped by high concentration of amino acids and low molecular chains. As results, amino acids in the rhizosphere are able to indirectly change the enthalpy of certain protein interaction with nanoparticles [66]. In addition, the proteins possess a very wide range of affinities for different nanoparticle surface, leading to a varied range of residence times for proteins at a nanoparticle surface.

1.6. Interaction of root exudate Amino Acids with Nanoparticles

The agglomeration of the nanoparticle is a critical phenomenon that occurs upon entrance of nanoparticle in a biological system which may be affected by the particle shape, size, surface area, and charge, as well as the adsorption properties of the nanoparticles [14, 69]. Furthermore, key factors including pH, ionic strength, water quality and the presence of organic/inorganic matter potentially modify nanoparticle aggregation, which govern the toxicity and reactivity of the nanoparticles [70].

In the plant root zone (the rhizosphere), amino acids are the second most significant component of the root exudates. The release of such molecules has been reported in numbers of plants by 50% ($w v^{-1}$) through the root exudates [71].

Representative amino acid solutions hold distinctive charges at a pH range (5.5–8.5) characterizing the natural environment. For example, four frequently reported amino acids in rhizosphere include positively charged (Histidine), neutral (Glycine), and negative charges (Aspartic acid and Glutamate) [71].

The nanoparticle colloidal stability in exposure to amino acids solution and their tendency to agglomerate corresponds to the surface charge of the nanoparticles as well as functional groups of the amino acids which overall interaction can be measured in the framework of multiple forces of electrostatic, steric, and van der Waals, which can be articulated through application of the Derjaguin–Landau–Verwey–Overbeek (DLVO) theory [71].

In copresence of heavy metals and nanoparticles, several processes can lead to the lower adsorption of Cd on CeO₂NPs such as competitive adsorption of root exudates that occupy part of the adsorption sites for Cd; the formation of root exudate and Cd complexes which display lower

adsorption on CeO₂NPs than free Cd²⁺ or less available adsorption sites caused by CeO₂NPs aggregation.

In the presence of root exudates, if the adsorption density of Cd²⁺ is greater than that of other organic ions and charged organic ligands, the imbalance of adsorbed ions will contribute a net positive charge to the surface. Therefore, the charge imbalance might be described either in terms of unequal adsorption of the Cd²⁺ or nonstoichiometric dissolution of the CeO₂. The higher feasibility of Cd²⁺ adsorption in a substitution mechanism with Ce³⁺ with respect to higher dissolution of CeO₂ in co-presence of root exudates was further supported by reducing the trend of zeta potential and a higher concentration of cerium after equilibrium [13].

In the presence of the root exudate amino acids, the surface complexes form with Cd ions, in which the process is one of adsorption. Examples include binding of organic molecules on the surface of CeO₂ and formation of surface complexes between cadmium ions from solution and organic acid functional groups on the surface of NPs[50, 72].

However, these complexes in natural matrices seem to be more complicated. For example, Krishnamurti et al., 1997 reported that the complex of oxalic acid as a root exudate compound with cadmium as Cd-(oxalate)_n complexes could easily be decomposed by microbial activities and the resulting the readsorption of free Cd by the ENPs [73]. In contrary, D-serine is a rare amino acid which cannot be quickly metabolized by bacterial activities of the rhizosphere in soil [74]. Other ionizable functional groups in root exudates also impact the surface charge of the CeO₂NPs. For example, organic acids molecules (i.e., succinic acid and D-Serine) with both carboxyl (-COOH) and amino (-NH₂) groups [50, 72]. In a liquid medium, the carboxyl group is a stronger acid than the amino group. As a result, at low pH, both types of groups tend to be protonated (-COOH and -NH₃⁺), whereas, at high pH, both tend to be deprotonated (-COO⁻ and -NH₂); in

the intermediate pH range, most of the carboxyl groups are likely to be deprotonated, while most amino groups are protonated.

At high pH range, ($\text{pH} > 5$) the surface concentration of the organic acids far exceeds that of the amino groups. Hence, CeO_2NPs are generally negatively charged in this range of pH. Therefore, at lower pH values when CeO_2NPs that exposed to both types of functional groups, the surface carries more positive charges compared to negative charges at higher pH [50].

However, as it is illustrated in Figure 1, I proposed that adsorption of succinic acid and D-glucose occur through its two carboxyl groups binding to two adjacent cadmium surface sites, and not only one. Also, l-malic acid adsorption binds via one carboxyl group and one hydroxyl, which forms a “claw” on CeO_2NPs surface. This mechanism was in a good agreement with the proposed mechanism of the other scientists[75]. However, in such medium, the strength of the surface complex of l-malic acid is thought to be far stronger than a weak surface complex of succinic acid. To support this mechanism, it is worth to note that l-malic acid adsorption can reach the equilibrium state four times faster than succinic acid (12/48 h)[75].

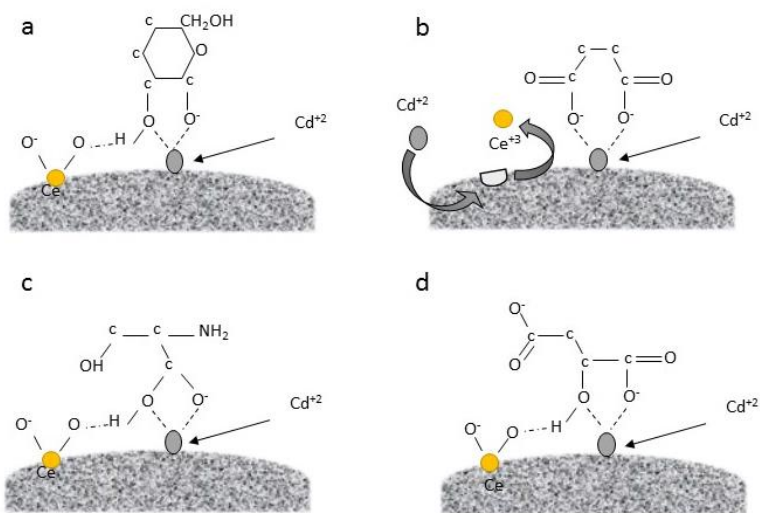


Figure 1.1. The schematic diagram for the CeO₂NPs and possible binding between synthetic root exudate molecules and Cd²⁺ on the surface of CeO₂NPs during adsorption. a) Illustrate the binding of the oxygen molecule in D-glucose with Cd and Ce. B) Succinic acid. c) D-serine amino acid and d) L-malic acid

In addition to the behavior of CeO₂NPs in exposure to root exudate, a similar correlation was found between the ZnO nanoparticles behavior and four commonly found amino acids in rhizosphere area (Glycine, L-Glutamic, L-Aspartic, and L-Histidine) at different concentrations. It was shown that the nanoparticle size distribution was reduced as the pH changed into more acidic and nanoparticles became less agglomerated [71].

Further, in exposure to the ZnO, the charge of the amino acid functional groups affected the colloidal stability of the ZnO nanoparticle and its size distribution (agglomeration effects). The critical finding suggested that the amino acids holding more positively charged seems to be more effective in lowering the agglomeration rate compared to the neutral or negative charged amino

acids. Overall, the more significant concentration of amino acids is associated with the reduction of the zeta potential at a broad range of environmental pH [71].

In soil complex, the most critical example of adsorption that affects the surface charge of particles is that of large organic molecules, such as those identified as natural organic matter (NOM). Such molecules are often strongly adsorbed onto both inorganic minerals and manufactured nanoparticles. The functional groups that are part of these molecules are often charged in the dominant pH of the environment so that when the molecules adsorb, they contribute charge to the particle surface. It is now widely accepted that the adsorption of NOM onto particles in natural waters is almost always the principal determinant of their surface charge. The fact is accepted that the charge on nanoparticles in natural waters is dictated by NOM.

1.7. Cerium oxide nanoparticles (CeO₂)

Cerium oxide nanoparticles (CeO₂ NPs) is one of those ENPs that have been extensively applied in various industries over the past several years particularly as a fuel additive [76, 77]. The main introduction pathway of the CeO₂ into soil and plants is reported through deposition of vehicle exhausts and diffusion of municipal runoff into the top soil [76]. It is very important to understand the uptake mechanism of such ENPs into crop plants due to their bioaccumulation in the human food, their chemical interaction with essential trace elements, delivering toxic ions to the plants, biotransformation, and potential biological inheritance to the next plant generations [76, 78].

Cerium oxide possesses the lowest solubility against acid among the rare earth metal oxides and does not elute during the removal of harmful ions in water[79]. Also, natural organic matter

(NOM) including root exudates in a growth medium can enhance in the stability of CeO₂ [5]. Elemental Ce belongs to a lanthanide family and is the most abundant and reactive rare element of the earth (20-60 mg/kg)[80]. It is a soft, ductile metal with silver color, which acts as a strong oxidizer in exposure to air — cerium with a molecular weight of the 140.116 g mol⁻¹ represents density of 6.770 g cm⁻³. Its melting point has been reported as of 798 °C and respectively a boiling point of 3443 °C. It also solves in dilute, mineral acids.

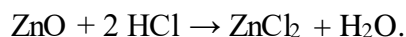
Elemental Ce tarnishes gradually in exposure to air and actively react at 150 °C to form CeO₂[81]. CeO₂ is the most common form for Ce in the earth's crust. CeO₂ nanoparticles are massively applied in different industries due to their catalytic ability, which is basically subjected to redox behavior depending on the Ce's redox state[82]. The CeO₂ nanoparticles are mainly contained of Ce(III) (up to 60%) and Ce(IV), which the higher ratio of Ce(IV) cause the stronger the catalytic activity. In the lattice structural form of CeO₂, the cationic form of Ce will be coordinated via eight oxygen anions at the corner of the crystal form while the anionic oxygen tetrahedrally corresponds to four Ce cations. Once the oxygen anions (O²⁻) gets off from the lattice structure, the oxygen vacancies will increase the reactivity of the nanoparticle, concerning the temperature and environmental parameters [83]. Thus it is believed to be a promising alternative nano-adsorbents to eliminate toxic elements. In environmental remediation, cerium oxide had demonstrated a high adsorption capacity for hazardous anions, such as fluoride, bichromate, [79] and cations including As(V), Cr(VI) and Pb (II) [84].

The loss of O²⁻ creates an electrostatic balance which is associated with the reduction of two Ce⁴⁺ to Ce³⁺ [85]. On the surface of CeO₂ nanoparticle, Ce³⁺ can potentially oxidize to Ce⁴⁺ in exposure to environmental oxidants. At smaller CeO₂ nanoparticle sizes, the density of oxygen vacancy, as well as Ce³⁺/Ce⁴⁺, will increase[83, 85].

1.8. Zinc oxide (ZnO)

Zinc oxide with the formula of ZnO is an inorganic compound, which typically appears in the form of insoluble white powder[86]. ZnO has been massively applied as an additive into many products including glass, plastics, sunscreen, ceramics, rubber, cement, lubricants, paints, and batteries[14, 87]. ZnO is currently being used as food additives and has been recognized as safe material by the Food and Drug Administration[88]. ZnO can be found on the Earth crust as a natural mineral zincite, but mostly available as a commercial product through chemical synthetases. ZnO is also known as II-VI semiconductor due to representing the groups of II and VI in the periodic table, respectively for zinc and oxygen[89]. It exhibits specific properties which make it favorable for many implications; this properties includes decent transparency, high electron mobility as well as strong room temperature luminescence[90]. Also, ZnO is a multipurpose functional material that is available within diverse morphologic groups such as nanorings, nanocombs, nanosprings, nanobelts, and nanowires[91]. Such ZnO nanostructures can be economically synthesized at very low cost. Therefore it has a high promising potential in the development of nanotechnology [92].

As and an amphoteric oxide, ZnO is almost insoluble in water and alcohol, but it can be solved in many acidic solutions, such as hydrochloric acid:



Also, basic solutions can be dissolve the ZnO and lead to the production of soluble zincates:



ZnO nanostructures are also attractive for biological and agricultural application because of their safe properties and large surface area[92, 93]. For example, in biological systems, ZnO enters into a slow reaction with fatty acids and produce carboxylates compounds, such as oleate or

stearate[94]. Also, ZnO nanoparticle represents strong antibacterial characteristics which may stem from the generation of reactive oxygen species (ROS)[95, 96]. Such ROS could be induced on the nanosurface of ZnO, which have been investigated through a conductometric technique. In this regard, ZnO being exhibit a wide band-gap semiconductor (3.36 eV), which make it an ideal nanoparticle for agricultural applications[69]. Its application as an antimicrobial agent against various pathogens including *Escherichia coli*, *Campylobacter jejuni*, *Pseudomonas aeruginosa* has been frequently reported[70, 97].

The benefits of using ZnO as antimicrobial agents is that Zn is an essential mineral element for humans and crops, which exhibit strong activity in the form of oxide at very small amounts. For example, Zn is the sole metal formulated in all six enzyme classes (transferases, viz. oxidoreductases, hydrolases and ligases, lyases, isomerases)[70]. Zn plays a vital role in different integral metabolic processes, promotes the synthesis of carotenoids and chlorophylls leading to higher photosynthetic apparatus of the crops [94]. However, it has been reported that particle size and surface charge of coating materials can affect the activity of the ZnO in plants[98, 99].

Different studies reported the impact of ZnO ENPs on crop plants. For instance, it has demonstrated to enhance germination rate, pigments synthesis, the contents of carbs and protein as well as activities of antioxidant enzymes[100, 101].

1.9. Inhibitors of biological process in plants

1.9.1. Lanthanum (La³⁺) and Gadolinium (Gd³⁺)

Calcium-permeable channels represent an extremely high affinity for divalent cations like Ca²⁺, Sr²⁺, and Ba²⁺ [102]. The trivalent lanthanide gadolinium (Gd³⁺) and lanthanum (La³⁺) are chemically very close to the divalent calcium ion (Ca²⁺) in terms of size (radius of Gd³⁺ 1.05–1.11

Å and Ca^{2+} 1.00–1.06 Å), donor atom preference, bonding, and coordination [103, 104]. These trivalent cations can indicate high potency and completely block the current through an open channel at concentration levels less than 10 μM [102]. Several studies indicated VIC channels that exist in all root cell-types, as well as voltage dependent channels, could be inhibited by Gd^{3+} and La^{3+} [105]

The inhibitory behavior of Gd^{3+} and La^{3+} , primarily stems from inhibiting the influx of extracellular calcium into cells through calcium channels in the plasma membrane [106] because they are competing with Ca^{2+} for binding at the same site [102, 107]. The regulation of calcium flux through this class of lanthanide is a highly concentration dependent. For example, Liu et al. (2012) indicated that at lower concentration levels, La^{3+} could inhibit Ca^{2+} flux, while the higher concentration levels induce Ca^{2+} in the root cells [108]. It has been reported that in certain cell types, La^{3+} and Gd^{3+} can passively diffuse into the cytosol where their intracellular inhibitory effects take place stronger in comparison to extracellular effects [107]. In this case, lanthanides may appear in two forms of free ions or complexes through binding with negatively charged compounds [107].

1.9.2. 2,4-Dinitrophenol (DNP)

Calcium-permeable channels require energy (in the form of ATP) for their maintenance and activities including gate action and transport of certain divalent cations. These channels can be activated directly through i) depolarization ii) cyclic-AMP-mediated phosphorylation and iii) fluoride-mediated inhibition of phosphatase-induced dephosphorylation [106].

The formation of Adenosine triphosphate (ATP) is the ultimate product of the tricarboxylic acid (Krebs) cycle in mitochondria with simultaneous formation of CO_2 and H_2O . Through glycolysis,

there is a net production of two ATP molecules, but the majority of energy-rich phosphate bonds are produced during the final oxidative phosphorylation process[109].

Within the final phase, ATP synthetase converts adenosine diphosphate to ATP with the addition of an inorganic phosphate molecule [110]. 2,4-Dinitrophenol (DNP), reduces the production of high-energy phosphate bonds in mitochondria and simultaneously encourages systemic oxygen intake. This dissociative progression is recognized as uncoupling of oxidative phosphorylation [109, 110].

In oxidative phosphorylation, the current of electrons from NADH and FADH₂ to oxygen occur through exporting of H⁺ from the matrix to the inner mitochondrial membrane. This gradient of H⁺ can yield to the synthesis of ATP by flowing through ATP synthetase in the mitochondrial inner membrane. DNP interfere with the H⁺ gradient and decrease the synthesis of required cellular ATP [110].

Also, DNP interferes with the synthesis of ATP at the final energy production phase by preventing the uptake of inorganic phosphate molecules into the mitochondria. Consequently, all energy-requiring processes block and the extra-mitochondrial accumulation of inorganic phosphate occur[110].

The effects of DNP vary with the age of the plants as well as applied concentration [111, 112]. For example in a 6 day barley plant, DNP inhibits the absorption of phosphate by approximately %40 while in 18 days plant it increases as high as 98%. This observation implies a possible correlation between glycolytic phosphorylation, oxidative phosphorylation and root development [111]. This can be strongly linked to species of leguminous plants that possess phosphomannoseisomerase activities which may display higher sensitivity to DNP on phosphate absorption.

DNP also inhibit the transport of inorganic phosphate to the shoots, indicating that the inhibition of metabolic mechanisms is critically effective not only within the entry process but also through the exit process into the shoot[111].

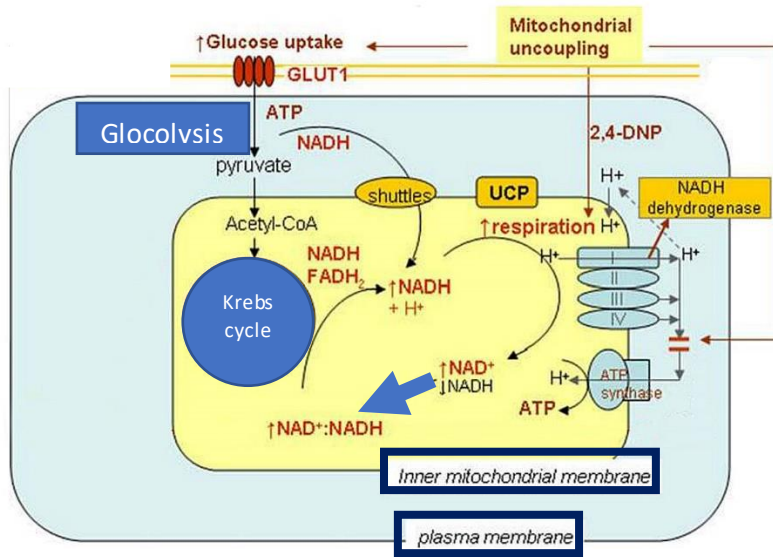


Figure 1.3. Proposed model by Liu et al. 2008[113] for the uncoupling effects of DNP which induces metabolic stress through interruption of the hydrogen ion shuttling across the inner membrane.

1.9.3. Cycloheximide (CHX)

Cycloheximide (CHX) represents the most common laboratory reagent used to block protein synthesis and is widely used in plant physiology. Cycloheximide was at first isolated from *Streptomyces griseus* and later was recognized as an inhibitor of eukaryotic translation blocking the translational elongation phase. Elongation is the step by step addition of amino acids to the growing protein chain. The order of amino acids is quantified by the sequence of codons in the mRNA, CHX is capable of binding the ribosomal E-site and inhibits eukaryotic elongation factors (eEF2)-mediated translocation[114].

Therefore, CHX blocks the synthesis of proteins in cell signaling. The use of CHX may represent other side effects. For example, inhibition of protein synthesis by CHX restrict the hydraulic conductivity of root through reducing cellular water transport from one cell to other[115]

Generally, effects of CHX on plants can be envisaged in three interdependence categories, i) inhibition of DNA synthesis ii), disruption of ion absorption, and iii) interfere the uptake of required amino acids. These effects are directly or indirectly governing by the ability of CHX concentration on blocking the protein synthesis[114].

1.10. Research Hypothesis and Goal

The applications of metallic oxide engineered nanoparticles (MONPs) in agriculture and food processing sectors including biosensors, nano-pesticides, plant growth stimulator, food additives, nano-fertilizers, delivery agents for micronutrient has massively increased [51, 116, 117]. Such nanoparticle can benefit the cultivation of dietary plants including crops and leafy vegetables by reducing the chance of heavy metals uptake or improve their post harvesting qualities such as chlorophyll content and anti-microbial properties [80, 118]. In addition, nanoparticles may contribute to increase the shelf life of vegetables by reducing the heavy metal content or act as a strong anti- microbial/fungal [118, 119]. The rationale to imply the MONPs in agrichemicals can be articulated into three specific goals: (i) efficient harvest of agricultural products with higher yield; (ii) to reduce the consumption of irrigation water and associated energy and (iii) minimizing the agri-waste production.

As a result of advances in nanotechnology-facilitated agrichemicals, MONPs are directly applied to agricultural systems [120, 121]. In addition, the progressive development of nano-biotechnology has resulted in noteworthy unintentional releases of MONPs into the agricultural soil as a primary

sink due to water irrigation and the collide deposition. Therefore, interactions of crops and leafy vegetables with MONPs with is fully expected.

Due to the different size-specific properties, surface charge, and phytotoxicity potential, the risk of bioaccumulation of MONPs in dietary plants and edible crop tissues, there is a need to understand the impacts of MONPs on plants, their uptake pathways and underlying mechanisms in plant tissues. In this regard, most ongoing research is centered on the potentially detrimental effects of MONPs [122, 123]. While, the effects of MONPs on plant uptake in exposure to a group of highly toxic contaminants, heavy metals, and metalloids, have not been adequately addressed.

In exposure to organic or inorganic contaminants, plant roots undertake different uptake mechanisms. For organic chemicals, hydrophobicity is a key parameter which mediates the entrance of compounds into the plant and dictates the primary mechanism for MONPs when they co-exist with the organic compounds[124]. This pathway is known as the “Trojan horse effect” in which adsorption of the organic compounds onto the MONPs surface lead to concomitantly uptake by plants[125, 126].

For inorganic elements including heavy metals and metalloids, sophisticated plant root systems can regulate their transport into root cytoplasm. Two pathways are well known, first, actively regulating the shuttle of heavy metals through various ion and protein channel which embedded in the cell membrane, second, passively transporting via passive diffusion which occurs through the cell membranes [94, 127].

Therefore, the interactions between MONPs and co-existing heavy metals and metalloids can be different from their interactions with organic compounds. In addition, MONPs have been observed to alter the gene expressions, interrupt the bilayer membrane of the cell, adsorb on cell wall and

interact with root exudate[128]. As a result, exposure to MONPs expected to alter plant uptake and accumulation of co-existing heavy metal and metalloid ions.

MONPs can be taken up by crops roots and translocated into edible parts of plants including leaf and fruits[129]. However, uptake and accumulation of MONPs in co-existence with heavy metals as well as the physiological effects of this co-exposure on plants are affected by the interference of various abiotic stresses [80, 130].

For example, the chemistry in the growth media has a strong impact on ENPs fate and transport and their interactions with coexisting pollutants. In particular, the presence of phosphate has been shown to drastically affect the speciation and uptake of MONPs by plants[131]. Addition of phosphate was shown to inhibit the redox cycle between Ce(III) and Ce(IV) on the CeO₂NPs surface due to the formation of CePO₄[132]. A similar phenomenon was also observed in plant roots that the transformation of Ce(IV) to Ce(III) was substantially reduced in the presence of 1 mM PO₄³⁺ in the growth media[133]. The presence of PO₄³⁺ also led to the formation of needle-like CePO₄ nanoparticles and different subcellular localizations of Ce in plant root cells[133]. A recent study found that the presence of PO₄³⁺ significantly increased the adsorption of Cd on graphene oxide (GO) at pH 5.3-10.0 due to the formation of a ternary surface complex [134]. Given the abundance of phosphate in biological systems and plant growth media and the strong impact of surface chemistry on MONPs fate and impact, it is imperative to understand the role of MONPs surface properties and the biogeochemical conditions in plant growth media on the mutual interactions of ENPs and co-occurring environmental chemicals.

There are several critical questions which raised from the previous studies: What biological mechanisms are involved in uptake of MONPs from media into root cells? Does the physiochemical properties of either MONPs or heavy metals/metalloid change in the presence of

root exudate? Does the nanoparticle surface charge impact the uptake and translocation of themselves and coexisting heavy metals? How the chemistry of growth medium can impact the uptake of both MONPs and heavy metals?

Mechanistic understanding of these research questions is imperative to elucidate of the altered plant heavy metal/metalloid uptake, determine the underling physiological mechanism in the accumulation of co-existing heavy metals and MONPs.

This dissertation aimed to investigate the interaction, involved mechanism in uptake and change of physiochemical properties of two important metallic oxide nanoparticles, CeO₂ and ZnO nanoparticles in biological systems of two crops; rice (*Oryza sativa* L.), Soybean (*Glycine max* (L.) Merr.) and four leafy vegetables including Spinach (*Spinaciae oleracea*), Parsley (*Petroselinum sativum*), Romaine lettuce (*Lactuca sativa* L. var. *Longifolia*), cilantro (*Coriandrum sativum*) in coexistence to heavy metals (Cadmium (Cd) and Lead (Pb)) and metalloids Arsenic III, V (As) under different growth conditions (soil and hydroponics).

The rationale to select these plants as the study model is due to their importance in human dietary system. Soybean was reported by the Food and Agricultural Organization (FAO) as the fifth most produced crop worldwide that provides about 30% vegetable oil and 77% nitrogen fixation[129]. Rice grains is one of the most staple food in the world[135]. The selected four leafy vegetables for this research are rich in bioactive compounds, essential minerals, and dietary fibers. The dry or fresh consumption of these vegetables through a variety of foods have been extensively increased due to rich flavor, anti-cancer properties, and high vitamin content. Therefore, these crops and vegetables are formulated in dietary supplements and are a proposed diet for infants, older adults, and patients[136, 137].

The rationale to select ZnO and CeO₂ nanoparticle due to their advancement in agriculture and food processing. CeO₂ has been introduced as a priority contaminant by the Organization for Economic Cooperation and Development (OECD). It has high potential impacts on dietary plants, strong stimulating impacts on the plant growth (i.e. chlorophyll content), and represented a high adsorption capacity of heavy metal contamination[129, 138].

ZnO ENPs are closely related to agricultural food processing because Zn is an essential nutrient for crops and many vegetables and progressing advancement aims to formulate ZnO into the composition of nano-fertilizers. ZnO ENPs represent high efficiency, low toxicity, and act as antimicrobial/ fungicides which have been extensively applied to protect vegetables, fruit, and grain crops among many promising organic antimicrobial agents [116, 139].

To achieve the overall goal of this research, six research hypotheses were developed:

Hypothesis 1: heavy metals of Cd and Pb with ZnO nanoparticles can represent competitive behavior on ZnO surface adsorption and may alter the heavy metals uptake pattern and microbial community in root zone and physiology of plants.

Hypothesis 2: The response of the leafy greens to the co-contamination of two divalent heavy metals Cd and Pb may differ from plants to plants, leading to alteration of the nutritional values of minerals (Fe, Cu).

Hypothesis 3: Co-existence of CeO₂ ENPs and Cd, ENPs surface charge and chemistry of growth media can alter their uptake by soybean plants and change the defense mechanism of plants such as the release of root exudates.

Hypothesis 4: The release of root exudate can lead to the transformation of CeO₂ ENPs and co-existing heavy metals and metalloids in terms of nanoparticle size and shape and impact the adsorption potential of the nanoparticle for reducing the heavy metals

Hypothesis 5: Coexistence of CeO₂ ENPs and Cd can impact active or passive transport of the chemicals. Suspecting the active transport will play a role in the transport of heavy metals, CeO₂

1.11. References

1. Navarro, E., et al., *Environmental behavior and ecotoxicity of engineered nanoparticles to algae, plants, and fungi*. *Ecotoxicology*, 2008. **17**(5): p. 372-386.
2. Lin, D., et al., *Fate and transport of engineered nanomaterials in the environment*. *Journal of Environmental Quality*, 2010. **39**(6): p. 1896-1908.
3. Tourinho, P.S., et al., *Metal-based nanoparticles in soil: Fate, behavior, and effects on soil invertebrates*. *Environmental Toxicology and Chemistry*, 2012. **31**(8): p. 1679-1692.
4. Picó, Y., *Challenges in the determination of engineered nanomaterials in foods*. *TrAC Trends in Analytical Chemistry*, 2016. **84, Part A**: p. 149-159.
5. Grillo, R., A.H. Rosa, and L.F. Fraceto, *Engineered nanoparticles and organic matter: A review of the state-of-the-art*. *Chemosphere*, 2015. **119**: p. 608-619.
6. Mihindukulasuriya, S.D.F. and L.T. Lim, *Nanotechnology development in food packaging: A review*. *Trends in Food Science & Technology*, 2014. **40**(2): p. 149-167.
7. Dreher, K.L., *Health and environmental impact of nanotechnology: toxicological assessment of manufactured nanoparticles*. *Toxicological sciences*, 2004. **77**(1): p. 3-5.
8. Alfadul, S., A.J.A.J.o.F. Elneshwy, *Agriculture, Nutrition, and Development, Use of nanotechnology in food processing, packaging and safety—review*. 2010. **10**(6).

9. Stowers, C., et al., *Initial Sterilization of Soil Affected the Interactions of Cerium Oxide Nanoparticles and Soybean Seedlings (Glycine max (L.) Merr.) in a Greenhouse Study*. 2018.
10. Rossi, L., et al., *Uptake, Accumulation, and in Planta Distribution of Coexisting Cerium Oxide Nanoparticles and Cadmium in Glycine max (L.) Merr.* 2017. **51**(21): p. 12815-12824.
11. Chorianopoulos, N., et al., *Use of titanium dioxide (TiO₂) photocatalysts as alternative means for Listeria monocytogenes biofilm disinfection in food processing*. 2011. **28**(1): p. 164-170.
12. Kim, J.S., et al., *Antimicrobial effects of silver nanoparticles*. 2007. **3**(1): p. 95-101.
13. Sharifan, H., et al., *Investigation on the Modification of Physicochemical Properties of Cerium Oxide Nanoparticles through Adsorption of Cd and As(III)/As(V)*. ACS Sustainable Chemistry & Engineering, 2018. **6**(10): p. 13454-13461.
14. Wang, X., et al., *Elucidating the Effects of Cerium Oxide Nanoparticles and Zinc Oxide Nanoparticles on Arsenic Uptake and Speciation in Rice (Oryza sativa) in a Hydroponic System*. 2018. **52**(17): p. 10040-10047.
15. Zhu, N., J. Qiao, and T.J.S.o.t.t.e. Yan, *Arsenic immobilization through regulated ferrolysis in paddy field amendment with bismuth impregnated biochar*. 2019. **648**: p. 993-1001.
16. Rossi, L., et al., *Mutual effects and in planta accumulation of co-existing cerium oxide nanoparticles and cadmium in hydroponically grown soybean (Glycine max (L.) Merr.)*. 2018. **5**(1): p. 150-157.

17. Sharma, V.K., et al., *Interactions between silver nanoparticles and other metal nanoparticles under environmentally relevant conditions: A review*. 2019. **653**: p. 1042-1051.
18. Hidangmayum, A., et al., *Application of chitosan on plant responses with special reference to abiotic stress*. 2019: p. 1-14.
19. Khan, Z. and H. Upadhyaya, *Impact of Nanoparticles on Abiotic Stress Responses in Plants: An Overview*, in *Nanomaterials in Plants, Algae and Microorganisms*. 2019, Elsevier. p. 305-322.
20. Zhang, W., et al., *Impact of Nanoparticle Surface Properties on the Attachment of Cerium Oxide Nanoparticles to Sand and Kaolin*. 2017.
21. Ma, X., J.J.C.O.i.E.S. Yan, and Health, *Plant Uptake and Accumulation of Engineered Metallic Nanoparticles from Lab to Field Conditions*. 2018.
22. Rafique, M., et al., *Dependence of the structural optical and thermo-physical properties of gold nano-particles synthesized by laser ablation method on the nature of laser*. *Optik - International Journal for Light and Electron Optics*, 2017. **134**: p. 140-148.
23. Benn, T.M. and P. Westerhoff, *Nanoparticle silver released into water from commercially available sock fabrics*. *Environmental science & technology*, 2008. **42**(11): p. 4133-4139.
24. Lateef, A., et al., *Synthesis and characterization of zeolite based nano-composite: An environment friendly slow release fertilizer*. *Microporous and Mesoporous Materials*, 2016. **232**: p. 174-183.
25. Theng, B.K. and G. Yuan, *Nanoparticles in the soil environment*. *Elements*, 2008. **4**(6): p. 395-399.

26. Wang, M., B. Gao, and D. Tang, *Review of key factors controlling engineered nanoparticle transport in porous media*. Journal of Hazardous Materials, 2016. **318**: p. 233-246.
27. Yaron, B., I. Dror, and B. Berkowitz, *Engineered nanomaterials as a potential metaprogenetic factor: A perspective*. CATENA, 2016. **146**: p. 30-37.
28. Tolaymat, T., et al., *The effects of metallic engineered nanoparticles upon plant systems: An analytic examination of scientific evidence*. Science of The Total Environment, 2017. **579**: p. 93-106.
29. Zhang, W., et al., *Elucidating the mechanisms for plant uptake and in-planta speciation of cerium in radish (*Raphanus sativus* L.) treated with cerium oxide nanoparticles*. Journal of Environmental Chemical Engineering, 2017. **5**(1): p. 572-577.
30. Khot, L.R., et al., *Applications of nanomaterials in agricultural production and crop protection: a review*. Crop protection, 2012. **35**: p. 64-70.
31. Zheng, L., et al., *Effect of nano-TiO₂ on strength of naturally aged seeds and growth of spinach*. Biological trace element research, 2005. **104**(1): p. 83-91.
32. Khodakovskaya, M., et al., *Carbon nanotubes are able to penetrate plant seed coat and dramatically affect seed germination and plant growth*. ACS nano, 2009. **3**(10): p. 3221-3227.
33. Kole, C., et al., *Nanobiotechnology can boost crop production and quality: first evidence from increased plant biomass, fruit yield and phytochemistry content in bitter melon (*Momordica charantia*)*. BMC biotechnology, 2013. **13**(1): p. 37.
34. Borišev, M., et al., *Drought Impact Is Alleviated in Sugar Beets (*Beta vulgaris* L.) by Foliar Application of Fullerenol Nanoparticles*. PloS one, 2016. **11**(11): p. e0166248.

35. Davarpanah, S., et al., *Effects of foliar applications of zinc and boron nano-fertilizers on pomegranate (Punica granatum cv. Ardestani) fruit yield and quality*. Scientia Horticulturae, 2016. **210**: p. 57-64.
36. Liu, F., et al., *Porous hollow silica nanoparticles as controlled delivery system for water-soluble pesticide*. Materials Research Bulletin, 2006. **41**(12): p. 2268-2275.
37. Rani, M., U. Shanker, and V. Jassal, *Recent strategies for removal and degradation of persistent & toxic organochlorine pesticides using nanoparticles: A review*. Journal of Environmental Management, 2017. **190**: p. 208-222.
38. Bala, R., et al., *Detection of organophosphorus pesticide – Malathion in environmental samples using peptide and aptamer based nanoprobe*s. Chemical Engineering Journal, 2017. **311**: p. 111-116.
39. Dehghani, M.H., et al., *Optimizing the removal of organophosphorus pesticide malathion from water using multi-walled carbon nanotubes*. Chemical Engineering Journal, 2017. **310, Part 1**: p. 22-32.
40. de la Rosa, G., et al., *Physiological and biochemical response of plants to engineered NMs: Implications on future design*. Plant Physiology and Biochemistry, 2017. **110**: p. 226-235.
41. Husen, A. and K.S. Siddiqi, *Phytosynthesis of nanoparticles: concept, controversy and application*. Nanoscale research letters, 2014. **9**(1): p. 1-24.
42. Siddiqi, K.S. and A. Husen, *Recent advances in plant-mediated engineered gold nanoparticles and their application in biological system*. Journal of Trace Elements in Medicine and Biology, 2017. **40**: p. 10-23.

43. Arokiyaraj, S., et al., *Enhanced antibacterial activity of iron oxide magnetic nanoparticles treated with Argemone mexicana L. leaf extract: An in vitro study*. Materials Research Bulletin, 2013. **48**(9): p. 3323-3327.
44. Tran, N., et al., *Bactericidal effect of iron oxide nanoparticles on Staphylococcus aureus*. Int J Nanomedicine, 2010. **5**: p. 277-283.
45. Barik, T.K., B. Sahu, and V. Swain, *Nanosilica—from medicine to pest control*. Parasitology Research, 2008. **103**(2): p. 253.
46. Stadler, T., M. Buteler, and D.K. Weaver, *Novel use of nanostructured alumina as an insecticide*. Pest management science, 2010. **66**(6): p. 577-579.
47. Li, C., et al., *Production of copper nanoparticles by the flow-levitation method*. Nanotechnology, 2004. **15**(12): p. 1866.
48. Wang, P., et al., *Nanotechnology: a new opportunity in plant sciences*. Trends in plant science, 2016. **21**(8): p. 699-712.
49. Tian, Y., et al., *Transport of engineered nanoparticles in saturated porous media*. Journal of Nanoparticle Research, 2010. **12**(7): p. 2371-2380.
50. Benjamin, M.M. and D.F. Lawler, *Water quality engineering: physical/chemical treatment processes*. 2013: John Wiley & Sons.
51. Dasgupta, N., S. Ranjan, and C. Ramalingam, *Applications of nanotechnology in agriculture and water quality management*. Environmental Chemistry Letters, 2017. **15**(4): p. 591-605.
52. Zhang, W., et al., *Nanomaterial based Biosensors for Detection of Biomarkers of Exposure to OP Pesticides and Nerve Agents: A Review*. Electroanalysis, 2017.

53. Wang, Y. and T.V. Duncan, *Nanoscale sensors for assuring the safety of food products*. *Current Opinion in Biotechnology*, 2017. **44**: p. 74-86.
54. Sharma, D., et al., *Analytical methods for estimation of organophosphorus pesticide residues in fruits and vegetables: A review*. *Talanta*, 2010. **82**(4): p. 1077-1089.
55. Dahman, Y., *Chapter 4 - Nanosensors**, in *Nanotechnology and Functional Materials for Engineers*. 2017, Elsevier. p. 67-91.
56. Grieshaber, D., et al., *Electrochemical biosensors-sensor principles and architectures*. *Sensors*, 2008. **8**(3): p. 1400-1458.
57. Yeh, J.I., M.B. Zimmt, and A.L. Zimmerman, *Nanowiring of a redox enzyme by metallized peptides*. *Biosensors and Bioelectronics*, 2005. **21**(6): p. 973-978.
58. Apak, R.a., et al., *Selective determination of catechin among phenolic antioxidants with the use of a novel optical fiber reflectance sensor based on indophenol dye formation on nano-sized TiO₂*. *Journal of agricultural and food chemistry*, 2012. **60**(11): p. 2769-2777.
59. Wang, L., et al., *Two-Photon Sensing and Imaging of Endogenous Biological Cyanide in Plant Tissues Using Graphene Quantum Dot/Gold Nanoparticle Conjugate*. *ACS Applied Materials & Interfaces*, 2015. **7**(34): p. 19509-19515.
60. Chaiyo, S., et al., *Highly selective and sensitive paper-based colorimetric sensor using thiosulfate catalytic etching of silver nanoplates for trace determination of copper ions*. *Analytica Chimica Acta*, 2015. **866**: p. 75-83.
61. Terenteva, E.A., et al., *Simple and rapid method for screening of pyrophosphate using 6,6-ionene-stabilized gold and silver nanoparticles*. *Sensors and Actuators B: Chemical*, 2017. **241**: p. 390-397.

62. Campos, B.B., et al., *Carbon dots coated with vitamin B12 as selective ratiometric nanosensor for phenolic carbofuran*. *Sensors and Actuators B: Chemical*, 2017. **239**: p. 553-561.
63. Liou, P., et al., *Cellulose nanofibers coated with silver nanoparticles as a SERS platform for detection of pesticides in apples*. *Carbohydrate Polymers*, 2017. **157**: p. 643-650.
64. Caballero-Díaz, E., S. Benítez-Martínez, and M. Valcárcel, *Rapid and simple nanosensor by combination of graphene quantum dots and enzymatic inhibition mechanisms*. *Sensors and Actuators B: Chemical*, 2017. **240**: p. 90-99.
65. Gopal, J., et al., *Nondestructive detection of the freshness of fruits and vegetables using gold and silver nanoparticle mediated graphene enhanced Raman spectroscopy*. *Sensors and Actuators B: Chemical*, 2016. **224**: p. 413-424.
66. Lynch, I. and K.A. Dawson, *Protein-nanoparticle interactions*. *Nano today*, 2008. **3**(1-2): p. 40-47.
67. Lundqvist, M., et al., *Nanoparticle size and surface properties determine the protein corona with possible implications for biological impacts*. *Proceedings of the National Academy of Sciences*, 2008. **105**(38): p. 14265-14270.
68. Cedervall, T., et al., *Understanding the nanoparticle–protein corona using methods to quantify exchange rates and affinities of proteins for nanoparticles*. *Proceedings of the National Academy of Sciences*, 2007. **104**(7): p. 2050-2055.
69. Espitia, P.J.P., et al., *Zinc Oxide Nanoparticles: Synthesis, Antimicrobial Activity and Food Packaging Applications*. 2012. **5**(5): p. 1447-1464.

70. Singh, A., et al., *Zinc oxide nanoparticles: a review of their biological synthesis, antimicrobial activity, uptake, translocation and biotransformation in plants*. 2018. **53**(1): p. 185-201.
71. Molina, R., et al., *Potential environmental influence of amino acids on the behavior of ZnO nanoparticles*. Chemosphere, 2011. **83**(4): p. 545-551.
72. Huang, S.-H. and D.-H. Chen, *Rapid removal of heavy metal cations and anions from aqueous solutions by an amino-functionalized magnetic nano-adsorbent*. Journal of Hazardous Materials, 2009. **163**(1): p. 174-179.
73. Krishnamurti, G., et al., *Kinetics of cadmium release from soils as influenced by organic acids: implication in cadmium availability*. Journal of Environmental Quality, 1997. **26**(1): p. 271-277.
74. Kumar, M., et al., *Plants impact structure and function of bacterial communities in Arctic soils*. Plant and soil, 2016. **399**(1-2): p. 319-332.
75. Li, Z., et al., *Comparative study of carboxylic acid adsorption on calcite: l-malic acid, d-malic acid and succinic acid*. Carbonates and Evaporites, 2018.
76. Schymura, S., et al., *Elucidating the Role of Dissolution in CeO₂ Nanoparticle Plant Uptake by Smart Radiolabeling*. Angewandte Chemie International Edition, 2017.
77. Zhang, W., et al., *Uptake and accumulation of bulk and nanosized cerium oxide particles and ionic cerium by radish (*Raphanus sativus* L.)*. Journal of agricultural and food chemistry, 2015. **63**(2): p. 382-390.
78. Zuverza-Mena, N., et al., *Exposure of engineered nanomaterials to plants: Insights into the physiological and biochemical responses-A review*. Plant Physiology and Biochemistry, 2017. **110**: p. 236-264.

79. Li, R., et al., *Exceptional arsenic adsorption performance of hydrous cerium oxide nanoparticles: Part A. Adsorption capacity and mechanism*. Chemical Engineering Journal, 2012. **185–186**: p. 127-135.
80. Li, J., et al., *Effect of CeO₂ nanomaterial surface functional groups on tissue and subcellular distribution of Ce in tomato (*Solanum lycopersicum*)*. Environmental Science: Nano, 2019.
81. Fernández-García, M., et al., *Structural characteristics and redox behavior of CeO₂–ZrO₂/Al₂O₃ supports*. Journal of Catalysis, 2000. **194**(2): p. 385-392.
82. Chai, Y., et al., *Insights into the Relationship of the Heterojunction Structure and Excellent Activity: Photo-Oxidative Coupling of Benzylamine on CeO₂-rod/g-C₃N₄ Hybrid under Mild Reaction Conditions*. ACS Sustainable Chemistry & Engineering, 2018. **6**(8): p. 10526-10535.
83. Deshpande, S., et al., *Size dependency variation in lattice parameter and valency states in nanocrystalline cerium oxide*. Applied Physics Letters, 2005. **87**(13): p. 133113.
84. Cao, C.-Y., et al., *Ceria hollow nanospheres produced by a template-free microwave-assisted hydrothermal method for heavy metal ion removal and catalysis*. The Journal of Physical Chemistry C, 2010. **114**(21): p. 9865-9870.
85. Perullini, M., S.A. Aldabe Bilmes, and M. Jobbágy, *Cerium Oxide Nanoparticles: Structure, Applications, Reactivity, and Eco-Toxicology*, in *Nanomaterials: A Danger or a Promise? A Chemical and Biological Perspective*, R. Brayner, F. Fiévet, and T. Coradin, Editors. 2013, Springer London: London. p. 307-333.
86. Abe, T., et al., *Improvement of the Photoconductive Characteristics of ZnO Single Crystals by Annealing*. 2018. **47**(8): p. 4272-4276.

87. Sharifan, H. and X.J.M.-R.i.O.C. Ma, *Potential Photochemical Interactions of UV Filter Molecules with Multichlorinated Structure of Pymnesins in Harmful Algal Bloom Events*. 2017. **14**(5): p. 391-399.
88. Rossi, L., et al., *Effects of foliar application of zinc sulfate and zinc nanoparticles in coffee (Coffea arabica L.) plants*. 2019. **135**: p. 160-166.
89. Xaba, T., et al., *SYNTHESIS OF HEXADECYLAMINE CAPPED ZnO NANOPARTICLES USING BIS (2-HYDROXY-1-NAPHTHALDEHYDATO) ZINC (II) AS A SINGLE SOURCE PRECURSOR*. 2018. **13**(1).
90. Makino, T., et al., *Room-temperature luminescence of excitons in ZnO/(Mg, Zn) O multiple quantum wells on lattice-matched substrates*. Applied Physics Letters, 2000. **77**(7): p. 975-977.
91. Wei, A., L. Pan, and W. Huang, *Recent progress in the ZnO nanostructure-based sensors*. Materials Science and Engineering: B, 2011. **176**(18): p. 1409-1421.
92. Wang, Z.L., *ZnO nanowire and nanobelt platform for nanotechnology*. Materials Science and Engineering: R: Reports, 2009. **64**(3-4): p. 33-71.
93. McNeil, S.E., *Nanotechnology for the biologist*. Journal of Leukocyte Biology, 2005. **78**(3): p. 585-594.
94. Hussain, A., et al., *Zinc oxide nanoparticles alter the wheat physiological response and reduce the cadmium uptake by plants*. Environmental Pollution, 2018. **242**: p. 1518-1526.
95. Sirelkhatim, A., et al., *Review on zinc oxide nanoparticles: antibacterial activity and toxicity mechanism*. Nano-Micro Letters, 2015. **7**(3): p. 219-242.

96. Zhang, L., et al., *Investigation into the antibacterial behaviour of suspensions of ZnO nanoparticles (ZnO nanofluids)*. Journal of Nanoparticle Research, 2007. **9**(3): p. 479-489.
97. Wang, L., et al., *Removing Escherichia coli from water using zinc oxide-coated zeolite*. Water research, 2018. **141**: p. 145-151.
98. Kaphle, A., et al., *Nanomaterials for agriculture, food and environment: applications, toxicity and regulation*. Environmental chemistry letters, 2018. **16**(1): p. 43-58.
99. Mishra, Y.K. and R. Adelung, *ZnO tetrapod materials for functional applications*. Materials Today, 2018. **21**(6): p. 631-651.
100. Scott, N.R., H. Chen, and H. Cui, *Nanotechnology applications and implications of agrochemicals toward sustainable agriculture and food systems*. 2018, ACS Publications.
101. Medina-Velo, I.A., et al., *Minimal transgenerational effect of ZnO nanomaterials on the physiology and nutrient profile of Phaseolus vulgaris*. ACS Sustainable Chemistry & Engineering, 2018.
102. Malasics, A., et al., *Simulations of calcium channel block by trivalent cations: Gd³⁺ competes with permeant ions for the selectivity filter*. Biochimica et Biophysica Acta (BBA) - Biomembranes, 2010. **1798**(11): p. 2013-2021.
103. Adding, L.C., G.L. Bannenberg, and L.E. Gustafsson, *Basic experimental studies and clinical aspects of gadolinium salts and chelates*. Cardiovascular Therapeutics, 2001. **19**(1): p. 41-56.
104. Leonard, R.T., G. Nagahashi, and W.W. Thomson, *Effect of Lanthanum on Ion Absorption in Corn Roots*. Plant Physiology, 1975. **55**(3): p. 542-546.

105. White, P.J., et al., *Genes for calcium-permeable channels in the plasma membrane of plant root cells*. *Biochimica et Biophysica Acta (BBA) - Biomembranes*, 2002. **1564**(2): p. 299-309.
106. Rahwan, R.G., D.T. Witiak, and W.W. Muir, *Chapter 23. Calcium Antagonists*. *Annual Reports in Medicinal Chemistry*, 1981. **16**: p. 257-268.
107. Bouron, A., K. Kiselyov, and J. Oberwinkler, *Permeation, regulation and control of expression of TRP channels by trace metal ions*. *Pflügers Archiv - European Journal of Physiology*, 2015. **467**(6): p. 1143-1164.
108. Liu, D., et al., *Effects of lanthanum on the change of calcium level in the root cells of rice*. *Communications in soil science and plant analysis*, 2012. **43**(15): p. 1994-2003.
109. Fry, D.W., J.C. White, and I.D. Goldman, *Effects of 2, 4-dinitrophenol and other metabolic inhibitors on the bidirectional carrier fluxes, net transport, and intracellular binding of methotrexate in Ehrlich ascites tumor cells*. *Cancer research*, 1980. **40**(10): p. 3669-3673.
110. Grundlingh, J., et al., *2, 4-dinitrophenol (DNP): a weight loss agent with significant acute toxicity and risk of death*. *Journal of Medical Toxicology*, 2011. **7**(3): p. 205-212.
111. Loughman, B.C., *METABOLIC PROCESSES IN ROOTS RELATED TO ABSORPTION AND TRANSPORT OF PHOSPHATE A2 - SUNDERLAND, N*, in *Botany*. 1976, Pergamon. p. 423-431.
112. Votrubová-Vaňousová, O., *The effect of 2,4-dinitrophenol on the absorption and translocation of calcium by pumpkin plants*. *Biologia Plantarum*, 1977. **19**(3): p. 166-172.

113. Liu, D., M. Pitta, and M.P. Mattson, *Preventing NAD⁺ depletion protects neurons against excitotoxicity: bioenergetic effects of mild mitochondrial uncoupling and caloric restriction*. Annals of the New York Academy of Sciences, 2008. **1147**(1): p. 275-282.
114. Oksvold, M.P., et al., *Effect of cycloheximide on epidermal growth factor receptor trafficking and signaling*. FEBS Letters, 2012. **586**(20): p. 3575-3581.
115. Voicu, M. and J. Zwiazek, *Cycloheximide inhibits root water flow and stomatal conductance in aspen (*Populus tremuloides*) seedlings*. Plant, Cell & Environment, 2004. **27**(2): p. 199-208.
116. Rossi, L., et al., *Effects of foliar application of zinc sulfate and zinc nanoparticles in coffee (*Coffea arabica* L.) plants*. Plant Physiology and Biochemistry, 2019. **135**: p. 160-166.
117. Rossi, L., et al., *Uptake, Accumulation, and in Planta Distribution of Coexisting Cerium Oxide Nanoparticles and Cadmium in Glycine max (L.) Merr.* Environmental science & technology, 2017. **51**(21): p. 12815-12824.
118. Donovan, A.R., et al., *Detection of zinc oxide and cerium dioxide nanoparticles during drinking water treatment by rapid single particle ICP-MS methods*. Analytical and bioanalytical chemistry, 2016. **408**(19): p. 5137-5145.
119. Londono, N., et al., *Impact of TiO₂ and ZnO nanoparticles on an aquatic microbial community: effect at environmentally relevant concentrations*. Nanotoxicology, 2017. **11**(9-10): p. 1140-1156.
120. Oliveira, J.L.d., et al., *Zein nanoparticles as eco-friendly carrier systems for botanical repellents aiming sustainable agriculture*. Journal of agricultural and food chemistry, 2018. **66**(6): p. 1330-1340.

121. Ma, X. and J. Yan, *Plant uptake and accumulation of engineered metallic nanoparticles from lab to field conditions*. Current Opinion in Environmental Science & Health, 2018.
122. Meesters, J.A., et al., *Multimedia environmental fate and speciation of engineered nanoparticles: a probabilistic modeling approach*. Environmental Science: Nano, 2016. **3**(4): p. 715-727.
123. Liu, R. and R. Lal, *Potentials of engineered nanoparticles as fertilizers for increasing agronomic productions*. Science of the total environment, 2015. **514**: p. 131-139.
124. Dan, Y., et al., *Characterization of gold nanoparticle uptake by tomato plants using enzymatic extraction followed by single-particle inductively coupled plasma–mass spectrometry analysis*. Environmental science & technology, 2015. **49**(5): p. 3007-3014.
125. Zhao, L., et al., *Effect of surface coating and organic matter on the uptake of CeO₂ NPs by corn plants grown in soil: Insight into the uptake mechanism*. Journal of hazardous materials, 2012. **225**: p. 131-138.
126. Ma, C., et al., *Uptake of Engineered Nanoparticles by Food Crops: Characterization, Mechanisms, and Implications*. Annual review of food science and technology, 2018. **9**: p. 129-153.
127. Sharifan, H., et al., *Investigation on the Modification of Physicochemical Properties of Cerium Oxide Nanoparticles through Adsorption of Cd and As (III)/As (V)*. ACS Sustainable Chemistry & Engineering, 2018. **6**(10): p. 13454-13461.
128. Shang, L., K. Nienhaus, and G.U. Nienhaus, *Engineered nanoparticles interacting with cells: size matters*. Journal of nanobiotechnology, 2014. **12**(1): p. 5.

129. Rossi, L., et al., *Mutual effects and in planta accumulation of co-existing cerium oxide nanoparticles and cadmium in hydroponically grown soybean (Glycine max (L.) Merr.)*. Environmental Science: Nano, 2018. **5**(1): p. 150-157.
130. Yang, Y., et al., *Phosphate deprivation decreases cadmium (Cd) uptake but enhances sensitivity to Cd by increasing iron (Fe) uptake and inhibiting phytochelatin synthesis in rice (Oryza sativa)*. Acta physiologiae plantarum, 2016. **38**(1): p. 28.
131. Williams, C. and D. David, *The accumulation in soil of cadmium residues from phosphate fertilizers and their effect on the cadmium content of plants*. Soil Science, 1976. **121**(2): p. 86-93.
132. Singh, S., et al., *A phosphate-dependent shift in redox state of cerium oxide nanoparticles and its effects on catalytic properties*. Biomaterials, 2011. **32**(28): p. 6745-6753.
133. Wang, G., et al., *Influence of phosphate on phytotoxicity of ceria nanoparticles in an agar medium*. Environmental Pollution, 2017. **224**: p. 392-399.
134. Ren, X., et al., *New insight into GO, cadmium (II), phosphate interaction and its role in GO colloidal behavior*. Environmental science & technology, 2016. **50**(17): p. 9361-9369.
135. Wang, H., et al., *Foliar application of Zn can reduce Cd concentrations in rice (Oryza sativa L.) under field conditions*. Environmental Science and Pollution Research, 2018. **25**(29): p. 29287-29294.
136. López-Cervantes, J. and D.I. Sánchez-Machado, *Astaxanthin, Lutein, and Zeaxanthin*, in *Nonvitamin and Nonmineral Nutritional Supplements*. 2019, Elsevier. p. 19-25.
137. Venu, S., et al., *Phytochemical Profile and Therapeutic Properties of Leafy Vegetables*, in *Plant and Human Health, Volume 2*. 2019, Springer. p. 627-660.

138. Gui, X., et al., *Fate and phytotoxicity of CeO₂ nanoparticles on lettuce cultured in the potting soil environment*. PloS one, 2015. **10**(8): p. e0134261.
139. da Cruz, T.N., et al., *Shedding light on the mechanisms of absorption and transport of ZnO nanoparticles by plants via in vivo X-ray spectroscopy*. Environmental Science: Nano, 2017. **4**(12): p. 2367-2376.

CHAPTER II

INVESTIGATION ON THE PLANT ROOT EXUDATE EFFECTS ON THE MODIFICATION OF PHYSICOCHEMICAL PROPERTIES OF CERIUM OXIDE NANOPARTICLES THROUGH ADSORPTION OF CD AND AS(III)/AS(V)¹

2.1. Summary

Contamination of agricultural soils by cadmium (Cd) and arsenic (As) has caused many concerns on the production of safe food crops. Rapid development and application of nanotechnology in the recent decade raise new concerns on the accumulation of emerging nanoparticles in crop tissues. Evidence has also been reported that in the co-presence of heavy metals and engineered nanoparticles (ENPs), plant uptake of these chemicals are mutually affected by each other. Adsorption of heavy metal ions on the surface of ENPs has been identified as an important mechanism for the altered plant metal uptake by ENPs. However, quantitative information on the extent of adsorption in the environmentally relevant conditions such as in the presence of root exudates has not been reported. Information is also lacking on how the interaction of ENPs and various heavy metals through adsorption may alter the physicochemical properties of ENPs, and consequently change the plant uptake of these ENPs. This study investigated the adsorption of Cd and As(III)/As(V) onto 100 mg L⁻¹ cerium oxide nanoparticles (CeO₂NPs) both in the presence and absence of synthetic root exudates (SRE). The results indicated that both As and Cd displayed strong adsorption on CeO₂NPs, and the presence of SRE reduced the adsorption for both metals,

¹ Reprinted with permission from (1. Sharifan, H.; Wang, X.; Guo, B.; Ma, X., Investigation on the Modification of Physicochemical Properties of Cerium Oxide Nanoparticles through Adsorption of Cd and As(III)/As(V). *ACS Sustainable Chemistry & Engineering* **2018**, *6*, (10), 13454-13461.). Copyright (2018) American Chemical Society."

but to different extents. Importantly, the interactions of heavy metal ions with CeO₂NPs significantly changed the physicochemical properties of CeO₂NPs including their zeta potential and size distribution. Different effects on CeO₂NPs properties were noticed for Cd and As at different oxidation states. The results shed new lights on the reciprocal effect of CeO₂NPs and these two metals on their plant uptake and accumulation.

2.2. Introduction

Heavy metals are ubiquitous in the environment and their concentrations in agricultural soils are steadily increasing because of their excessive uses in industries. Arsenic (As) and cadmium (Cd) are of high concern due to their carcinogenic and mutagenic effects ². As and Cd are listed as the first and fourth most problematic substances on the 2013 Priority List of Hazardous Substances developed by the U.S. Agency for Toxic Substances and Disease Registry (ATSDR), (<http://www.atsdr.cdc.gov/spl>). The background Cd in U.S soil is in the range of 0.1 to 0.5 mg/kg in most cases, increased by 43% in the past century due to various industrial activities (*e.g.*, plastic manufacturing, mining, paint pigments, production of household appliances, automobiles and fungicides). The background concentration of As in soil ranges from 0.4-40 mg/kg, with an average concentration of >10 mg/kg in many agricultural soils ³. Both chemicals can be easily accumulated in edible tissues of plants, exposing humans to them through diet ². Prolonged exposure to these chemicals has been shown to be damaging to human health.

Nanotechnology is a rapidly growing industry and its contribution to the global economy was estimated to be \$3 trillion in 2015 ⁴. Nanotechnology is used in a wide variety of industries including water and wastewater treatment, agriculture, medicine, and manufacturing. In the agricultural sector, ENPs have been incorporated into fertilizers, nanosensors and pathogen combating formulas, and directly applied to crop plants throughout the world ^{5,6}. In addition, the

rapid development of nanotechnology has resulted in significant unintentional releases of ENPs into the environment, with agricultural soil as a primary sink due to water irrigation and biosolid land application ^{7,8}. Cerium oxide nanoparticles (CeO₂NPs) is a widely used metallic ENPs in a wide range of industries and holds great potential as an agrichemical stimulator to enhance plant's capacity to fight against various abiotic stresses such as salt stress ⁹. Consequently, the accumulation of CeO₂NPs in agricultural soils is highly expected and numerous studies have been conducted to evaluate the physiological and biochemical impact of CeO₂NPs on plants from bench scale hydroponic studies to large-scale field conditions ¹⁰⁻¹². These studies have demonstrated strong impact of CeO₂NPs on plant physiology such as plant net photosynthesis rate and plant root anatomy. The previous studies also demonstrated the uptake and accumulation of elemental Ce in plant tissues through both direct uptake of CeO₂NPs and their dissolved ions ^{7,13}.

In addition to the direct impact of CeO₂NPs on plants, an emerging topic concerning the CeO₂NPs plant interactions is to understand the impact of CeO₂NPs on the fate and transport of co-existing environmental pollutants ^{14,15}. Some studies have shown that CeO₂NPs can alter the plant uptake and accumulation of several freshly added or historic pesticides in soil ¹⁶⁻¹⁸. The extent of impact depends on both the physiochemical properties of the pesticides and the plant species. Recently, we showed that CeO₂NPs can modify the plant uptake and accumulation of co-existing Cd in both hydroponic and soil systems ^{10,19}. Several mechanisms have been identified for the altered Cd uptake and accumulation by CeO₂NPs including the adsorption of Cd on CeO₂NPs to form Cd-CeO₂NPs complexes, the altered excretion of root exudates and plant root anatomical structure changes in the co-presence of Cd and CeO₂NPs¹⁰. Even though the adsorption of Cd on CeO₂NPs has been identified as an important mechanism, quantitative information on the extent of adsorption of Cd on CeO₂NPs is lacking. Similarly, As is another concerning heavy metal in soil

and water and evidence has shown that As has high adsorption capacity on ENPs at both oxidation states, including CeO₂NPs, but quantitative information on the adsorption of As on CeO₂NPs in typical plant growing conditions is not available²⁰. It is well recognized that the environment in the root region is very different from the most test systems (e.g. in DI water) used to quantify the adsorption of As and other heavy metals on CeO₂NPs. For instance, there are a high amount of organic acids in the root region excreted from plant roots and these compounds could have a significant impact on the adsorption process. Studies on the adsorption of Cd and As on CeO₂NPs in an environment relevant for plant growth is critical to obtain accurate information on the impact of ENPs on the fate and plant uptake of co-occurring heavy metal ions.

One interesting phenomenon we have noticed in our previous studies with the co-existing CeO₂NPs and Cd was that the alteration of plant uptake and accumulation of these chemicals was mutual. We have investigated the plant root physiology in the co-presence of Cd and CeO₂NPs and partially explained the altered plant uptake of CeO₂NPs from that perspective^{10,20}, however, possibilities exist that the co-present Cd or As may modify the physiochemical properties of CeO₂NPs, leading to a different plant uptake and accumulation of Ce. Such possibility has not been explored in the literature. The objectives of this study therefore were: (1) to determine the adsorption of Cd and As on CeO₂NPs, both in the presence and absence of a synthetic root exudate (SRE) and (2) to evaluate the potential impact of Cd and As on the physiological and chemical properties of CeO₂NPs. Both As(III) and As(V) were investigated in this study due to the broad presence of these two oxidation states for As and their different fate and toxicity to plants.

2.2. Materials and Methods

2.2.1. Reagents

CeO₂NPs coated with polyvinylpyrrolidone (PVP) was purchased from the US Research Nanomaterials, Inc. (Houston, TX) and was extensively characterized through our previous studies^{10,21}. The average size of the primary nanoparticles fell in the range of 30-50 nm, with a dominant hydrodynamic size of 210.1 ±4.6 nm in DI water at 100 mg L⁻¹. The nanoparticles are primarily spherical and have a zeta potential of -51.8 mV at pH 7. Cd sulfate (CdSO₄) was obtained from Fisher Scientific Inc. (Pittsburgh, PA). High purity As (V) (Na₂HAsO₄·7H₂O >98%) and As (III) (NaAsO₂ >99%), was purchased from Sigma Aldrich (St. Louis, MO) and Lab Chem, (Zelienople, PA) respectively. D-Glucose was purchased from Fisher Scientific, the succinic acid and L-malic acid (>99%) were bought from Acros Organics (Fair Lawn, NJ) and D-serine (>99%) from Alfa Aesar (Lancashire, UK).

2.2.2. Synthetic root exudates (SRE) preparation

SRE, consisting of L-malic acid (25 mM), D-glucose (50 mM), succinic acid (25 mM), and D-serine (12.5 mM), was prepared according to a published recipe^{13,22}. Different amounts of those four chemicals were added to a liter of sterilized DI water and stirred vigorously at room temperature with a plastic-coated magnetic bar for 2 hours until they were fully dissolved. To minimize the oxidation of As (III), the SRE was prepared using boiled water for As (III) treatments.

2.2.3. Adsorption of Cd and As on CeO₂NPs without synthetic root exudates

CeO₂NPs solution was freshly prepared at a concentration of 100 mg L⁻¹ in sterilized ultra-pure water (18.3 MΩ). CdSO₄ and both forms of arsenic were dissolved in a solution containing 100 mg L⁻¹ of CeO₂ to obtain eight final elemental concentrations of Cd or As (III/V) (0, 0.2, 0.5, 1,

1.5, 3, 4, 5 mg L⁻¹). To minimize the oxidation of As (III), the deionized water (DI) was boiled in a beaker for two hours to remove the dissolved oxygen. Immediately after boiling, the beaker was covered with a glass lid and was allowed to cool down to room temperature before As (III) was added at the above-mentioned concentrations. The prepared solutions (30 mL) containing different concentrations of Cd or As and 100 mg L⁻¹ of CeO₂NPs were transferred to 50 mL centrifuge tubes and each treatment had three replicates. The tubes were shaken at 180 rpm on a shaking table for 48 h at 25 °C (New Brunswick Scientific, Edison, NJ), adequate for the system to reach equilibrium^{23,24}. Afterward, the pH of the solution was measured with a pH probe. To separate the remaining dissolved metal ions from the ions adsorbed onto CeO₂NPs, 10 mL of the solution was centrifuged (7000 x g) for 45 minutes with a syringe centrifuge (NMWL = 3 kDa, Merck Millipore) and the concentrations of heavy metals in the filtrate was considered as the un-adsorbed heavy metal ions and were determined by an Inductively Coupled Plasma Mass Spectrometry (ICP-MS). Briefly, 2 mL of each filtrate was diluted with 10 mL of 1% nitric acid in a 15 mL centrifuge tube first. The diluted solutions were directly introduced to ICP-MS (Perkin Elmer mod. DRCII, Waltham, MA) for the quantification of Cd and As as well as the dissolved Ce ion. The adsorbed heavy metals on CeO₂NPs (q_e) were calculated based on the mass balance as follows:

$$q_e = \frac{(C_0 - C_e)V}{m}$$

Where C_e is the concentration of Cd or As(III)/As(V) in solution (mg L⁻¹) at equilibrium, C_0 is the initial concentration of the heavy metal ions; V is the volume of the solution (30 mL), and m is the mass of CeO₂NPs, (100 mg L⁻¹ x 30 mL). The adsorption data were fitted with the Freundlich model as shown below:

$$q_e = K_f C_e^{1/n}$$

Where, $K_f (\text{mg g}^{-1})(\text{L g}^{-1})^n$ indicates the adsorption affinity and capacity and, $1/n$ refers to the Freundlich exponential coefficient.

2.2.4. Adsorption of Cd and As on CeO₂NPs with synthetic root exudates

The experimental setup was similar to what was described above without SRE. The major difference was that the SRE compounds were dissolved into the sterilized water before adding the heavy metal ions and CeO₂NPs. In order to further investigate mechanisms for the impact of root exudates on the adsorption of heavy metals on CeO₂NPs, two additional experiments were carried out with Cd. In the first treatment, SRE was first mixed with 4 mg L⁻¹ of Cd in a 50 mL centrifuge tube for 48 hours, and then 100 mg L⁻¹ CeO₂NPs was added to the mixture and the total mixture was shaken for additional 48 hours. In the second experiment, 100 mg L⁻¹ of CeO₂NPs was first mixed with SRE for 48 hours. Then 4 mg L⁻¹ of Cd was added to the mixture and shaken for another 48 hours.

2.2.5. Analysis of the particle size distribution and zeta potential changes after adsorption

At the end of the adsorption, 2 mL of solution from each sample was transferred to a 4.5 mL polystyrene cuvette with 10 mm optical path length (Fisher Scientific, USA) and the hydrodynamic size and zeta potential of CeO₂NPs were analyzed using a DelsaNano C, (Beckman Coulter Inc., Miami, FL). The hydrodynamic particle size distribution for each sample was determined through two 5-min sequences and the reported values were the average of five continuous measurements. Part of the solutions was also examined under a transmission electron microscope (TEM) (JEOL JEM-1200EX, JEOL Ltd., Tokyo, Japan).

Zeta potential of CeO₂NPs was measured with the same instrument. Solutions containing 100 mg L⁻¹ of CeO₂NPs and different concentrations of As or Cd were analyzed using a glass cell with the

optical surface of 1 mm at the scattering angle of $\theta = 90^\circ$ (633 nm) for 15 min to determine the zeta potential of CeO₂NPs. Three replicates were measured for each treatment.

2.2.6. Statistical analysis

All results were subjected to analysis of variance, means and standard deviation. One-way ANOVA was performed and means separation between treatments was obtained by the Tukey's post-hoc test. Data were analyzed using the Minitab 18 Statistical Software (Minitab Inc., State College, PA).

2.3. Results

2.3.1. Adsorption of cadmium on CeO₂NPs

Cd adsorption isotherms in the presence and absence of SRE are shown in **Figure 2.1**. Cd²⁺ displayed strong adsorption onto CeO₂NPs in the absence of synthetic root exudates. The presence of SRE significantly reduced the adsorption of Cd²⁺. For instance, the K_f values from the Freundlich model fitting dropped from 0.082 to 0.015 after SRE was included in the system.

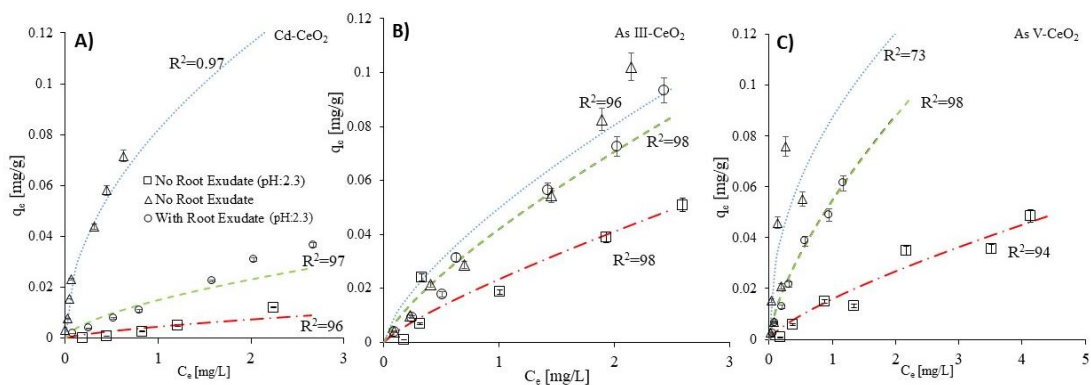


Fig. 2.1. The adsorption isotherms of A) Cd, B) As (III) and C) As (V) onto CeO₂NPs. q_e (mg g⁻¹) is the amount of Cd or As adsorbed per unit weight of CeO₂NPs at equilibrium, and C_e (mg L⁻¹)

is the adsorbate concentration in solution at equilibrium. Error bars indicate standard deviation ($n = 3$). Data points with no error bars designate very small error bars. Dotted lines indicate Freundlich isotherm fittings.

2.3.2. Impact of Cd adsorption on the physicochemical properties of cerium oxide nanoparticles

Figure 2.2 shows the dissolution of CeO_2NPs in the presence of Cd with and without SRE after 48 hours of mixing. As indicated, Cd alone did not affect the dissolution of CeO_2NPs . However, the mixture with both Cd and SRE significantly increased the dissolution of CeO_2NPs ($p < 0.05$).

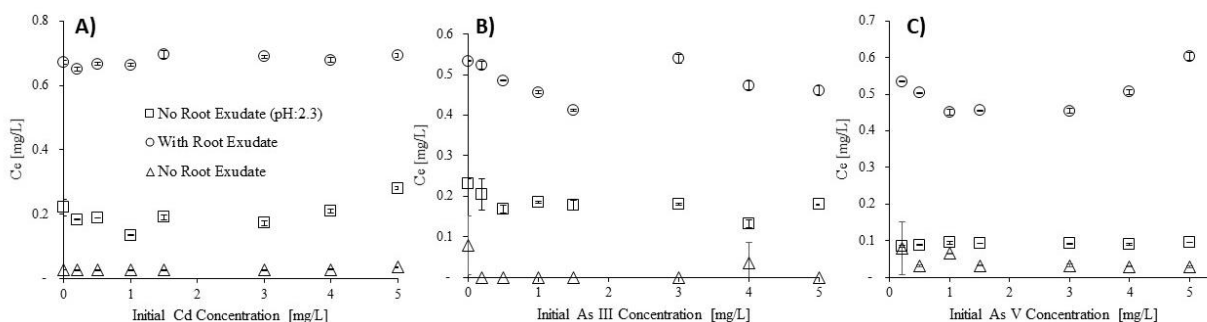


Fig. 2.2. Average concentrations of Ce^{3+} (mg L^{-1}) in solution after CeO_2NPs were mixed with A) Cd B) As (III) and C) As (V), alone or in combination with the synthetic root exudates (SRE). The concentration level in both scenarios (with and without SRE) were statistically meaningful ($p < 0.05$).

Both Cd and SRE significantly modified the zeta potential of CeO_2NPs , Figure 2.3. In the absence of SRE, the zeta potential of CeO_2NPs increased from -45 mV to about -5 mV when the Cd concentration increased from 0 to 5 mg L^{-1} . SRE alone drastically increased the zeta potential of CeO_2NPs from -45 mV to $+20$ mV. The zeta potential of CeO_2NPs became less positive with the

increase of Cd concentration in the presence of SRE. The solution pH was not significantly affected by Cd and the addition of SRE significantly lowered the pH from 5-6.0 to 1.9-2.5.

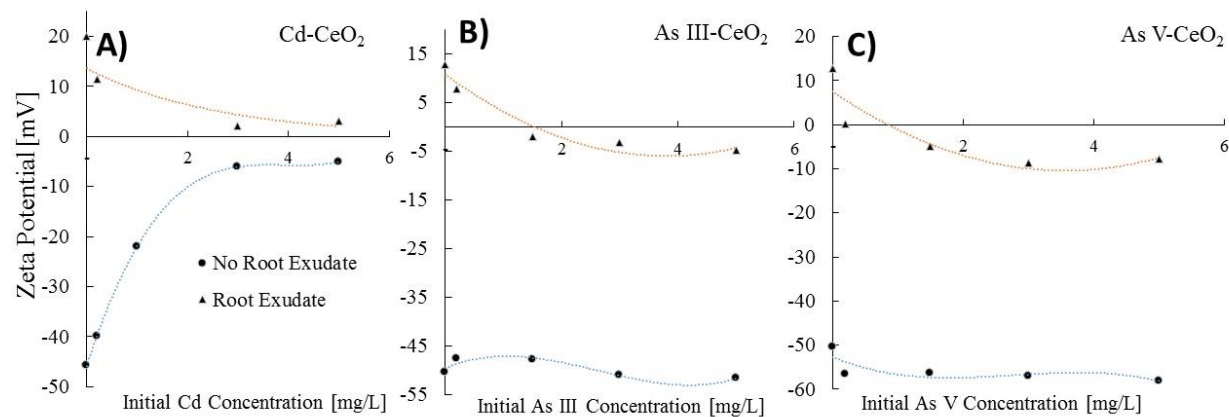


Fig. 2.3. Zeta potential of CeO₂NPs as a function of the adsorbate doses in the presence and absence of SRE. Reported values are the average of three replicates with A) Cd B) As (III) and C) As (V) alone or in combination with the synthetic root exudates (SRE).

Figure 2.4 illustrates the mean hydrodynamic diameter of CeO₂NPs after equilibrium. Without SRE, Cd increased the hydrodynamic size of some CeO₂NPs as indicated by the fractions of larger CeO₂NPs in solutions with the increase of Cd. However, the predominant sizes of CeO₂NPs remained unchanged by Cd. In contrast, SRE drastically increased the hydrodynamic size of CeO₂NPs, Figure 2.5. The results indicated that SRE led to the formation of two dominant size groups of CeO₂NPs (100-2000 nm) and (46-100 μm). The appearance of multiple peaks with varying sizes did not correlate with the concentration of Cd, suggesting that SRE is the dominant factor leading to the aggregation of CeO₂NPs.

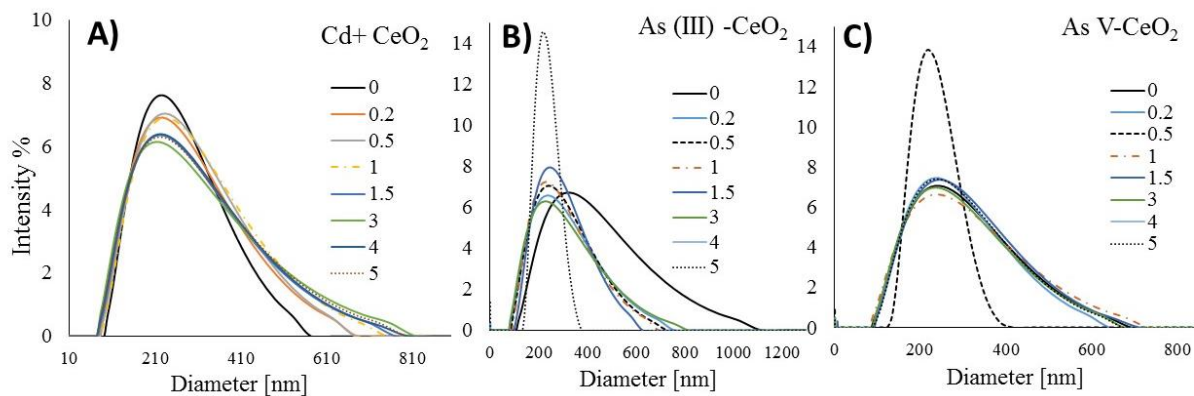


Fig. 2.4. Distribution of the hydrodynamic sizes of CeO₂NPs after exposure to different concentrations of A) Cd; B) As (III) and C) As (V) in DI water. The reported curves are representative of three replicates at each concentration.

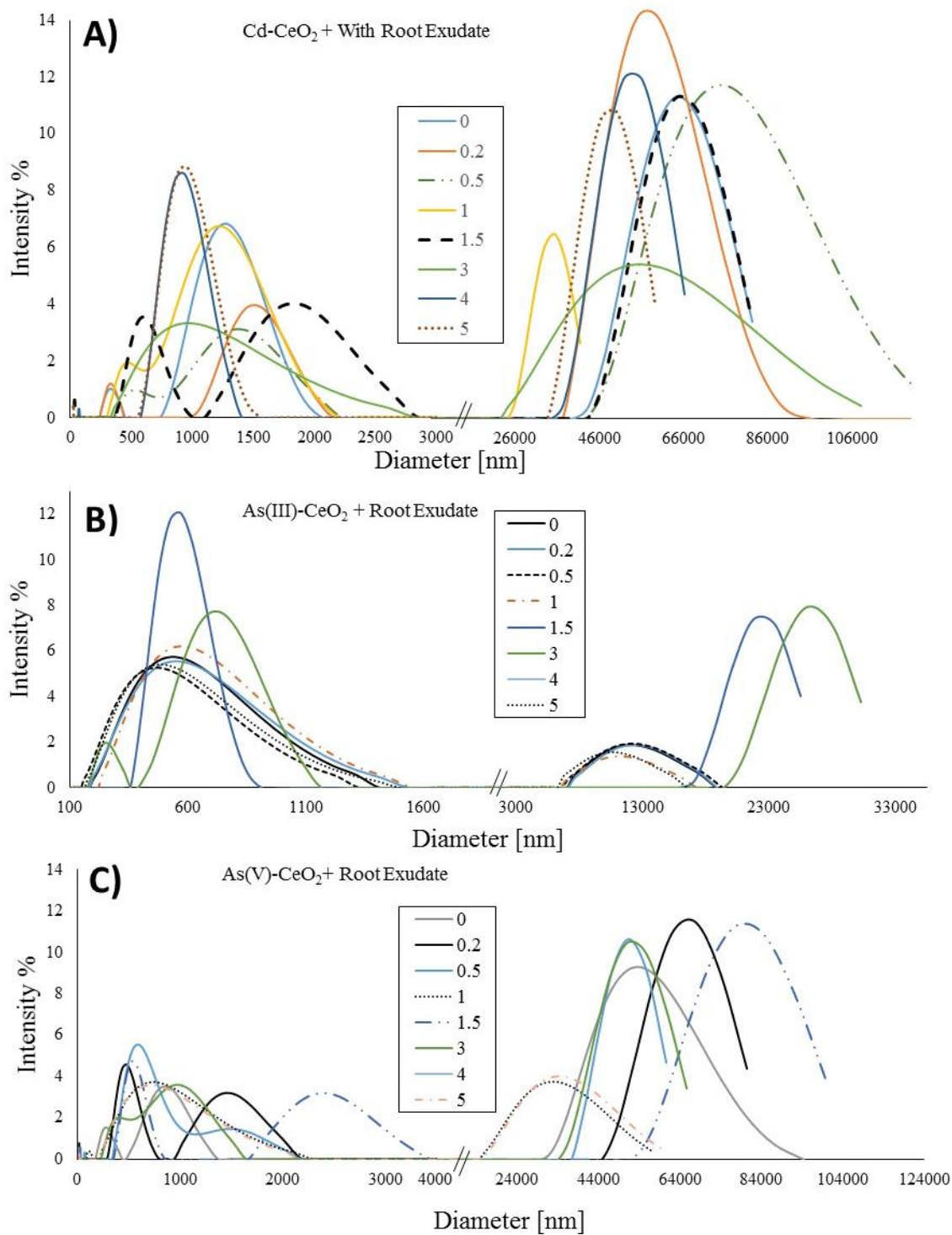


Fig. 2.5. Distribution of the hydrodynamic sizes of CeO₂NPs after exposure to A) Cd; B) As (III) and C) As (V) concurrently with SRE. The reported curves are representative of three replicates at each concentration.

2.3.3. Adsorption of Arsenic on CeO₂NPs

As shown in Figure 2.1, both As (III) and As (V) exhibited strong adsorption on CeO₂NPs without SRE and the adsorption was greater for As (III) than As (V). As observed for Cd, the presence of SRE reduced the adsorption of both As (III) and As (V), but to a less extent compared to its impact on Cd adsorption. In particular, the impact of SRE on the adsorption of As (III) on CeO₂NPs was minimal. For instance, the K_f from Freundlich fitting was 0.049 and 0.042 respectively for As (III) in the absence and presence of SRE. Other fitting parameters for As(III), As(V) and Cd are summarized in the Table 2.1.

Table. 2.1. Freundlich isotherm fitting parameters for the adsorption of Cd and As (III)/As(V) onto cerium oxide nanoparticles (CeO₂NPs) with and without presence of SRE.

Adsorbent	CeO ₂ NPs								
Adsorbate	Cd			As (III)			As (V)		
	No SRE	With SRE	No SRE	No SRE	With SRE	No SRE	No SRE	With SRE	No SRE
PH	5.9	2.3	2.3	5.9	2.3	2.3	5.9	2.3	2.3
K [mg g ⁻¹ (L mg ⁻¹) ⁻¹]	0.082	0.015	0.0045	0.049	0.042	0.0165	0.08	0.05	0.016
1/n	0.5	0.62	0.68	0.69	0.75	0.77	0.33	0.68	0.75
R ²	0.97	0.97	0.96	0.96	0.98	0.98	0.73	0.98	0.94

2.3.4. Impact of Arsenic adsorption on the physiochemical properties of CeO₂NPs

Figure 2.2 illustrates the concentrations of dissolved Ce from CeO₂NPs after 48h of mixing with different concentrations of As (III) and As (V). Without SRE, As (III) appeared to completely stop the dissolution of Ce³⁺ from the nanoparticle surfaces while As (V) displayed minimal effect on Ce dissolution. In the presence of SRE, Ce dissolution was significantly increased to a level similar to what was observed in the mixture with Cd and SRE, suggesting that enhanced dissolution of CeO₂NPs was primarily attributed to the presence of SRE.

As observed in the Cd study, SRE drastically changed the zeta potential of CeO₂NPs from around -50 mV to about +13 mV and the adsorption of As gradually reduced the zeta potential to the negative territory with increasing As concentration, Figure 2.3. However, the As alone at both oxidation states did not markedly change the zeta potential of CeO₂NPs. The zeta potential of CeO₂NPs was around -45 to -50 mV and -47 to -57 mV in the presence of up to 5 mg/L of As(III) and As(V) respectively.

The hydrodynamic size distributions of 100 mg L⁻¹ of CeO₂NPs at equilibrium with different concentrations of As (III) and As (V) are presented in Figures 2.4 and 2.5. The average hydrodynamic size of CeO₂NPs was about 233±10 nm after contact with As (V) or As (III) for 48 hours without SRE. Interestingly, unlike the impact of Cd which increased the fractions of larger CeO₂NPs, both As (III) and As (V) appeared to reduce the hydrodynamic sizes of CeO₂NPs even though the predominant sizes were similar at different concentrations of As. The observation was particularly obvious at the highest concentration of As (III) and As (V). No specific correlation was observed between the increasing doses of As and the hydrodynamic size of CeO₂NPs.

In agreement with the study with Cd, the presence of SRE significantly increased the hydrodynamic size of CeO₂NPs. However, the impact of SRE seemed to be far greater in the presence of As (V) than As (III). For example, while SRE led to larger aggregates in both cases, the size of larger aggregates in the presence of As (V) was about five times bigger than that in the presence of As (III). In addition, the large CeO₂NPs aggregates accounted for a smaller fraction of the total CeO₂NPs in the mixture with As (III) than As (V).

2.4. Discussion

As expected, both Cd and As displayed strong adsorption on the surface of CeO₂NPs and this can be a significant mechanism affecting the plant uptake of heavy metals in their co-presence with CeO₂NPs. Plant root exudates is a considerable factor in the interactions of Cd and As with CeO₂NPs and generally reduced their adsorption on CeO₂NPs. The reduction is particularly significant for Cd, and to a less extent to As (V). To gain more insights into the effects of root exudates on the adsorption of Cd, two hypotheses were formulated: one is that in the mixture of SRE and Cd, SRE occupied most of the available spaces for Cd adsorption and the other one is that Cd and SRE form complexes and the complexes had lower adsorption affinity and capacity to CeO₂NPs surfaces. Based on our results shown in Figure 2.6, the Cd and SRE complexes (if they were formed) showed similar adsorption capacity on CeO₂NPs, hence the second hypothesis was not correct. But when we mixed the SRE with CeO₂NPs first, the adsorption of Cd was drastically reduced, suggesting that the first hypothesis is more plausible.

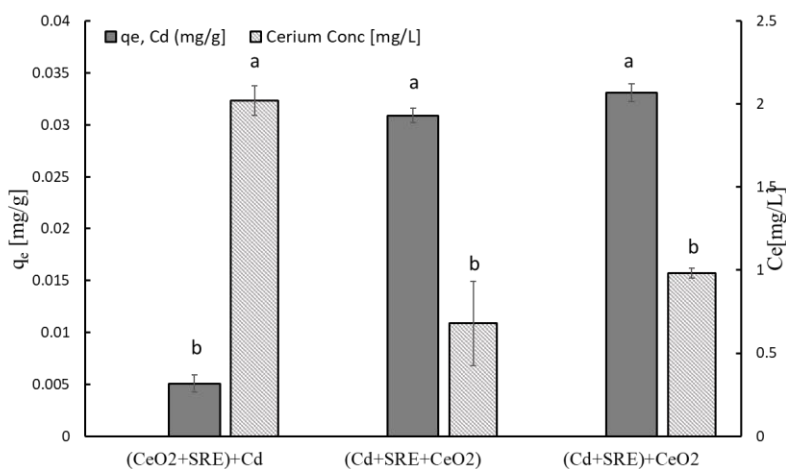


Fig. 2.6. Liquid concentration of Ce^{3+} ($mg L^{-1}$) and solid concentration of Cd on CeO_2 NPs in three different treatments with an initial concentration of $4 mg L^{-1}$ of Cd; $(CeO_2+SRE)+Cd$ refers to the treatment that CeO_2 NPs were first mixed with SRE for 48 hours before the introduction of Cd; $(Cd+SRE)+ CeO_2$ NPs refers to the treatment that Cd and SRE were first mixed for 48 hours before the addition of CeO_2 NPs; $(Cd+SRE+CeO_2)$ indicates that the three components were mixed simultaneously. Error bars represent standard deviation ($n = 3$). Different letters indicate significant differences between treatments ($p < 0.05$).

In addition to these two hypotheses, the reduced accessibility of adsorption sites by Cd due to the aggregation of CeO_2 NPs in the presence of SRE may contribute to the lower Cd adsorption on CeO_2 NPs. However, the aggregation of CeO_2 NPs was greater for both As species and the effect of SRE on their adsorption on CeO_2 NPs was weaker, implying that lower accessibility of adsorption sites was not a dominant reason for the reduced Cd adsorption.

For the adsorption of As, two observations stood out as particularly interesting. One is the much weaker effect of SRE on the adsorption of As compared to Cd, in particular the adsorption of As

(III) on CeO₂NPs, indicating that the effects of SRE on As and Cd adsorption might be different. This weaker effect of SRE on As may be ascribed to the chemistry of As. Unlike Cd, As did not exist as free-standing cations, instead, As (III) was predominantly in the form H₃AsO₃ (pK_a = 9.17) and As (V) a mixture of H₃AsO₄ (pK_{a1} = 2.20) and H₂AsO₄⁻ in this study. It is likely that the adsorption of neutral As(III) and part of the neutral As (V) occupied different adsorption sites from the charged ions of SRE, therefore competition was weak between the neutral molecules and SRE molecules. In the SRE mixture, the NH₂ functional group in D-serine molecule would be protonated to carry a positive charge at pH 1.9-2.5, which might attract the negatively charged H₂AsO₄⁻ and reduce its adsorption to CeO₂NPs. They would have minimum effect on the adsorption of H₃AsO₃. The second interesting observation was the stronger adsorption of As (III) on CeO₂NPs than As (V). The general consensus about the fate of As species in the environment is that As (III) is more mobile and bioavailable than As (V) based on their adsorption to iron hydroxides minerals^{25, 26}, however, such conclusion may not hold true in the presence of ENPs, depending on whether ENPs loaded with As are more bioavailable to plants or not. If the ENPs loaded with As are less bioavailable to plant uptake, then As associated with these ENPs would also be retained in the root region, without being taken up by plants. In this scenario, the stronger adsorption of As (III) on ENPs may make it less bioavailable than As (V). Therefore, the availability of these heavy metal ions in the presence of emerging ENPs needs more detailed evaluation.

A key finding of this study was that not only the fate of heavy metal ions was affected by CeO₂NPs, co-existing heavy metal ions could also modify the key properties of CeO₂NPs. In this study, three aspects of the physicochemical properties of CeO₂NPs were closely examined, including their size distribution, zeta potential and the dissolution rate. Dissolution of Ce³⁺ from CeO₂NPs was mostly

unaffected by Cd and As (V) and was reduced by As (III), possibly because the adsorption of neutral H_3AsO_3 blocked some sites for dissolution. SRE alone markedly increased the dissolution rate of Ce^{3+} because once SRE was complexed with Cd, they did not affect CeO_2NPs dissolution, Figure 2.6. The enhanced dissolution was attributed to the redox reactions between low molecular weight acids in SRE mixture with CeO_2NPs in a previous study and our results agree with that conclusion.

Surprisingly, the zeta potential of CeO_2NPs was significantly changed by either SRE or Cd, but not by As species. We attribute the SRE effect to the adsorption of NH_2 -containing molecules on the surface of CeO_2NPs , because at acidic condition, these molecules carry a positive charge and their adsorption to the negatively charged CeO_2NPs neutralized the surface charge and bestowed the surface some positive charge, leading to a positive zeta potential. For Cd^{2+} , similar reasoning can be made. For example, Cd^{2+} may bind to the $=\text{Ce}-\text{O}^-$ group on CeO_2NP surface to form $=\text{Ce}-\text{O}-\text{Cd}^+$ complexes or form a claw structure with two of the surface groups as $=(\text{Ce}-\text{O})_2-\text{Cd}$ ^{27, 28}. Consequently, the adsorption of Cd^{2+} on CeO_2NPs steadily increased the zeta potential of CeO_2NPs , but the modified zeta potentials were both in the unstable range ($-30 \text{ mV} < \text{zeta potential} < 30 \text{ mV}$). Neutral H_3AsO_3 or H_3AsO_4 were not expected to significantly change the zeta potential of CeO_2NPs , consistent with what was observed in our study.

The zeta potential of CeO_2NPs play a significant role in nanoparticle aggregation and as shown in Figure 2.5, CeO_2NPs aggregated to a great extent in the presence of SRE and to a less extent, in the presence of Cd^{2+} . The result was supported by TEM images, Figure 2.7. No CeO_2NPs were detected in the solution with SRE by TEM, likely due to the precipitation of micro-sized particles and greater dissolution caused by SRE.

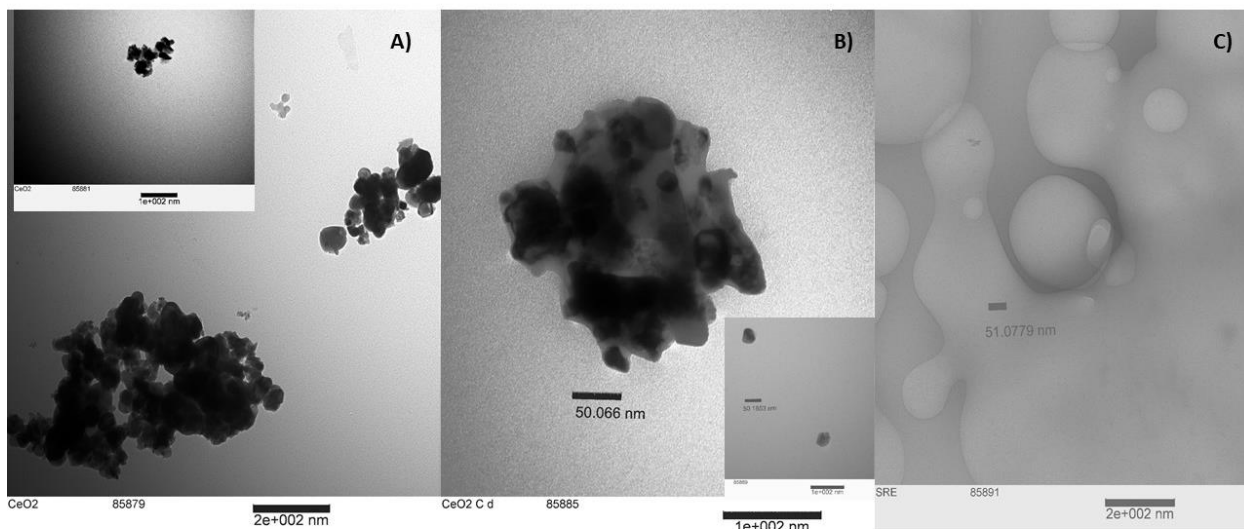


Figure 2.7. High resolution of Transmission electron microscopy TEM (JEOL JEM-1200EX, JEOL Ltd., Tokyo, Japan) studies of 100 mg/L CeO₂ ENP (A) the TEM image of intact CeO₂ ENPs. (B) It represent the physical transformation of CeO₂ENPs after adsorption of Cd. (C) It indicate the macro transformation of ENPs that are not observable at nanoscale when the SRE was introduced in adsorption batch.

2.5. Conclusion

The size distribution of CeO₂NPs narrowed at high As concentrations which might be associated with the even more negative zeta potential of these nanoparticles at high As concentrations, but additional investigation is needed for a mechanistic understanding. CeO₂NPs aggregation, zeta potential and dissolution rate have a significant impact on their fate and accumulation in agricultural systems and this study is probably the first study to demonstrate that co-existing heavy metals can significantly modify the physicochemical properties of CeO₂NPs, providing new insights into the mechanisms of altered plant uptake of CeO₂NPs and co-existing heavy metals.

2.6. References

1. Sharifan, H.; Wang, X.; Guo, B.; Ma, X., Investigation on the Modification of Physicochemical Properties of Cerium Oxide Nanoparticles through Adsorption of Cd and As(III)/As(V). *ACS Sustainable Chemistry & Engineering* **2018**, *6*, (10), 13454-13461.
2. Clemens, S.; Ma, J. F., Toxic heavy metal and metalloid accumulation in crop plants and foods. *Annual review of plant biology* **2016**, *67*, 489-512.
3. Caussy, D., Case studies of the impact of understanding bioavailability: arsenic. *Ecotoxicology and Environmental Safety* **2003**, *56*, (1), 164-173.
4. Roco, M. C.; Mirkin, C. A.; Hersam, M. C., *Nanotechnology research directions for societal needs in 2020*. Springer Netherlands: 2011; Vol. 1.
5. Peters, R. J.; Bouwmeester, H.; Gottardo, S.; Amenta, V.; Arena, M.; Brandhoff, P.; Marvin, H. J.; Mech, A.; Moniz, F. B.; Pesudo, L. Q., Nanomaterials for products and application in agriculture, feed and food. *Trends in Food Science & Technology* **2016**, *54*, 155-164.
6. Zhang, W.; Guo, Z.; Chen, Y.; Cao, Y., Nanomaterial based Biosensors for Detection of Biomarkers of Exposure to OP Pesticides and Nerve Agents: A Review. *Electroanalysis* **2017**.
7. Schymura, S.; Fricke, T.; Hildebrand, H.; Franke, K., Elucidating the Role of Dissolution in CeO₂ Nanoparticle Plant Uptake by Smart Radiolabeling. *Angewandte Chemie International Edition* **2017**.
8. Cao, Z.; Stowers, C.; Rossi, L.; Zhang, W.; Lombardini, L.; Ma, X., Physiological effects of cerium oxide nanoparticles on the photosynthesis and water use efficiency of soybean (*Glycine max* (L.) Merr.). *Environmental Science: Nano* **2017**, *4*, (5), 1086-1094.

9. Rossi, L.; Zhang, W.; Ma, X., Cerium oxide nanoparticles alter the salt stress tolerance of *Brassica napus* L. by modifying the formation of root apoplastic barriers. *Environmental Pollution* **2017**, *229*, 132-138.
10. Rossi, L.; Sharifan, H.; Zhang, W.; Schwab, A. P.; Ma, X., Mutual effects and in planta accumulation of co-existing cerium oxide nanoparticles and cadmium in hydroponically grown soybean (*Glycine max* (L.) Merr.). *Environmental Science: Nano* **2018**, *5*, (1), 150-157.
11. Cao, Z. The Impact of Cerium Oxide Nanoparticles on Photosynthesis and Water Use Efficiency of Soybean (*Glycine Max* (L.) Merr.). 2016.
12. Zhiming Cao, C. S., Lorenzo Rossi, Weilan Zhang, Leonardo Lombardini , Xingmao Ma, Physiological effects of cerium oxide nanoparticles on the photosynthesis and water use efficiency of soybean (*Glycine max* L.). *Environmental Science: Nano* **2017**, *4*, 1086-1094.
13. Zhang, W.; Dan, Y.; Shi, H.; Ma, X., Elucidating the mechanisms for plant uptake and in-planta speciation of cerium in radish (*Raphanus sativus* L.) treated with cerium oxide nanoparticles. *Journal of Environmental Chemical Engineering* **2017**, *5*, (1), 572-577.
14. Contreras, A. R.; Garcia, A.; Gonzalez, E.; Casals, E.; Puentes, V.; Sanchez, A.; Font, X.; Recillas, S., Potential use of CeO₂, TiO₂ and Fe₃O₄ nanoparticles for the removal of cadmium from water. *Desalination and water treatment* **2012**, *41*, (1-3), 296-300.
15. Contreras, A.; Casals, E.; Puentes, V.; Komilis, D.; Sánchez, A.; Font, X., Use of cerium oxide (CeO₂) nanoparticles for the adsorption of dissolved cadmium (II), lead (II) and chromium (VI) at two different pHs in single and multi-component systems. *Global Nest Journal* **2015**, *17*, (3), 536-543.

16. Ma, X.; Geiser-Lee, J.; Deng, Y.; Kolmakov, A., Interactions between engineered nanoparticles (ENPs) and plants: phytotoxicity, uptake and accumulation. *Science of the total environment* **2010**, *408*, (16), 3053-3061.
17. De La Torre-Roche, R.; Hawthorne, J.; Deng, Y.; Xing, B.; Cai, W.; Newman, L. A.; Wang, Q.; Ma, X.; Hamdi, H.; White, J. C., Multiwalled carbon nanotubes and C60 fullerenes differentially impact the accumulation of weathered pesticides in four agricultural plants. *Environmental Science & Technology* **2013**, *47*, (21), 12539-12547.
18. De La Torre-Roche, R.; Hawthorne, J.; Musante, C.; Xing, B.; Newman, L. A.; Ma, X.; White, J. C., Impact of Ag nanoparticle exposure on p, p'-DDE bioaccumulation by Cucurbita pepo (Zucchini) and Glycine max (Soybean). *Environmental science & technology* **2013**, *47*, (2), 718-725.
19. Rossi, L.; Zhang, W.; Schwab, A. P.; Ma, X., Uptake, Accumulation, and in Planta Distribution of Coexisting Cerium Oxide Nanoparticles and Cadmium in Glycine max (L.) Merr. *Environmental science & technology* **2017**, *51*, (21), 12815-12824.
20. Mishra, P. K.; Saxena, A.; Rawat, A. S.; Dixit, P. K.; Kumar, R.; Rai, P. K., Surfactant-Free One-Pot Synthesis of Low-Density Cerium Oxide Nanoparticles for Adsorptive Removal of Arsenic Species. *Environmental Progress & Sustainable Energy* **2018**, *37*, (1), 221-231.
21. Rossi, L.; Zhang, W.; Lombardini, L.; Ma, X., The impact of cerium oxide nanoparticles on the salt stress responses of Brassica napus L. *Environmental Pollution* **2016**, *219*, 28-36.
22. Krishnamurti, G.; Cieslinski, G.; Huang, P.; Van Rees, K., Kinetics of cadmium release from soils as influenced by organic acids: implication in cadmium availability. *Journal of Environmental Quality* **1997**, *26*, (1), 271-277.

23. Komárek, M.; Koretsky, C. M.; Stephen, K. J.; Alessi, D. S.; Chrastný, V., Competitive adsorption of Cd (II), Cr (VI), and Pb (II) onto nanomaghemite: a spectroscopic and modeling approach. *Environmental science & technology* **2015**, *49*, (21), 12851-12859.
24. Li, B.; Yang, L.; Wang, C.-q.; Zhang, Q.-p.; Liu, Q.-c.; Li, Y.-d.; Xiao, R., Adsorption of Cd(II) from aqueous solutions by rape straw biochar derived from different modification processes. *Chemosphere* **2017**, *175*, 332-340.
25. Xu, T.; Catalano, J. G., Effects of Ionic Strength on Arsenate Adsorption at Aluminum Hydroxide–Water Interfaces. *Soils* **2018**, *2*, (1), 1.
26. Rawson, J.; Prommer, H.; Siade, A.; Carr, J.; Berg, M.; Davis, J. A.; Fendorf, S., Numerical modeling of arsenic mobility during reductive iron-mineral transformations. *Environmental science & technology* **2016**, *50*, (5), 2459-2467.
27. Benjamin, M. M.; Lawler, D. F., *Water quality engineering: physical/chemical treatment processes*. John Wiley & Sons: 2013.
28. Grulke, E.; Reed, K.; Beck, M.; Huang, X.; Cormack, A.; Seal, S., Nanoceria: factors affecting its pro-and anti-oxidant properties. *Environmental Science: Nano* **2014**, *1*, (5), 429-444.

CHAPTER III

IMPACT OF NANOPARTICLE SURFACE CHARGE AND PHOSPHATE ON THE UPTAKE OF COEXISTING CERIUM OXIDE NANOPARTICLES AND CADMIUM BY SOYBEAN (*GLYCINE MAX. (L.) MERR.*)²

3.1. Summary

Engineered nanoparticles (ENPs) often interact closely with co-existing environmental pollutants; however, the effects of nanoparticle properties, such as surface charge, on the interactions of ENPs with co-present environmental pollutants in a plant system has not been examined. This study investigated the roles of surface charge of nanoparticles and growth media chemistry on the mutual effects of cerium oxide nanoparticles (CeO₂NPs) and cadmium (Cd) on their plant uptake and accumulation in a hydroponic system. Soybean seedlings were exposed to five nanoparticle/Cd treatments including: 100 mg L⁻¹ CeO₂NPs⁽⁺⁾; 100 mg L⁻¹ CeO₂NPs⁽⁻⁾; 100 mg L⁻¹ CeO₂NPs⁽⁺⁾ + 1 mg L⁻¹ Cd; 100 mg L⁻¹ CeO₂NPs⁽⁻⁾ + 1 mg L⁻¹ Cd; and 1 mg L⁻¹ Cd only. The previous treatments were imposed in the presence and absence of 50 mg L⁻¹ phosphate. After four days of exposure to the treatments, concentrations of Cd and Ce in plant tissues were quantified by inductively coupled plasma-mass spectrometry (ICP-MS). Roots exposed to CeO₂NPs⁽⁺⁾ contained 87% higher Ce than plants exposed to CeO₂NPs⁽⁻⁾. The presence of phosphate significantly increased the root

² Taylor & Francis is pleased to offer reuses of its content for a thesis or dissertation free of charge contingent on resubmission of permission request if work is published. Impact of nanoparticle surface charge and phosphate on the uptake of coexisting cerium oxide nanoparticles and cadmium by soybean (*Glycine max. (L.) merr.*),. Hamidreza Sharifan, , Xiaoxuan Wang, X Ma,. International Journal of Phytoremediation,. aylor & Francis 1522-6514 (Print) 1549-7879 (Online) Journal homepage: <https://www.tandfonline.com/loi/bijp20>

concentration of Ce exposed to both CeO₂NPs. As previously reported, CeO₂NPs and Cd mutually affected their plant uptake and accumulation. The interactions of CeO₂NPs and Cd are heavily affected by nanoparticle surface charge, and phosphate, a common nutrient in the growth medium, plays a significant role in the plant uptake and accumulation of Cd and CeO₂NPs.

Key Words: surface charge, phosphate, cerium oxide, nanoparticle, cadmium, soybean

3.2. Introduction

Nanotechnology is a driving force for innovations in the food-water-energy nexus (Rossi et al. 2019). Accompanying the rapid advancement of nanotechnology is the increasing manufacturing and discharge of engineered nanoparticle (ENPs). Agricultural soil is a primary sink of ENPs in the environment (Meesters et al. 2016). Direct applications of ENP-incorporated agrichemicals further increase the accumulation of ENPs in agricultural soils (Dasgupta, Ranjan, and Ramalingam 2017). As a result, numerous studies have evaluated the effects of ENPs on plants and their accumulation in edible tissues of agricultural crops (Ma and Yan 2018; Ma et al. 2015). In addition to the direct impact and accumulation of ENP elements in plant tissues, however, ENPs may affect plant growth and food safety through their alteration of plant uptake and accumulation of coexisting environmental pollutants (Ma and Yan 2018). Co-occurring ENPs change the plant uptake of both organic (De La Torre-Roche et al. 2012) and inorganic pollutants (Wang et al. 2018) in soil and hydroponic systems. In particular, we have shown that cerium oxide nanoparticles (CeO_2NPs) and cadmium (Cd) mutually affect their plant uptake and accumulation in soybeans through a variety of mechanisms including the adsorption of Cd on CeO_2NPs surface (Sharifan et al. 2018), the modification of rhizosphere environments through greater excretion of root exudates (Rossi et al. 2018) and modified root endodermal barriers (Rossi et al. 2017). Despite an increased understanding of the mutual effects of these two chemicals, the impact of surface properties of CeO_2NPs on their interaction with Cd has not been examined.

Surface charge plays a distinctive role in the fate and transport of CeO_2NPs . For example, after wheat seedlings were treated with CeO_2NPs possessing different surface charges for 34 h, positively charged CeO_2NPs were mostly retained on the root surface while the neutral and negatively charged CeO_2NPs showed much higher accumulation in wheat shoots, despite that the

Ce concentrations in roots exposed to neutral and negatively charged ENPs were much lower (Spielman-Sun et al. 2017). Similarly, positively charged gold nanoparticles (AuNPs) are readily retained by plant roots while negatively charged AuNPs are more efficiently translocated from roots to shoots (Zhu et al. 2012). Different surface charge of ENPs also leads to different subcellular localization in plant roots and different biochemical impacts (Ma and Quah 2016). Using an ultra-high resolution X-ray fluorescence imaging technique, large quantity of negatively charged CeO₂NPs was found in root cell cytoplasm in cortex tissues in addition to their presence in intercellular spaces while positively charged CeO₂NPs were mostly associated with the root epidermal cells, indicating the predominant impact of surface charge on ENP fate and transport (Li et al. 2019). The surface charge also affects the adsorption of Cd on CeO₂NP surfaces due to the significant role of electrostatic forces in the adsorption process (Sharifan et al. 2018).

In addition to the physiochemical properties of ENPs, the chemistry of the growth media has a strong impact on ENPs fate and transport. In particular, the presence of phosphate affects the speciation and uptake of CeO₂NPs by plants. Addition of phosphate inhibits the redox cycle between Ce³⁺ and Ce⁴⁺ on CeO₂NPs surface due to the formation of CePO₄ (Singh et al. 2011). Also, in plant roots, the transformation of Ce⁴⁺ to Ce³⁺ was markedly reduced in the presence of 1 mM PO₄ in the growth media (Wang et al. 2017). The presence of PO₄ also led to the formation of needle-like CePO₄ nanoparticles and different subcellular localizations of Ce in plant root cells. A recent study found that the presence of PO₄ significantly increased the adsorption of Cd on graphene oxide (GO) at pH 5.3-10.0 due to the formation of a ternary surface complex (Ren et al. 2016). Given the abundance of phosphate in biological systems and plant growth media and the strong impact of surface chemistry on ENPs fate and impact, it is important to understand the role of ENP surface properties and the biogeochemical conditions in plant growth media on the mutual

interactions of ENPs and co-occurring environmental chemicals. The primary goal of this study was to understand the effects of surface charge of CeO₂NPs and the presence of phosphate on the uptake and accumulation of coexisting CeO₂NPs and Cd by soybeans (*Glycine max* (L.) Merr. var. 'Tohya'). We chose CeO₂NPs as a model ENP because of its broad applications in industry and our previous experiences with this ENP, and Cd due to its prevalence in agricultural soils. Soybean was used in this study because of its global importance as a food crop.

3.3. Materials and Methods

3.3.1 Materials

An aqueous dispersion of negatively charged CeO₂NPs (CeO₂NPs⁽⁻⁾) (20% by weight, 10-30 nm) was purchased from the US Research Nanomaterials, Inc. (Houston, TX). Positively charged CeO₂NPs (CeO₂NPs⁽⁺⁾) (10% by weight, <25 nm) was obtained from Sigma Aldrich (St. Louis, MO). Both ENPs were fully characterized through our previous studies (Rossi et al. 2018; Zhang et al. 2018). Both ENPs have irregular polygonal shapes, the zeta potential for CeO₂NPs⁽⁻⁾ was approximately -51.8 mV and for CeO₂NPs⁽⁺⁾, +47.3 mV in 200 mg/L suspensions (Zhang et al. 2018). Cd sulfate (CdSO₄) was purchased from Fisher Scientific Inc. (Pittsburgh, PA). High purity sodium phosphate monobasic (NaH₂PO₄ >98%) was purchased from Sigma Aldrich (St. Louis, MO).

3.3.2. Plant growth

The seeds of *Glycine max* (L.) Merr. var. 'Tohya' (soybean) were purchased from Johnny's Selected Seeds (Fairfield, MN). The seeds were disinfected with 2.7% sodium hypochlorite solution for 5 min, washed with deionized water (DI) three times and then germinated in a moist potting soil mix (Miracle Gro®, the Scotts Company, Marysville, OH) for four days. The seedlings were transplanted to 50 mL

centrifuge tubes containing quarter strength Hoagland solution. The plant seedlings were cultivated in the nutrient solution at room temperature under a 16/8 h fluorescent illumination cycle ($250 \mu\text{mol m}^2 \text{s}^{-1}$) for 14 days before any treatment. The seedlings were randomly rotated every other day during the cultivation stage to reduce possible differences in light reception. The nutrient solution was replenished every morning and evening. Similarly-sized seedlings were selected for different treatments as described below.

3.3.3. Treatments with CeO₂NPs, Cd and phosphate

Five treatments without the presence of phosphate salt were prepared in deionized (DI) water as follow: $100 \text{ mg L}^{-1} \text{ CeO}_2\text{NPs}^{(+)}$; $100 \text{ mg L}^{-1} \text{ CeO}_2\text{NPs}^{(-)}$; $100 \text{ mg L}^{-1} \text{ CeO}_2\text{NPs}^{(+)} + 1 \text{ mg L}^{-1} \text{ Cd}$; $100 \text{ mg L}^{-1} \text{ CeO}_2\text{NPs}^{(-)} + 1 \text{ mg L}^{-1} \text{ Cd}$; and $1 \text{ mg L}^{-1} \text{ Cd}$ without nanoparticles. A parallel series of treatments containing 50 mg L^{-1} phosphate salt (NaH_2PO_4) in addition to the above-mentioned CeO₂NPs and/or Cd were also prepared. 100 mg L^{-1} of CeO₂NPs were freshly prepared in sterilized ultra-pure water before use ($18.3 \text{ M}\Omega$). A known amount of CdSO₄ or NaH₂PO₄ were then dissolved in a solution containing 100 mg L^{-1} of CeO₂NPs to obtain concentrations of $1 \text{ mg L}^{-1} \text{ Cd}$ or 50 mg L^{-1} phosphate in the solution. The phosphate concentration was selected based on the recommended concentrations in literature (Lv et al. 2012). All solutions were mixed on a shaker table for ten minutes before use. A negative control with seedlings growing in DI water was also prepared.

After solution preparation, 14-day old seedlings were removed from Hoagland solutions and rinsed five times with DI water to remove the residue of the nutrient solution from seedling roots. These seedlings were then transferred to 50 mL polypropylene centrifuge tubes containing 50 mL of different treatment solutions as described above. Three replicates were prepared for each treatment. Altogether, 33 seedlings were grown in 11 different treatment solutions for four days.

During the period of treatment, the centrifuge tubes were replenished with DI water twice per day (morning-evening) to compensate for the transpired water. The water transpiration in all treatments was recorded.

3.3.4. Plant uptake of cerium and cadmium

At termination, the seedlings were removed from the tubes and the roots were rinsed three times with DI water. The seedlings were then dried with a paper towel. Afterward, the seedlings were separated into roots and shoots, dried in an oven at 75 °C for 48 hours and acid digested following published protocols (Wang et al. 2018). Briefly, 5 mL of 70% (w/w) nitric acid (Certified ACS Plus) was added to a 50 mL digestion tube containing 0.5 g (shoots) or 0.25 g (roots) of dry biomass and heated at 95 °C for 5 h on a DigiPREP MS hot block digester (SCP Science, Clark Graham, Canada). After being cooled down to room temperature, 2 mL of hydrogen peroxide (30%, Certified ACS) was added to each tube and re-heated on the hot block to 95 °C until the biomass was fully digested (Zhang et al. 2015; Zhang et al. 2017). The amount of Ce and Cd in each sample was then quantified by an inductively coupled plasma–mass spectrometry (ICP-MS) (Agilent 7500i, Agilent Technologies Co. Ltd, USA). Detailed information on the operational parameters of ICP-MS and sample quality control can be found from our previous publications (Sharifan et al. 2018).

3.3.5. Statistical Analysis

Statistical analysis of Ce and Cd concentrations in plant tissues was performed using the Minitab 18 Statistical Software (Minitab Inc., State College, PA, USA). The comparison between the mean values of different treatments was carried out using One-Way ANOVA, followed by Tukey's test at the significance level of 5% ($p < 0.05$).

3.4. Results and Discussion

The dry biomass of soybean roots and shoots exposed to different treatments of Cd and CeO₂NPs in the presence and absence of the 50 mM phosphate is shown in **Figure 1**. No significant differences were detected between different treatments. For the plant transpiration (**Figure S1**), the only significant difference was the CeO₂⁽⁻⁾-Cd transpiration was higher than that for CeO₂⁽⁺⁾-Cd treated plants.

In agreement with a previous study (Spielman-Sun et al. 2017), soybean roots exposed to CeO₂NPs⁽⁺⁾ had 87% higher Ce than plants exposed to the same concentration of CeO₂NPs⁽⁻⁾ in the absence of phosphate, **Figure 2**. However, Ce concentrations in soybean shoots were statistically equivalent in most treatments, but indicating greater transport of CeO₂NPs⁽⁻⁾ compared to CeO₂NPs⁽⁺⁾. The presence of PO₄ increased the root concentration of Ce exposed to CeO₂NPs, regardless of the surface charge, and some of the increases were significant. The Ce concentration in soybean roots increased by 61% and 66% for plants exposed to CeO₂NPs⁽⁺⁾ and CeO₂NPs⁽⁻⁾, respectively. The presence of PO₄ displayed different impacts on Ce concentration in soybean shoots exposed to CeO₂NPs with different surface charges. While 50 mg/L of PO₄ significantly increased Ce concentration by 58% in soybean shoots exposed to CeO₂NPs⁽⁻⁾, this increase was insignificant in soybean shoots exposed to CeO₂NPs⁽⁺⁾. The impact of PO₄ on the transformation of CeO₂NPs is well recognized due to the formation of CePO₄ by Ce³⁺ and PO₄, which can be either deposited back on nanoparticle surface (Schwabe et al. 2014), or immobilized on root epidermis and intercellular spaces (Zhang et al. 2012). It is likely that the formation of CePO₄ reduced the potential migration of dissolved Ce³⁺ away from the root surface and hence increased the root Ce concentration in the presence of PO₄. While similar processes might have occurred in the soybean rhizosphere exposed to CeO₂NPs⁽⁺⁾, the electrostatic interactions between CeO₂NPs⁽⁺⁾

and negatively charged root surfaces may be stronger than the potential effects of PO_4 , leading to an insignificant impact of PO_4 on the root concentration of Ce in plants exposed to $\text{CeO}_2\text{NPs}^{(+)}$.

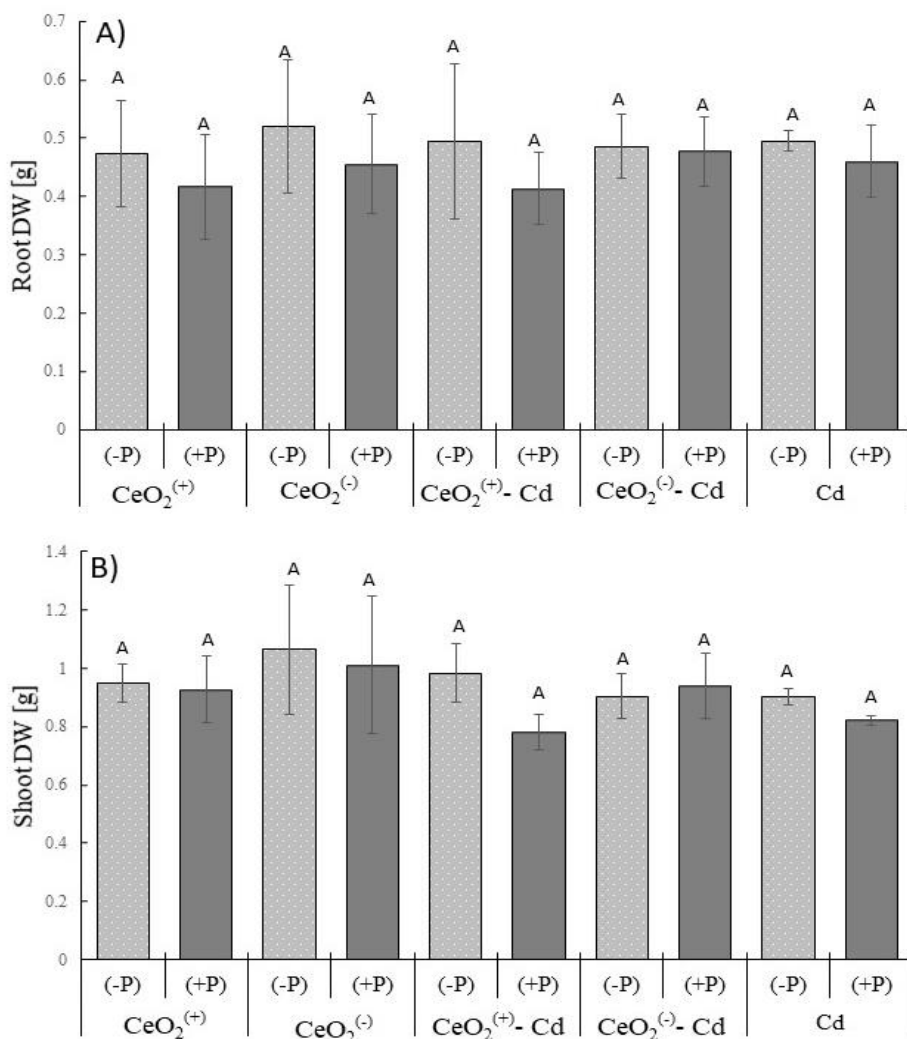


Figure 3.1: Dry weight (g) of soybean roots (A) and shoots (B) grown in 1.0 mg L^{-1} Cd and 100 mg L^{-1} $\text{CeO}_2\text{NPs}^{(+)}$ or $\text{CeO}_2\text{NPs}^{(-)}$ separately or in combination. (-P) and (+P) indicates the absence and presence of 50 mg L^{-1} of phosphate in the growth media. Different letters above each column indicate significant differences by Tukey's post hoc test ($p < 0.05$) and the error bars represent standard deviation ($n = 3$).

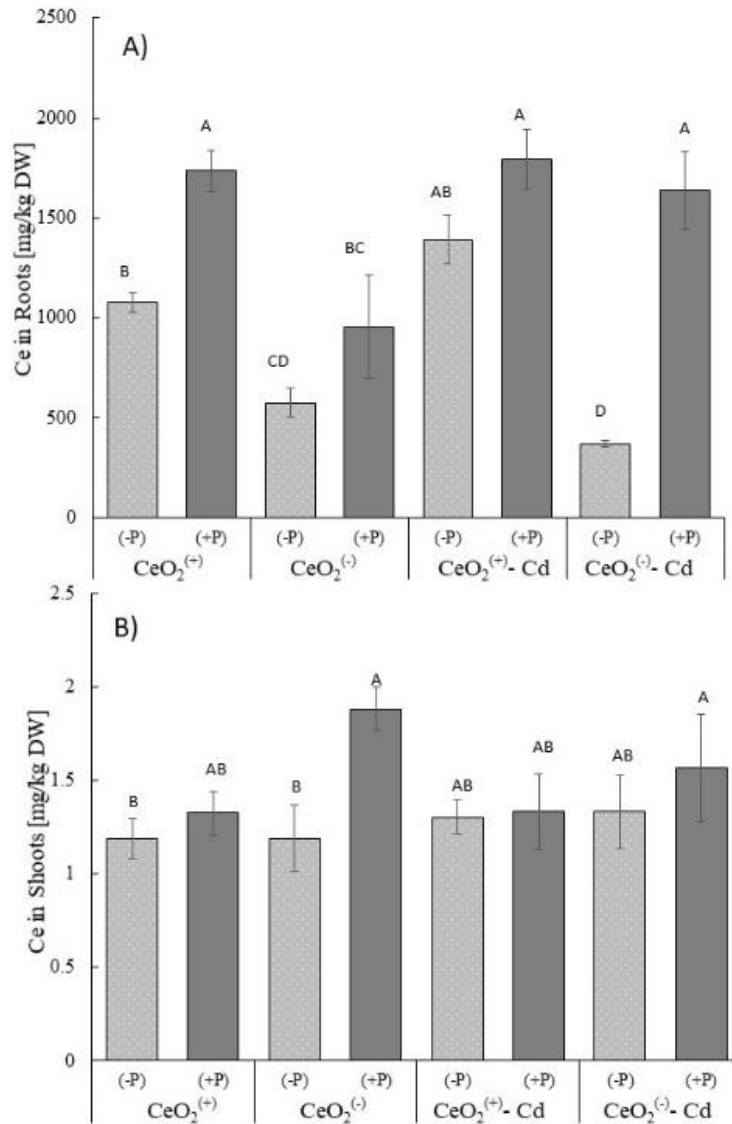


Figure 3.2: Cerium concentrations in soybean roots (A) and shoots (B) grown in 1.0 mg L^{-1} Cd and 100 mg L^{-1} $\text{CeO}_2\text{NPs}^{(+)}$ or $\text{CeO}_2\text{NPs}^{(-)}$ separately or in combination. (-P) and (+P) indicates the absence and presence of 50 mg L^{-1} of phosphate in the growth media. Different letters above each column indicate significant differences by Tukey's post hoc test ($p < 0.05$) and the error bars represent standard deviation ($n = 3$).

Cadmium affected plant uptake of Ce in the absence of PO_4 . Herein, we further demonstrate that the impact was dependent on the surface charge of CeO_2NPs . The co-presence of 1.0 mg/L of Cd and $\text{CeO}_2\text{NPs}^{(+)}$ increased the Ce concentration in roots by 29% compared to the absence of Cd but decreased Ce concentration in roots by 35% in $\text{CeO}_2\text{NPs}^{(-)}$ -exposed soybean seedlings. The presence of PO_4 resulted in a slightly but not significantly higher Ce concentration in soybean roots which concurrently exposed to Cd and $\text{CeO}_2\text{NPs}^{(+)}$. However, the presence of PO_4 increased Ce concentration in soybean roots exposed to both Cd and $\text{CeO}_2\text{NPs}^{(-)}$ by almost 4 times compared with soybean plants exposed to the same concentrations of Cd and Ce but without PO_4 . Cadmium could affect plant Ce accumulation from coexisting $\text{CeO}_2\text{NPs}^{(-)}$ through the modification of nanoparticle physicochemical properties such as their size, surface charge and dissolution (Sharifan et al. 2018), the anatomical structures of plant roots (Rossi et al. 2017), and the chemistry around root rhizosphere (Rossi et al. 2018). However, the overall effect of Cd on Ce concentration in soybean roots hydroponically grown in the medium with both Cd and $\text{CeO}_2\text{NPs}^{(-)}$ was not significant due to the competing effects of affected processes on Ce accumulation. The underlying mechanism on PO_4 behavior in exposure to Ce in soybean roots rhizosphere in the co-presence of Cd and $\text{CeO}_2\text{NPs}^{(-)}$ is unclear, but may be ascribed to the formation of $\text{CeO}_2\text{NPs}^{(-)}\text{-Cd-PO}_4^{3-}$ ternary complex (Ren et al. 2016) which had larger hydrodynamic size than $\text{CeO}_2\text{NPs}^{(-)}$ and therefore, greatly enhanced their deposition on soybean roots. Similar $\text{CeO}_2\text{NPs}^{(+)}\text{-PO}_4^{3-}\text{-Cd}$ complex might have occurred too, but to a lesser extent. If the postulation of the ternary complex is correct, lower transport of Ce from roots to shoots should be expected. Indeed, we observed insignificant impact of Ce concentration in soybean shoots by co-present Cd in the presence of PO_4 , regardless of the surface charge of the nanoparticles. In comparison, the Ce concentration in soybean shoots in a previous study was

increased by 60% by co-occurring Cd when the plants were jointly exposed to CeO₂NPs⁽⁻⁾ and Cd hydroponically without PO₄, while the Ce concentration in the shoots is reduced by 15% in the presence of PO₄ in the CeO₂NPs⁽⁻⁾-Cd treatment.

Soybean seedlings showed high uptake of Cd in plant roots and shoots. The presence of PO₄ significantly increased Cd concentration in soybean roots but only slightly increased its concentration in soybean shoots (**Figure 3**). The formation of a Cd-phosphate solid phase might be the primary reason for the elevated Cd concentration in soybean roots because the particulate Cd-phosphate is more likely to be retained by soybean roots, and thus higher Cd concentration in soybean roots did not lead to higher Cd concentration in the shoots. Consistent with a previous study, CeO₂NPs⁽⁻⁾ had little impact on Cd root concentration in soybean seedlings hydroponically grown in the absence of PO₄ (Rossi et al. 2018). However, CeO₂NPs⁽⁺⁾ significantly increased Cd concentration in soybean roots by approximately 48%. The greater attachment of CeO₂NPs⁽⁺⁾ on root surfaces could have lowered the pore sizes of root epidermal cells and increased their adsorption on the root surface, however, this is unlikely a dominant reason because of the relative insignificance of apoplastic transport for Cd (Song, Jin, and Wang 2017) and comparable water transpiration by plants from different treatment groups in this study, **Figure 41**. It is more likely that the symplastic pathways of Cd uptake, regulated by various active transporters, are more heavily affected by CeO₂NPs⁽⁺⁾ than CeO₂NPs⁽⁻⁾. Detailed studies concerning the impact of ENPs on heavy metal transporters in plant root cells are rare, and future studies are needed to elucidate the interactions of heavy metals with co-existing ENPs with different physicochemical properties. Neither nanoparticles significantly affected Cd concentration in soybean shoots in this study, in contrast to a previous study that CeO₂NPs⁽⁻⁾ reduced Cd concentration in soybean shoots by almost 70% (Rossi et al. 2018).

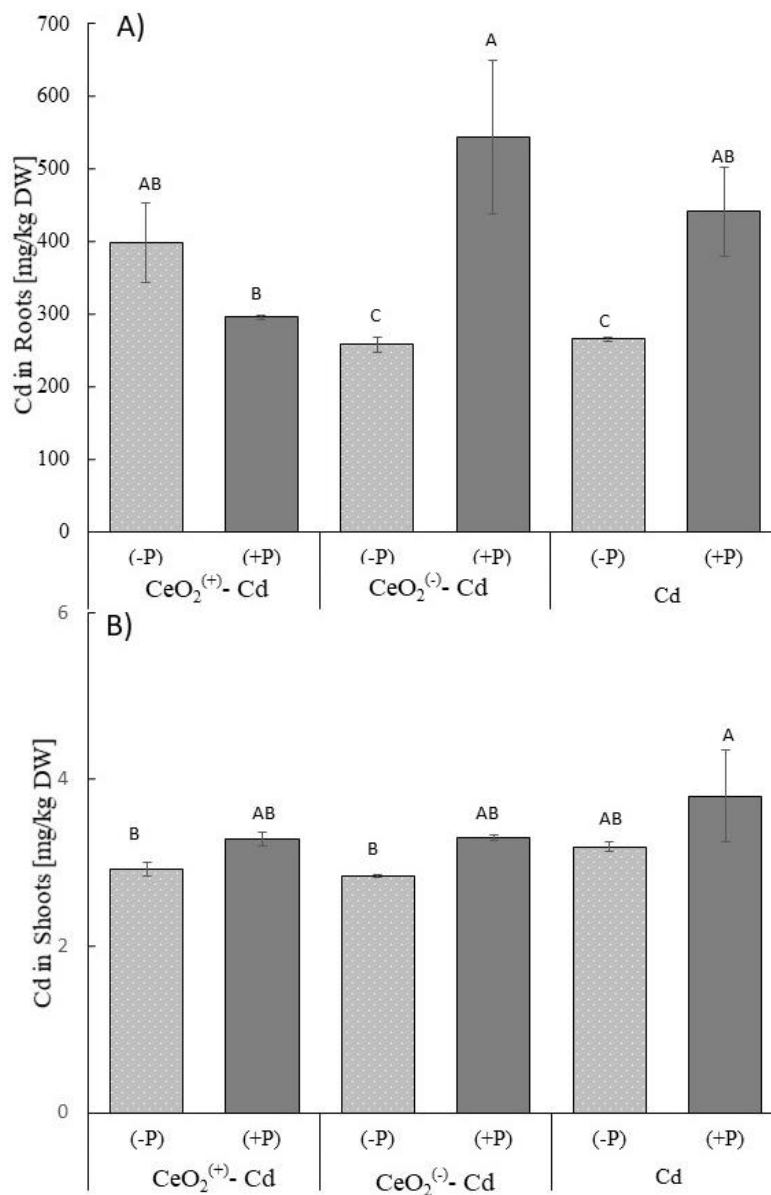


Figure 3.3: Cadmium concentrations in soybean roots (A) and shoots (B) grown in 1.0 mg L⁻¹ Cd and 100 mg L⁻¹ CeO₂NPs⁽⁺⁾ or CeO₂NPs⁽⁻⁾ separately or in combination. (-P) and (+P) indicates the absence and presence of 50 mg L⁻¹ of phosphate in the growth media. Different letters above each column indicate significant differences by Tukey's post hoc test (p < 0.05) and

the error bars represent standard deviation (n = 3).

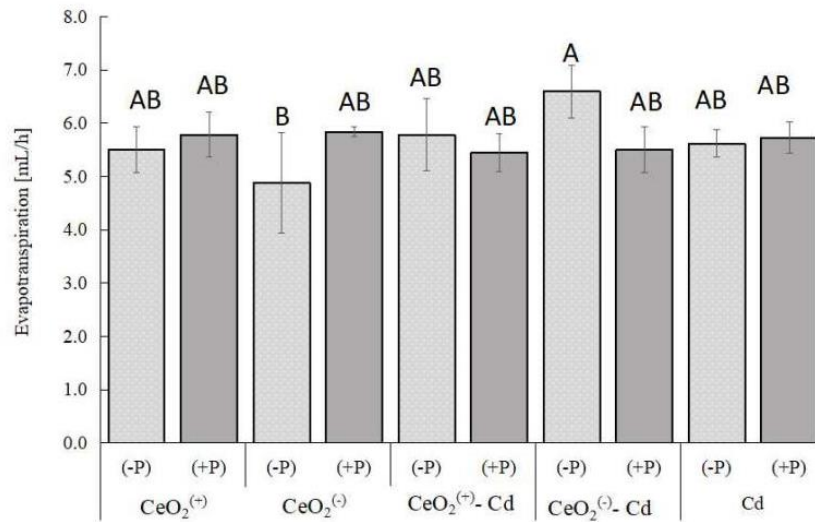


Figure 3.4: Accumulative transpiration of soybean seedlings exposed to 1.0 mg L⁻¹ Cd and 100 mg L⁻¹ CeO₂NPs⁽⁺⁾ or CeO₂NPs⁽⁻⁾ separately or in combination. (-P) and (+P) indicates the absence and presence of 50 mg L⁻¹ of phosphate in the growth media. Different letters above each column indicate significant differences by Tukey's post hoc test (p < 0.05) and the error bars represent standard deviation (n = 3).

Interestingly, the presence of PO_4 almost doubled the Cd concentration in soybean roots grown in the media containing $\text{CeO}_2\text{NPs}^{(-)}$ and Cd, compared with soybean seedlings co-exposed to these two chemicals but without PO_4 . On the contrary, the presence of PO_4 lowered the root Cd concentration by about 30% in the system containing $\text{CeO}_2\text{NPs}^{(+)}$ and Cd, suggesting that PO_4 interfered the interactions between CeO_2NPs and Cd and the interference differed with the surface charge of CeO_2NPs .

3.5. Conclusion

Understanding the mutual interactions of ENPs with co-occurring environmental chemicals and how these interactions affect their fate and transport in different environmental systems is an emerging topic in sustainable nanotechnology. Several previous studies have demonstrated that the close interactions of coexisting CeO_2NPs and Cd in a plant system reciprocally affect their plant uptake and accumulation. Our present study confirmed those interactions and demonstrated for the first time that the mutual effect of CeO_2NPs and Cd is heavily affected by the nanoparticles surface charge. In addition, our study revealed that PO_4 , a common nutrient in the growth medium, plays a significant role in the plant uptake and accumulation of Cd and CeO_2NPs .

3.6. References

- Dasgupta, Nandita, Shivendu Ranjan, and Chidambaram Ramalingam. 2017. 'Applications of nanotechnology in agriculture and water quality management', *Environmental Chemistry Letters*, 15: 591-605.
- De La Torre-Roche, Roberto, Joseph Hawthorne, Yingqing Deng, Baoshan Xing, Wenjun Cai, Lee A Newman, Chen Wang, Xingmao Ma, and Jason C White. 2012. 'Fullerene-enhanced accumulation of p, p'-DDE in agricultural crop species', *Environmental Science & Technology*, 46: 9315-23.
- Li, Jieran, Ryan V. Tappero, Alvin S. Acerbo, Hanfei Yan, Yong Chu, Gregory V. Lowry, and Jason M. Unrine. 2019. 'Effect of CeO₂ nanomaterial surface functional groups on tissue and subcellular distribution of Ce in tomato (*Solanum lycopersicum*)', *Environmental Science: Nano*.
- Lv, Jitao, Shuzhen Zhang, Lei Luo, Wei Han, Jing Zhang, Ke Yang, and Peter Christie. 2012. 'Dissolution and microstructural transformation of ZnO nanoparticles under the influence of phosphate', *Environmental Science & Technology*, 46: 7215-21.
- Ma, Chuanxin, Jason C White, Om Parkash Dhankher, and Baoshan Xing. 2015. 'Metal-based nanotoxicity and detoxification pathways in higher plants', *Environmental Science & Technology*, 49: 7109-22.
- Ma, X, and B Quah. 2016. 'Effects of Surface Charge on the Fate and Phytotoxicity of Gold Nanoparticles to *Phaseolus vulgaris*', *Food Chem. Nanotechnol*, 2: 57-65.

- Ma, Xingmao, and Jun Yan. 2018. 'Plant uptake and accumulation of engineered metallic nanoparticles from lab to field conditions', *Current Opinion in Environmental Science & Health*.
- Meesters, Johannes AJ, JTK Quik, AA Koelmans, AJ Hendriks, and D Van de Meent. 2016. 'Multimedia environmental fate and speciation of engineered nanoparticles: a probabilistic modeling approach', *Environmental Science: Nano*, 3: 715-27.
- Ren, Xuemei, Qunyan Wu, Huan Xu, Dadong Shao, Xiaoli Tan, Weiqun Shi, Changlun Chen, Jiaxing Li, Zhifang Chai, and Tasawar Hayat. 2016. 'New insight into GO, cadmium (II), phosphate interaction and its role in GO colloidal behavior', *Environmental Science & Technology*, 50: 9361-69.
- Rossi, Lorenzo, Lauren N. Fedenia, Hamidreza Sharifan, Xingmao Ma, and Leonardo Lombardini. 2019. 'Effects of foliar application of zinc sulfate and zinc nanoparticles in coffee (*Coffea arabica* L.) plants', *Plant Physiology and Biochemistry*, 135: 160-66.
- Rossi, Lorenzo, Hamidreza Sharifan, Weilan Zhang, Arthur P Schwab, and Xingmao Ma. 2018. 'Mutual effects and in planta accumulation of co-existing cerium oxide nanoparticles and cadmium in hydroponically grown soybean (*Glycine max* (L.) Merr.)', *Environmental Science: Nano*, 5: 150-57.
- Rossi, Lorenzo, Weilan Zhang, Arthur P Schwab, and Xingmao Ma. 2017. 'Uptake, Accumulation, and in Planta Distribution of Coexisting Cerium Oxide Nanoparticles and Cadmium in *Glycine max* (L.) Merr', *Environmental Science & Technology*, 51: 12815-24.

- Schwabe, Franziska, Rainer Schulin, Patrick Rupper, Aline Rotzetter, Wendelin Stark, and Bernd Nowack. 2014. 'Dissolution and transformation of cerium oxide nanoparticles in plant growth media', *Journal of nanoparticle research*, 16: 2668.
- Sharifan, Hamidreza, Xiaoxuan Wang, Binglin Guo, and Xingmao Ma. 2018. 'Investigation on the Modification of Physicochemical Properties of Cerium Oxide Nanoparticles through Adsorption of Cd and As(III)/As(V)', *ACS Sustainable Chemistry & Engineering*, 6: 13454-61.
- Singh, Sanjay, Talib Dosani, Ajay S Karakoti, Amit Kumar, Sudipta Seal, and William T Self. 2011. 'A phosphate-dependent shift in redox state of cerium oxide nanoparticles and its effects on catalytic properties', *Biomaterials*, 32: 6745-53.
- Song, Yu, Liang Jin, and Xiaojuan Wang. 2017. 'Cadmium absorption and transportation pathways in plants', *International journal of phytoremediation*, 19: 133-41.
- Spielman-Sun, Eleanor, Enzo Lombi, Erica Donner, Daryl Howard, Jason M Unrine, and Gregory V Lowry. 2017. 'Impact of surface charge on cerium oxide nanoparticle uptake and translocation by wheat (*Triticum aestivum*)', *Environmental Science & Technology*, 51: 7361-68.
- Wang, Guohua, Yuhui Ma, Peng Zhang, Xiao He, Zhaohui Zhang, Meihua Qu, Yayun Ding, Junzhe Zhang, Changjian Xie, and Wenhe Luo. 2017. 'Influence of phosphate on phytotoxicity of ceria nanoparticles in an agar medium', *Environmental Pollution*, 224: 392-99.
- Wang, Xiaoxuan, Wenjie Sun, Sha Zhang, Hamidreza Sharifan, and Xingmao Ma. 2018. 'Elucidating the Effects of Cerium Oxide Nanoparticles and Zinc Oxide Nanoparticles on

- Arsenic Uptake and Speciation in Rice (*Oryza sativa*) in a Hydroponic System', *Environmental Science & Technology*, 52: 10040-47.
- Zhang, Peng, Yuhui Ma, Zhiyong Zhang, Xiao He, Jing Zhang, Zhi Guo, Renzhong Tai, Yuliang Zhao, and Zhifang Chai. 2012. 'Biotransformation of ceria nanoparticles in cucumber plants', *ACS nano*, 6: 9943-50.
- Zhang, Weilan, Yongbo Dan, Honglan Shi, and Xingmao Ma. 2017. 'Elucidating the mechanisms for plant uptake and in-planta speciation of cerium in radish (*Raphanus sativus* L.) treated with cerium oxide nanoparticles', *Journal of Environmental Chemical Engineering*, 5: 572-77.
- Zhang, Weilan, Stephen D Ebbs, Craig Musante, Jason C White, Cunmei Gao, and Xingmao Ma. 2015. 'Uptake and accumulation of bulk and nanosized cerium oxide particles and ionic cerium by radish (*Raphanus sativus* L.)', *Journal of Agricultural and Food Chemistry*, 63: 382-90.
- Zhang, Weilan, Arthur P Schwab, Jason C White, and Xingmao Ma. 2018. 'Impact of Nanoparticle Surface Properties on the Attachment of Cerium Oxide Nanoparticles to Sand and Kaolin', *Journal of Environmental Quality*, 47: 129-38.
- Zhu, Zheng-Jiang, Huanhua Wang, Bo Yan, Hao Zheng, Ying Jiang, Oscar R Miranda, Vincent M Rotello, Baoshan Xing, and Richard W Vachet. 2012. 'Effect of surface charge on the uptake and distribution of gold nanoparticles in four plant species', *Environmental Science & Technology*, 46: 12391-98.

CHAPTER IV

MUTUAL EFFECTS AND *IN-PLANTA* UPTAKE OF CERIUM OXIDE NANOPARTICLES AND CADMIUM IN HYDROPONICALLY GROWN SOYBEAN (*GLYCINE MAX* (L.) MERR.)³

4.1. Summary

Cadmium (Cd) is an extremely toxic metal to humans even at very low concentrations. Elevated Cd in soil due to various anthropogenic activities has led to higher Cd concentration in various crop tissues, making it a serious food safety concern. With the progressive production and continued accumulation of engineered nanoparticles (ENPs) in agricultural soils, it is imperative to understand how ENPs may affect the plant metal uptake and accumulation. The goal of this study was to understand the mutual effects of cerium oxide nanoparticles (CeO₂NPs) and Cd²⁺ on their uptake and accumulation by soybean seedlings (*Glycine max* (L.) Merr.) in a hydroponic system. Soybean seedlings were exposed to four treatments (control, 1.0 mg L⁻¹ Cd²⁺, 1.0 mg L⁻¹ Cd²⁺ + 100 mg L⁻¹ CeO₂NPs, 100 mg L⁻¹ CeO₂NPs) for 10 days. At termination, plant roots and shoots were separated and the concentrations of Cd and Ce in these tissues determined. In addition, the amount of ionic Ce and particulate Ce within soybean roots were analyzed. Significant interactions between co-existing CeO₂NPs and Cd were found concerning their accumulation in plant tissues. While CeO₂NPs did not affect the total Cd associated with soybean roots, they significantly reduced the translocation of Cd from roots to shoots (p<0.05). In contrast, the co-

³ 1. Rossi, L.; Sharifan, H.; Zhang, W.; Schwab, A. P.; Ma, X., Mutual effects and in planta accumulation of co-existing cerium oxide nanoparticles and cadmium in hydroponically grown soybean (*Glycine max* (L.) Merr.). *Environmental Science: Nano* **2018**, 5, (1), 150-157.; Reproduced by permission of The Royal Society of Chemistry (RSC) on behalf of the Centre National de la Recherche Scientifique (CNRS) and the RSC

presence of Cd lowered the concentration of Ce in soybean roots but significantly increased the concentration of Ce in soybean shoots more than 90%. The altered plant accumulation of co-existing Cd and Ce was attributed to various physical, chemical and biological processes occurred in plant rhizosphere. Specifically, the co-presence of Cd and CeO₂NPs led to higher excretion of plant root exudates, which lowered the pH in plant rhizosphere, enhanced CeO₂NPs dissolution and likely facilitated Cd complexation with large biomolecules, leading to altered uptake accumulation of both chemicals.

Keywords: heavy metals, cerium oxide nanoparticles, cadmium, soybean

4.2. Introduction

Cadmium (Cd) is a ubiquitous environmental pollutant extremely toxic to humans. Chronic exposure to Cd has been shown to be associated with a wide variety of health problems such as renal dysfunction, cancer, osteoporosis and cardio vascular disease ^{2,3}. Consumption of Cd-tainted food is a predominant pathway for human exposure to Cd due to its highly efficient soil-to-plant transfer ^{4,5}. A recent study indicated that food consumption accounts for almost 90% of Cd exposure in the general non-smoking population, rendering it an urgent task to understand processes which may potentially aggravate the plant accumulation of Cd ³.

With the current embrace of nanotechnology in many industries including the agricultural industry, engineered nanoparticles (ENPs) are increasingly detected in agricultural soils. They have been shown to affect plant physiological and biochemical processes at various levels and altered plant uptake of co-existing environmental pollutants ^{6,7}. Earlier efforts to investigate the ENP and co-occurring environmental pollutants, mostly focused on organic contaminants ^{7,8}. Few studies have evaluated the effects of ENPs on plant uptake of co-existing heavy metals. Plant uptake of heavy metals involves complex transport processes and some are highly regulated. For example, Cd²⁺ is

taken up by plant roots both apoplastically and symplastically^{4,9}. In the symplastic pathway, Cd^{2+} may diffuse into plant root cells passively or be actively transported via different protein transporters embedded in root plasma membrane^{4,9,10}. Two types of Cd^{2+} transporters have been identified including the more specific Cd^{2+} ZIP transporters (Zn/Fe regulated transporter protein) and the less selective calcium permeable channels^{9,11,12}. If Cd^{2+} forms complexes with surrounding chelates such as chemicals in plant root exudates, the complexes are transported into plant roots through YSL (Yellow-Stripe 1-Like) proteins^{9,13}. Once Cd species are in plant root cells, they can be translocated to the leaves and grain tissues. The translocation from roots to shoots is greatly affected by the vacuolar compartmentation of Cd-phytochelatin complexes as well as the transporters involved in xylem loading of Cd^{4,10,14,15}.

Scientific evidences dictate that the ENPs are capable to may potentially interrupt many of the physiological processes involved in heavy metal uptake and transport. Consequently, it is of great interest to investigate the impact of ENPs on plant uptake of co-existing heavy metals. Cerium oxide nanoparticles (CeO_2NPs) are one of the ENPs that have been broadly used over the past years, particularly as a fuel additive^{16,17}. The main pathways for CeO_2NPs to enter into agricultural soils include deposition of vehicle exhausts, municipal runoff and land application of bio-solids¹⁶. Simultaneous exposure to both CeO_2NPs and heavy metals such as Cd^{2+} is increasingly possible for crops. Due to the disruptive impacts of CeO_2NPs on the cellular membrane as well as the plant physiology and root anatomy^{18,19}, CeO_2NPs may substantially change the plant uptake and accumulation of heavy metals.

In addition, CeO_2NPs display high adsorption capacity for hazardous heavy metals such as arsenic (As), lead (Pb) and Cd^{20,21} that implies the carrier role of CeO_2NPs in surface immobilizing the Cd^{2+} to penetrate into plant tissues or retain Cd^{2+} in plant rhizosphere when they are not taken up

by plants^{16,22}. The complex interactions of CeO₂NPs and other metals suggest that CeO₂NPs are likely to alter the plant uptake and accumulation of co-present heavy metals. A few available studies in the literature with different ENPs corroborate this assumption. For example, TiO₂NPs (100 mg L⁻¹) were shown to significantly reduce the phytotoxicity of Cd to rice (*Oryzasativa L*), likely due to the adsorption of Cd on TiO₂²³. However, comprehensive studies and mechanistic insight into ENP-heavy metal interactions in plant rhizosphere are lacking.

Meanwhile, evidence has been reported that plant uptake of ENPs may be affected by various abiotic stresses. In general, higher abiotic stresses such as salt stress, nutrient shortage stress appeared to increase plant uptake of ENPs elements²⁴. ENPs accumulation in plant tissues has been a great food safety concern due to multiple dietary exposure routes.. As a result, the plant uptake of ENPs in the presence of heavy metals (as a source of abiotic stress) is also pivotal to investigate. The objectives of this research were to investigate the reciprocal effects of CeO₂NPs and Cd on their uptake by soybeans and to explore the underlying physical and chemical mechanisms of the their uptake.

Soybean (*Glycine max.* (L.) Merr.) is a strong study model because it is a main protein source of human diet that can accumulate metals (including Cd) in the grains²⁵. Soybean was reported by the Food and Agricultural Organization (FAO) as the fifth most produced crop worldwide that provides about 30% vegetable oil and 77% nitrogen fixation. The global demand for soybean products increases by 2.2% annually²⁶. The concentration of Cd in soybean seeds is positively correlated with its concentration in soil and has surpassed the maximum permissible concentration (0.2 mg/kg) administrated by the Codex Alimentarius Commission in some studies (FAO)²⁷, making it a great choice for this study as a model plant.

4.3. Material and Methods

4.3.1. *CeO₂NPs and Cd*

CeO₂NPs coated with Poly Vinyl Pyrrolidone (PVP) were purchased from the US Research Nanomaterials, Inc. (Houston, TX). The average size of the nanoparticles was 41.7 ± 5.2 nm, calculated by averaging the diameter of over 100 individual nanoparticles measured with ImageJ on transmission electron microscopic images of the NPs. The pH of the CeO₂NPs dispersed in water at 100 mg L⁻¹ was 7.1 and the zeta potential was -48.6 mV, determined by a dynamic light scattering Zetasizer (Malvern, UK). X-ray photoelectron spectroscopy (XPS) analysis indicated that about 9.7 % of Ce on the nanoparticle surface exists as Ce³⁺ (Fig. 6).

The concentration of CeO₂NPs (100 mg L⁻¹) was chosen based on many previous nanotoxicity studies with terrestrial plants, which used concentrations mostly in the range of 1–1000 mg L⁻¹ ²⁸. ²⁹. In addition, the literature suggested that CeO₂NPs at this concentration display significant impact on plant physiology and biochemistry but not lethal effects³⁰. Cd sulfate (CdSO₄) was purchased from the Fisher Scientific Inc. (Pittsburgh, PA) and was dissolved in water to obtain the final concentration of 1.0 mg L⁻¹ Cd. This concentration falls in the typical range of Cd in agricultural soils ²⁵.

4.3.2. *Plant species and growth conditions*

Glycine max (L.) Merr. (soybean) cv. 'Tohya' seeds were purchased from Johnny's Selected Seeds (Winslow, ME). Soybean seeds were germinated in moist sand for 5 days. After germination, young seedlings were individually transplanted into 50 mL plastic centrifuge tubes (Becton, Dickinson and Co., Franklin Lakes, NJ, USA) filled with 25% Hoagland solution ³¹ (Phyto Technology Lab, Shawnee Mission, KS). The transpiration rate was recorded by daily water loss

(mL h⁻¹) shown in Suppl. Fig. 2. When the water transpiration reached 50 mL day⁻¹ (after 10 days), plants were transferred from the Hoagland solution to new tubes filled with solutions containing 1.0 mg L⁻¹ Cd²⁺ and/or 100 mg L⁻¹ CeO₂NPs. Soybean seedlings were cultivated in these solutions for additional 10 days at room temperature under fluorescent bulbs providing 250 μmol m² s⁻¹ photosynthetic photon flux density (16 h light – 8 h dark photoperiod). Seedlings grown in just tap water were used as controls. Six seedlings were grown under each treatment.

After the exposure, pH of the growth medium and root surface were measured respectively with a pH-meter (Thermo Orion Star A121, Fisher Scientific Int., Pittsburgh, PA) and pH-strips (Fisher Scientific Int., Pittsburgh, PA).

4.3.3. *Growth analyses and biomass partitioning*

Immediately after the exposure, plant roots were gently removed from the tubes and washed with 50 mL CaCl₂ solution (5 mM) five times to remove the Ce and Cd elements deposited on root surface. The washing solutions and the growth media were collected for further analysis. Fresh leaves and root samples of three replicates from each treatment were collected for cerium speciation analysis. Detailed descriptions of the analytical parameters and procedures are provided below. The rest three replicates from each treatment were rinsed with DI three times, divided into roots and shoots and dried in an oven at 70 °C for 7 days to determine the total concentrations of Cd and Ce associated with soybean roots and shoots.

4.3.4. *Total Organic Carbon determination*

Total organic carbon (TOC) in the growth media was measured as an indicator of the excretion of plant root exudates. The growth medium at termination was first diluted by tap water to 50 mL. The diluted solution was then shaken for 12 hours on a shaker table. Subsequently, TOC in those

samples was measured by a TOC analyzer (Shimadzu TOC-VWP Analyzer, Japan) following reported procedures^{32,33}. TOC in the growth medium was then obtained by correcting the measured TOC with the dilution factor for each sample. Three replicates from each treatment were measured.

4.3.5. Investigation on the Association of Cd with CeO₂NPs and Plant Root Exudates

A parallel experiment was performed to evaluate the potential chemical interactions Cd with CeO₂NPs and biomolecules in plant exudates. To begin with, forty-two soybean seedlings were grown in 20% strength Hoagland solution in 50 mL centrifuge tubes for 21 days. Transpired water was replenished with the same strength Hoagland solution during cultivation. At termination, plant seedlings were removed, and the growth medium containing root exudates was centrifuged at 10,000 rpm for 10 min. Afterwards, the supernatant was decanted and the pellet at the bottom of each centrifuge tube was gently collected and transferred to a new tube in which the pellet was combined with pellets from six other tubes to further concentrate them. The pellets were assumed to contain large molecular weight molecules from exudates such as proteins, polysaccharides and border cells. Low molecular weight molecules in exudates such as short-chain aliphatic acids were expected to remain in the supernatant and were decanted. The combined pellets were re-suspended in 40 mL DI water and altogether six such tubes were prepared. They were divided into three groups. The first group was injected with 30 mg L⁻¹ of Cd²⁺, the second group 100 mg L⁻¹ of CeO₂NPs and the third group the combination of these two materials at the same concentrations. The tubes were shaken for 24 h on a shaker table and then centrifuged at 10,000 rpm for 15 min. The supernatant was then decanted, and the residual was desiccated at 90 °C of heat blocker for 4 hours to form a dried pellet for X-ray photoelectron spectroscopy (XPS) analysis. XPS was carried out using an Omicron ESCA (Scientia Omicron GmbH, Germany) connected to a probe

spectrometer with polychromatic Mg Ka X-rays ($h\nu = 1253.6$ eV). The grounded sample was taken on a stainless-steel sample holder using double sided adhesive conductive carbon tape. The X-ray run was performed at the power of 225 W where the pass energy was set to 100 eV for survey scans and 50 eV for specific regions to ensure sufficient sensitivity under a base pressure of 10^{-6} Pa. The calibration of the binding energies of the core levels was fixed at 284.8 eV for the main C 1s B.E peak. The peaks of XPS spectrum were fitted by Gaussian function using Origin software 2017 (OriginLab, Northampton, MA).

4.3.6. Statistical analyses.

Data were subjected to analysis of variance using a completely randomized experimental design. Since the experiment was set up as a 2×2 factorial experiment, CeO₂NPs vs. Cd, a two-way ANOVA analysis was carried out to differentiate the significance of independent variables: CeO₂NPs and Cd. In addition, one-way ANOVA was performed and means separation between treatments was obtained by the Tukey's post-hoc test. Data were analyzed using the Minitab 18 Statistical Software (Minitab Inc., State College, PA).

4.4. Results

4.4.1. Growth analysis and plant uptake of CeO₂NPs and Cd

Neither CeO₂NPs nor Cd at the applied concentrations, separately or in combination, caused any significant changes in the root and shoot dry biomass of soybean seedlings (Fig. 1). As expected, Ce concentrations increased in roots and shoots in CeO₂NPs treated plants compared to the controls (Fig. 2). Interestingly, the co-existence of Cd markedly decreased the concentration of Ce in soybean roots but not in shoots (Fig. 2). The Ce associated with soybean roots decreased by

51% in CeO₂NPs+ Cd treated plants but increased by 44% in the shoots compared to plants treated with CeO₂NPs alone. Two-way ANOVA showed a high level of interactions between CeO₂NPs and Cd for Ce accumulation in soybean tissues. Total Cd associated with soybean roots was unaffected by the presence of CeO₂NPs (Fig. 3). By contrast, the presence of CeO₂NPs led to a significant decrease of Cd in plant shoots by 78%. Significant interactions between CeO₂NPs and Cd were only found in shoots for Cd accumulation.

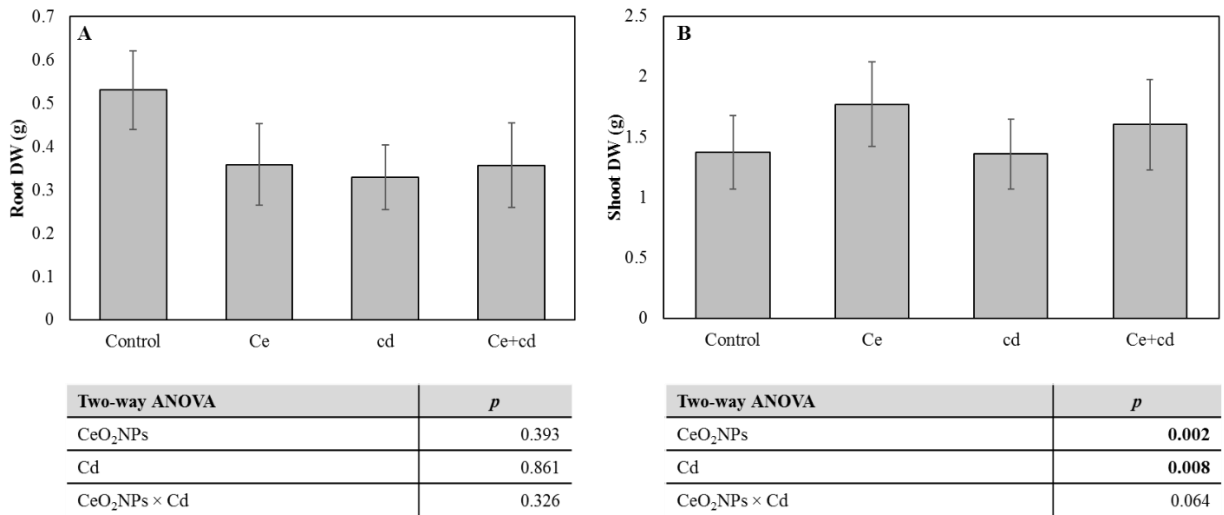


Fig. 4.1. Dry weight of *Glycine max* grown in the presence of 100 mg L⁻¹ CeO₂NPs and 1 mg L⁻¹ Cd. A: Root dry weigh, B: Shoot dry weight. Means labeled by different letters are significantly different by Tukey’s post-hoc test (*p* < 0.05). Error bars represent the standard deviation (n=3). Two-way ANOVA analysis are reported in tables.

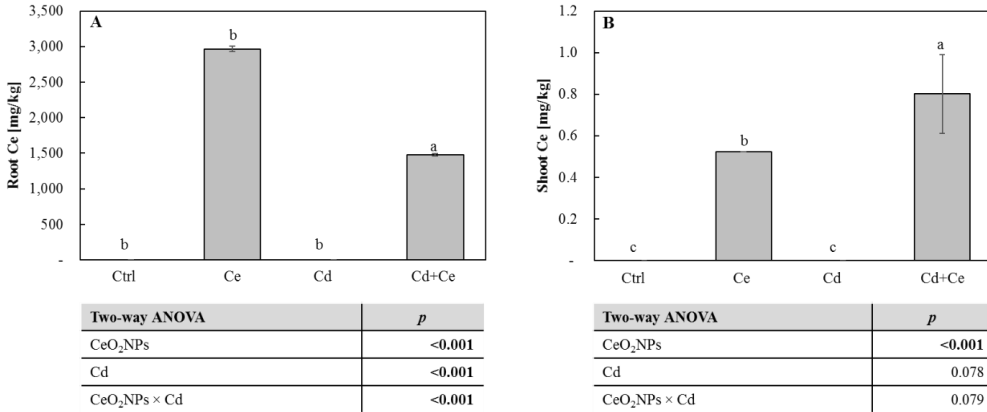


Fig. 4.2. Total cerium concentration in roots (A) and shoots (B) of *Glycine max* grown in the presence of 100 mg L⁻¹ CeO₂NPs and 1 mg L⁻¹ Cd. Means labeled by different letters are significantly different by Tukey's post-hoc test ($p < 0.05$). Error bars represent the standard deviation ($n=3$). Two-way ANOVA analysis are reported in tables.

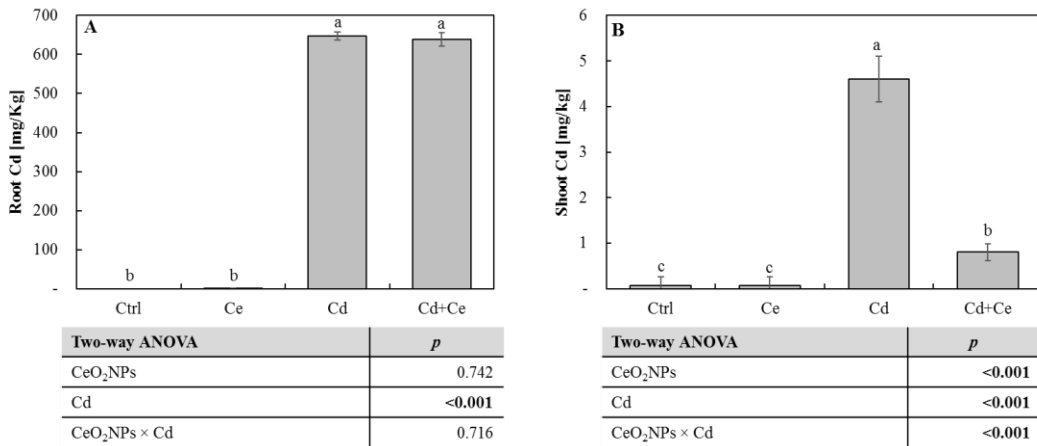


Fig. 4.3. Cadmium concentration (mg/kg) in root (A) and leaves (B) of *Glycine max* grew in the presence of 100 mg L⁻¹ CeO₂NPs and 1 mg L⁻¹ Cd. Means labeled by different letters are significantly different by Tukey's post-hoc test ($p < 0.05$). Error bars represent the standard deviation ($n=3$). Two-way ANOVA analysis are reported in tables.

4.4.2. Total organic carbon and pH

TOC in the growth media exposed to CeO₂NPs and/or Cd was higher than control plants. TOC in the growth medium from the joint treatment of CeO₂NPs and Cd was noticeably higher than that from the treatments with CeO₂NPs or Cd alone, even though the differences were not statistically significant (Fig. 4).

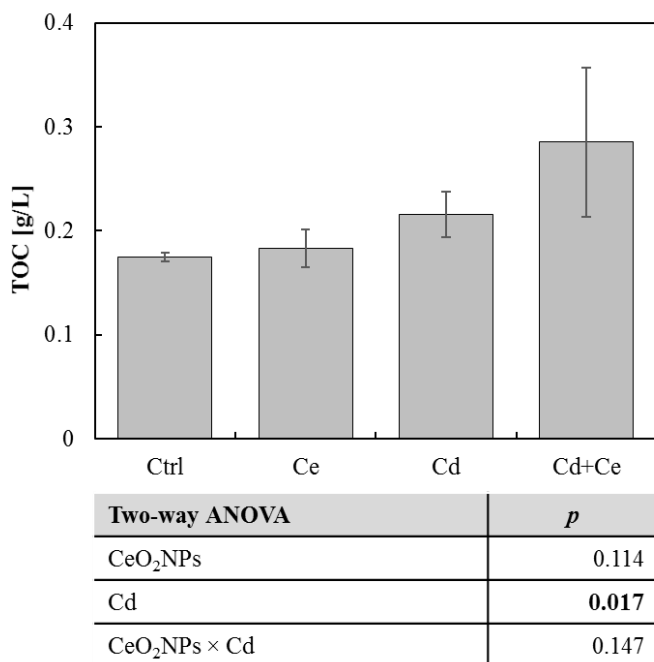


Fig. 4.4. Total organic carbon (TOC) in *Glycine max* grown in the presence of 100 mg L⁻¹ CeO₂NPs and 1 mg L⁻¹ Cd. A and D: Total biomass, B and E: Leaf biomass, C and F: Root biomass. Means labeled by different letters are significantly different by Tukey's post-hoc test (*p* < 0.05). Error bars represent the standard deviation (n=3). Two-way ANOVA analysis are reported in tables.

The pH values in the growth media and on root surface were significantly reduced by the joint exposure of CeO₂NPs and Cd (Table 1), and interactions between CeO₂NPs and Cd were found for pH on root surface. However, no significant interactions were found between CeO₂NPs and Cd in the growth media (Table 1).

Table 4.1. Root surface and growth medium pH values of *Glycine max* grown in the presence of 100 mg L⁻¹ CeO₂NPs and 1 mg L⁻¹ Cd. Means ± SD (n = 3) labeled by different letters are significantly different by Tukey's post-hoc test (p < 0.05).

<i>Treatments</i>	<i>Root pH</i>	<i>Medium pH</i>
Control	7.40 ± 0.10 <i>b</i>	7.69 ± 0.15 <i>ab</i>
CeO₂NPs	7.53 ± 0.06 <i>ab</i>	7.80 ± 0.06 <i>a</i>
Cd	7.40 ± 0.10 <i>ab</i>	7.66 ± 0.13 <i>ab</i>
Ce NPs + Cd	7.20 ± 0.10 <i>a</i>	7.50 ± 0.07 <i>b</i>
<i>Two-way ANOVA</i>	<i>p</i>	<i>p</i>
CeO₂NPs	0.527	0.633
Cd	0.014	0.025
CeO₂NPs × Cd	0.015	0.057

4.4.3. X-ray photoelectron spectroscopy

Cadmium spectra were shown in Fig. 5. Two fitting peaks (u and u') at the binding energy of 404.82 eV, and 411.82 eV were identified and they were assigned to Cd3d5/2 and Cd3d3/2 respectively^{34,35}. No Cd specific peaks were found in CeO₂ samples, but Cd peaks were detected in samples containing both root exudates and 30 mg L⁻¹ of Cd alone and samples containing part of the root exudates as well as 30 mg L⁻¹ of Cd and 100 mg L⁻¹ of CeO₂NPs. The results suggest that some Cd might have complexed with large molecules such as proteins and polysaccharides in plant root exudates or adsorbed on the surfaces of border cells, and some Cd might have adsorbed on the surface of CeO₂NPs. The evidence provided here is only qualitative, and quantitative characterization on the interactions between Cd and exudates and CeO₂NPs requires additional study, yet the results provided here do shed lights on the possible mechanisms for the interactions of CeO₂NPs and Cd in plant root rhizosphere.

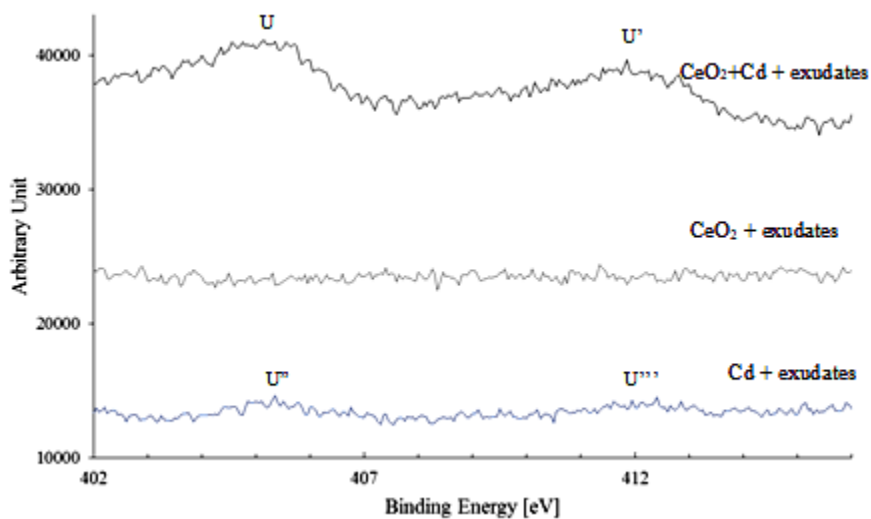


Fig. 4.5. The XPS spectrum of the presence of cadmium (30 mg/L) on the surface of CeO₂NPs (75 mg/L). Two peaks at B.E 404.82 eV, and 411.82 eV correspond to Cd3d5/2 and Cd3d3/2, respectively.

4.5. Discussion

Interests in the interactions between ENPs and co-present environmental pollutants in different environmental systems are growing ^{28,36,37}. Understanding their interactions in plant rhizosphere and the implications of these interactions for their accumulation in plant tissues have significant implications for food safety. In fact, consumption of food crops contaminated by various environmental pollutants represent a significant pathway for human exposure to these materials ³⁸⁻⁴⁰.

In this study we examined the reciprocal effects of CeO₂NPs and Cd in an aqueous system, avoiding many of the complications caused by soil particles, and allowing a mechanistic investigation on the interactions of CeO₂NPs and Cd in soybean rhizosphere. As shown in the results, CeO₂NPs, Cd and their interactions did not affect the overall dry weight and water transpiration, confirming that CeO₂NPs and Cd at the tested concentrations do not have any detrimental effects on plant growth and biomass, separately or together. Similar results have been reported in literature. In fact, Gui, Zhang, Liu, Ma, Zhang, He, Li, Zhang, Li, Rui, Liu and Cao ³⁹ reported that lettuce (*Lactuca sativa* L.) treated with 100 mg kg⁻¹ CeO₂NPs grew much faster than the controls. Similarly, Cao, et al. ⁴¹ demonstrated that 100 mg kg⁻¹ of CeO₂NPs improved the net photosynthesis rate and the Rubisco activity of soybean seedlings and enhanced the soybean water use efficiency (WUE).

A general observation in our study is that plant uptake and accumulation of Cd and Ce were affected by the co-presence of the other chemical, but the extent and pattern of alteration by co-existing chemicals differed. Cd led to a significant decrease of Ce in roots but a significant increase in leaves. For Cd, however, the co-occurrence of CeO₂NPs significantly reduced its concentration

in shoots but did not affect Cd associated with roots. This interesting observation was attributed to the complicated physical, chemical and biological processes co-occurring in soybean rhizosphere. First of all, as a result of the enhanced excretion of plant exudates as indicated by the higher TOC in the joint presence of CeO₂NPs and Cd, the pH in the rhizosphere and on plant root surface dropped in the co-presence of these two materials. The lower pH generally favors the dissolution of metals. But more importantly, in the cocktail of plant root exudates are many lower molecular weight acids, which can behave as reducing agents and enhance the reduction of Ce⁴⁺ to Ce³⁺, facilitating Ce uptake and transport to plant leaves⁴². Previous research has demonstrated that ionic Ce is much more efficiently transported from roots to shoots than CeO₂NPs^{17, 43}. Consequently, higher Ce was detected in soybean shoots exposed to both CeO₂NPs and Cd than those exposed to CeO₂NPs alone, even though the total Ce within root tissues was lower when plants were exposed to both materials simultaneously.

As described above, uptake of Cd is complicated, both apoplastic and symplastic pathways contribute to the entrance of Cd in plant root cells and then in the vascular system. The presence of CeO₂NPs can affect both pathways. In a recent study, we have found that the co-occurrence of CeO₂NPs and Cd altered the formation of “root apoplastic barriers” by depositing suberin on the cell wall of endodermal cells, compared to plants exposed to them separately¹⁹. The altered apoplastic barriers could affect Cd entrance through cellular hydraulic conductivity. It is also possible that CeO₂NPs may affect plant symplastic pathway by altering the functionality of ion transporters or the integrity of root cell membranes, leading to different Cd accumulation in plants. Such mechanisms have not been extensively explored, but some previous studies have shown that CeO₂NPs disrupt root membrane integrity^{30, 44}. Additionally, previous research with ENPs and co-existing organic contaminants has shown that the adsorption of organic compounds on ENPs

surfaces play a crucial role for the altered plant accumulation of organic compounds ^{8,45,46}. Similar process could occur between ENPs and heavy metal ions and indeed there have been many reports which showed the high adsorption capacity of heavy metals on ENP surfaces ^{20,47}. Particularly, Contreras, Garcia, Gonzalez, Casals, Puentes, Sanchez, Font and Recillas ²¹ showed that the adsorption capacity of Cd on CeO₂NPs was four times higher than that on TiO₂NPs. In our study, while detailed adsorption study was not performed, we have conducted a qualitative study in which CeO₂NPs and Cd were mixed in growth media containing some actual root exudates. Our results (Fig. 6) indicated that Cd was detected in dry pellets containing CeO₂NPs, suggesting a likely adsorption of Cd on CeO₂NPs. Because of the relatively less efficient root-to-shoot transport of CeO₂NPs, the adsorbed Cd would penetrate into roots with CeO₂NPs, but was less effectively transported to shoots. This possible interaction between Cd and CeO₂NPs is consistent with the lower Cd in plant shoots in the co-presence of CeO₂NPs and Cd, while Cd in the roots was unaffected. In addition, the co-existence of CeO₂NPs and Cd resulted in greater release of exudates as shown above, Cd may form complexes with organic exudates outside plant roots. Previous studies have shown that the Cd chelates are transported into plant root cells through different protein transporters such as YSL protein ^{48,49}. Earlier research also demonstrated that chelated Cd is more effectively sequestered in the vacuole of plant root cells, reducing the loading efficiency to xylem tissues and therefore less efficient translocation to shoots ^{4,10,14,15}. The formation of Cd-exudate complexes is supported by the XPS analysis (Fig. 6). The adsorption of Cd into biomolecules was shown to be strongest at pH>5 ³⁴. In this study, pH in the growth media was above 6, suggesting that affiliation between Cd and large size biomolecules in root exudates was possible.

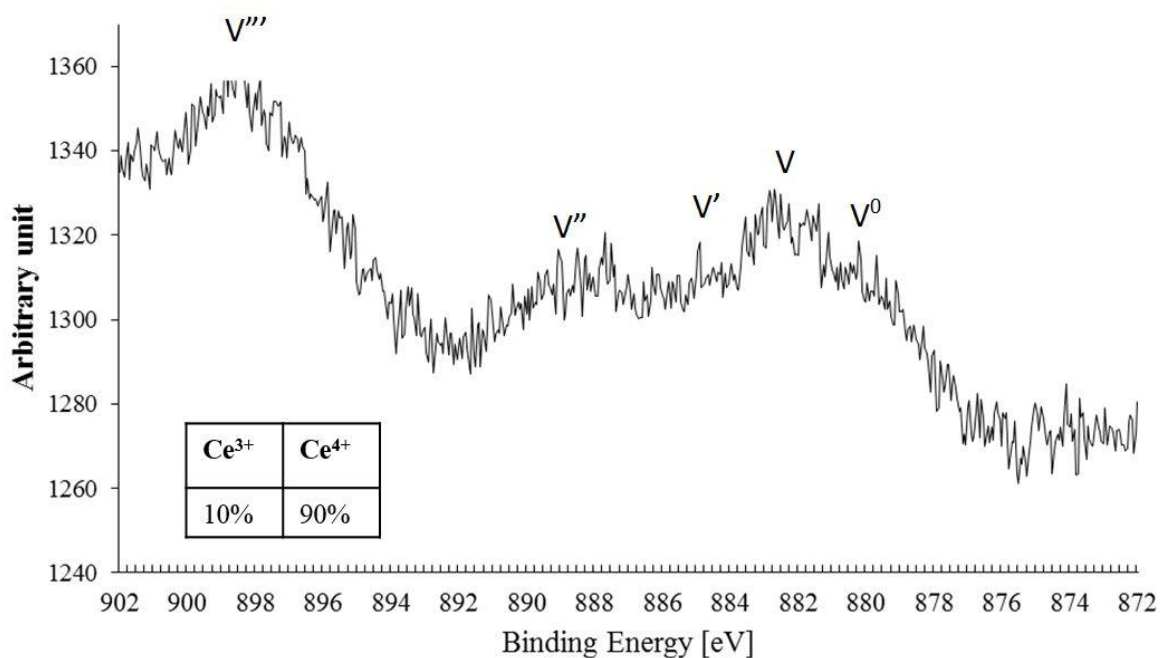


Fig. 4.6. illustrates the Ce $3d_{3/2,5/2}$ spectra obtained for the CeO_2 compound and dissociated ions. The CeO_2 spectrum is composed of two multiplets in five peaks Ce (IV) = v,v'',v''' and Ce(III) = v^o, v' with a ratio of Ce⁴⁺: Ce³⁺, 90%:10%. These multiplets attributed to the spin-orbit split $3d_{5/2}$ and $3d_{3/2}$ core holes [4]. The five identical peaks corresponding to the pairs of spin-orbit doublets were consistent with results from other authors[4]. The highest binding energy peaks, v''' located at B.E 898.3 ± 0.1 eV is the result of a Ce $3d^9 4f^0$ O $2p^6$ final state. The low binding energy states v and v' respectively located at 882.7 and 888.5 ± 0.1 eV are the result of Ce $3d^9 4f^2$ O $2p^4$ and Ce $3d^9 4f^1$ O $2p^5$ final states.

4.6. Conclusions

Overall, we have observed significant interactions between co-existing CeO_2 NPs and Cd on plant uptake of these metal elements. It appears that the co-presence of Cd with CeO_2 NPs led to higher excretion of plant root exudates, lowered the pH values on root surface and enhanced CeO_2 NPs dissolution, therefore resulted in lower accumulation of Ce in plant roots but higher accumulation

of Ce in plant shoots. This statement is supported by the higher Ce content in the root washing solution from the CeO₂NPs + Cd treated plants which indicated that higher amount of Ce was attached to plant root surface but did not penetrate into the tissues. Alternatively, the presence of CeO₂NPs may provide an adsorption site for Cd and reduces its uptake into plants. The elevated release of root exudates may be another possible reason for the reduced Cd in plant shoots. The study provides important new insights in the chemical mechanisms for Cd and CeO₂NPs interactions in plant root region. Due to the complex processes involved in both materials, future studies should aim to elucidate more molecular mechanisms on the mutual effects of these chemicals on their uptake and accumulation by plants.

4.7. References

1. Rossi, L.; Sharifan, H.; Zhang, W.; Schwab, A. P.; Ma, X., Mutual effects and in planta accumulation of co-existing cerium oxide nanoparticles and cadmium in hydroponically grown soybean (*Glycine max* (L.) Merr.). *Environmental Science: Nano* **2018**, *5*, (1), 150-157.
2. Clemens, S.; Ma, J. F., Toxic heavy metal and metalloid accumulation in crop plants and foods. *Annual review of plant biology* **2016**, *67*, 489-512.
3. Clemens, S.; Aarts, M. G.; Thomine, S.; Verbruggen, N., Plant science: the key to preventing slow cadmium poisoning. *Trends in plant science* **2013**, *18*, (2), 92-99.
4. Li, L.-Z.; Tu, C.; Peijnenburg, W. J. G. M.; Luo, Y.-M., Characteristics of cadmium uptake and membrane transport in roots of intact wheat (*Triticum aestivum* L.) seedlings. *Environmental Pollution* **2017**, *221*, 351-358.
5. Lu, L.-l.; Tian, S.-k.; Yang, X.-e.; Li, T.-q.; He, Z.-l., Cadmium uptake and xylem loading are active processes in the hyperaccumulator *Sedum alfredii*. *Journal of Plant Physiology* **2009**, *166*, (6), 579-587.

6. Cai, F.; Wu, X.; Zhang, H.; Shen, X.; Zhang, M.; Chen, W.; Gao, Q.; White, J. C.; Tao, S.; Wang, X., Impact of TiO₂ nanoparticles on lead uptake and bioaccumulation in rice (*Oryza sativa* L.). *NanoImpact* **2017**, *5*, 101-108.
7. De La Torre-Roche, R.; Hawthorne, J.; Deng, Y.; Xing, B.; Cai, W.; Newman, L. A.; Wang, Q.; Ma, X.; Hamdi, H.; White, J. C., Multiwalled carbon nanotubes and C60 fullerenes differentially impact the accumulation of weathered pesticides in four agricultural plants. *Environmental Science & Technology* **2013**, *47*, (21), 12539-12547.
8. Ma, X.; Wang, C., Fullerene nanoparticles affect the fate and uptake of trichloroethylene in phytoremediation systems. *Environmental Engineering Science* **2010**, *27*, (11), 989-992.
9. Lux, A.; Martinka, M.; Vaculík, M.; White, P. J., Root responses to cadmium in the rhizosphere: a review. *Journal of Experimental Botany* **2010**, *62*, (1), 21-37.
10. Cataldo, D. A.; Garland, T. R.; Wildung, R. E., Cadmium uptake kinetics in intact soybean plants. *Plant physiology* **1983**, *73*, (3), 844-848.
11. Lu, L.; Tian, S.; Zhang, M.; Zhang, J.; Yang, X.; Jiang, H., The role of Ca pathway in Cd uptake and translocation by the hyperaccumulator *Sedum alfredii*. *Journal of Hazardous Materials* **2010**, *183*, (1), 22-28.
12. Guerinot, M. L., The ZIP family of metal transporters. *Biochimica et Biophysica Acta (BBA)-Biomembranes* **2000**, *1465*, (1), 190-198.
13. Sharifan, H., Commentary on “Characteristics of cadmium uptake and membrane transport in roots of intact wheat (*Triticum aestivum* L.) seedlings” reported by Lian-Zhen Li, Chen Tu, Willie J.G.M. Peijnenburg, Yong-Ming Luo. *Environmental Pollution* **2017**.
14. Shute, T.; Macfie, S. M., Cadmium and zinc accumulation in soybean: A threat to food safety? *Science of The Total Environment* **2006**, *371*, (1), 63-73.

15. Tudoreanu, L.; Phillips, C., Modeling cadmium uptake and accumulation in plants. *Advances in agronomy* **2004**, *84*, 121-157.
16. Schymura, S.; Fricke, T.; Hildebrand, H.; Franke, K., Elucidating the Role of Dissolution in CeO₂ Nanoparticle Plant Uptake by Smart Radiolabeling. *Angewandte Chemie International Edition* **2017**.
17. Zhang, W.; Ebbs, S. D.; Musante, C.; White, J. C.; Gao, C.; Ma, X., Uptake and accumulation of bulk and nanosized cerium oxide particles and ionic cerium by radish (*Raphanus sativus* L.). *Journal of agricultural and food chemistry* **2015**, *63*, (2), 382-390.
18. Zhao, L.; Peng, B.; Hernandez-Viezcas, J. A.; Rico, C.; Sun, Y.; Peralta-Videa, J. R.; Tang, X.; Niu, G.; Jin, L.; Varela-Ramirez, A., Stress response and tolerance of Zea mays to CeO₂ nanoparticles: cross talk among H₂O₂, heat shock protein, and lipid peroxidation. *ACS nano* **2012**, *6*, (11), 9615-9622.
19. Rossi, L.; Zhang, W.; Ma, X., Cerium oxide nanoparticles alter the salt stress tolerance of *Brassica napus* L. by modifying the formation of root apoplastic barriers. *Environmental Pollution* **2017**, *229*, 132-138.
20. Cao, C.-Y.; Cui, Z.-M.; Chen, C.-Q.; Song, W.-G.; Cai, W., Ceria hollow nanospheres produced by a template-free microwave-assisted hydrothermal method for heavy metal ion removal and catalysis. *The Journal of Physical Chemistry C* **2010**, *114*, (21), 9865-9870.
21. Contreras, A. R.; Garcia, A.; Gonzalez, E.; Casals, E.; Puentes, V.; Sanchez, A.; Font, X.; Recillas, S., Potential use of CeO₂, TiO₂ and Fe₃O₄ nanoparticles for the removal of cadmium from water. *Desalination and water treatment* **2012**, *41*, (1-3), 296-300.

22. Casals, E.; Pfaller, T.; Duschl, A.; Oostingh, G. J.; Puentes, V. F., Hardening of the nanoparticle–protein corona in metal (Au, Ag) and oxide (Fe₃O₄, CoO, and CeO₂) nanoparticles. *Small* **2011**, *7*, (24), 3479-3486.
23. Ji, Y.; Zhou, Y.; Ma, C.; Feng, Y.; Hao, Y.; Rui, Y.; Wu, W.; Gui, X.; Le, V. N.; Han, Y.; Wang, Y.; Xing, B.; Liu, L.; Cao, W., Jointed toxicity of TiO₂ NPs and Cd to rice seedlings: NPs alleviated Cd toxicity and Cd promoted NPs uptake. *Plant Physiology and Biochemistry* **2017**, *110*, 82-93.
24. Keller, A. A.; Wang, H.; Zhou, D.; Lenihan, H. S.; Cherr, G.; Cardinale, B. J.; Miller, R.; Ji, Z., Stability and aggregation of metal oxide nanoparticles in natural aqueous matrices. *Environ. Sci. Technol* **2010**, *44*, (6), 1962-1967.
25. Zhao, Y.; Fang, X.; Mu, Y.; Cheng, Y.; Ma, Q.; Nian, H.; Yang, C., Metal pollution (Cd, Pb, Zn, and As) in agricultural soils and soybean, glycine max, in southern China. *Bulletin of environmental contamination and toxicology* **2014**, *92*, (4), 427-432.
26. Osborne, S. A.; Mills, G.; Hayes, F.; Ainsworth, E. A.; Bölker, P.; Emberson, L., Has the sensitivity of soybean cultivars to ozone pollution increased with time? An analysis of published dose–response data. *Global change biology* **2016**, *22*, (9), 3097-3111.
27. Newbigging, A. M.; Yan, X.; Le, X. C., Cadmium in soybeans and the relevance to human exposure. *Journal of Environmental Sciences* **2015**, *37*, (11), 157-162.
28. Holden, P. A.; Klaessig, F.; Turco, R. F.; Priester, J. H.; Rico, C. M.; Avila-Arias, H.; Mortimer, M.; Pacpaco, K.; Gardea-Torresdey, J. L., Evaluation of Exposure Concentrations Used in Assessing Manufactured Nanomaterial Environmental Hazards: Are They Relevant? *Environmental Science & Technology* **2014**, *48*, (18), 10541-10551.

29. Ma, X.; Wang, Q.; Rossi, L.; Ebbs, S.; White, J., Multigenerational Exposure to Cerium Oxide Nanoparticles: Physiological and Biochemical Analysis Reveals Transmissible Changes in Rapid Cycling Brassica rapa. *NanoImpact* **2016**.
30. López-Moreno, M. L.; de la Rosa, G.; Hernández-Viezcas, J. Á.; Castillo-Michel, H.; Botez, C. E.; Peralta-Videa, J. R.; Gardea-Torresdey, J. L., Evidence of the differential biotransformation and genotoxicity of ZnO and CeO₂ nanoparticles on soybean (*Glycine max*) plants. *Environmental science & technology* **2010**, *44*, (19), 7315-7320.
31. Hoagland, D. R.; Arnon, D. I., The water-culture method for growing plants without soil. *Circular. California Agricultural Experiment Station* **1950**, *347*, (2nd edit).
32. Wu, S.-Z.; Li, K.; Zhang, W.-D., On the heterostructured photocatalysts Ag₃VO₄/gC₃N₄ with enhanced visible light photocatalytic activity. *Applied Surface Science* **2015**, *324*, 324-331.
33. Ming, C. A.; Takako, T., High Sensitivity Total Organic Carbon Analysis. *Notes* **2003**, *2*, 0.9995.
34. Tan, G.; Xiao, D., Adsorption of cadmium ion from aqueous solution by ground wheat stems. *Journal of hazardous materials* **2009**, *164*, (2), 1359-1363.
35. Wang, F.-Z.; Shang, D.-C.; Wang, M.-G.; Hu, S.-G.; Li, Y.-Q., Incorporation and substitution mechanism of cadmium in cement clinker. *Journal of Cleaner Production* **2016**, *112*, 2292-2299.
36. Khan, M. N.; Mobin, M.; Abbas, Z. K.; AlMutairi, K. A.; Siddiqui, Z. H., Role of nanomaterials in plants under challenging environments. *Plant Physiol. Biochem.* **2017**, *110*, 194-209.

37. Grillo, R.; Rosa, A. H.; Fraceto, L. F., Engineered nanoparticles and organic matter: A review of the state-of-the-art. *Chemosphere* **2015**, *119*, 608-619.
38. Maurer-Jones, M. A.; Gunsolus, I. L.; Murphy, C. J.; Haynes, C. L., Toxicity of Engineered Nanoparticles in the Environment. *Analytical Chemistry* **2013**, *85*, (6), 3036-3049.
39. Gui, X.; Zhang, Z.; Liu, S.; Ma, Y.; Zhang, P.; He, X.; Li, Y.; Zhang, J.; Li, H.; Rui, Y.; Liu, L.; Cao, W., Fate and Phytotoxicity of CeO₂ Nanoparticles on Lettuce Cultured in the Potting Soil Environment. *PLoS One* **2015**, *10*, (8), e0134261.
40. Mustafa, G.; Komatsu, S., Toxicity of heavy metals and metal-containing nanoparticles on plants. *Biochimica et Biophysica Acta (BBA) - Proteins and Proteomics* **2016**, *1864*, (8), 932-944.
41. Cao, Z. M.; Stowers, C.; Rossi, L.; Zhang, W. L.; Lombardini, L.; Ma, X. M., Physiological effects of cerium oxide nanoparticles on the photosynthesis and water use efficiency of soybean (*Glycine max* (L.) Merr.). *Environ.-Sci. Nano* **2017**, *4*, (5), 1086-1094.
42. Zhang, W.; Dan, Y.; Shi, H.; Ma, X., Elucidating the mechanisms for plant uptake and in-planta speciation of cerium in radish (*Raphanus sativus* L.) treated with cerium oxide nanoparticles. *Journal of Environmental Chemical Engineering* **2017**, *5*, (1), 572-577.
43. Zhang, W.; Dan, Y.; Shi, H.; Ma, X., Effects of Aging on the Fate and Bioavailability of Cerium Oxide Nanoparticles to Radish (*Raphanus sativus* L.) in Soil. *ACS Sustainable Chemistry & Engineering* **2016**, *4*, (10), 5424-5431.
44. Peng, C.; Chen, Y.; Pu, Z.; Zhao, Q.; Tong, X.; Chen, Y.; Jiang, L., CeO₂ nanoparticles alter the outcome of species interactions. *Nanotoxicology* **2017**, (just-accepted), 1-38.

45. Ma, X.; Anand, D.; Zhang, X.; Talapatra, S., Adsorption and desorption of chlorinated compounds from pristine and thermally treated multiwalled carbon nanotubes. *The Journal of Physical Chemistry C* **2011**, *115*, (11), 4552-4557.
46. Zhang, W.; Musante, C.; White, J. C.; Schwab, P.; Wang, Q.; Ebbs, S. D.; Ma, X., Bioavailability of cerium oxide nanoparticles to *Raphanus sativus* L. in two soils. *Plant Physiol. Biochem.* **2017**, *110*, 185-193.
47. Contreras, A.; Casals, E.; Puentes, V.; Komilis, D.; Sánchez, A.; Font, X., Use of cerium oxide (CeO₂) nanoparticles for the adsorption of dissolved cadmium (II), lead (II) and chromium (VI) at two different pHs in single and multi-component systems. *Global Nest Journal* **2015**, *17*, (3), 536-543.
48. Song, Y.; Jin, L.; Wang, X., Cadmium absorption and transportation pathways in plants. *International journal of phytoremediation* **2017**, *19*, (2), 133-141.
49. Lin, Y.-F.; Aarts, M. G., The molecular mechanism of zinc and cadmium stress response in plants. *Cellular and molecular life sciences* **2012**, *69*, (19), 3187-3206.

CHAPTER V

ZINC OXIDE NANOPARTICLES ALLEVIATED THE BIOAVAILABILITY OF CADMIUM AND LEAD AND CHANGED THE UPTAKE OF IRON IN HYDROPONICALLY GROWN LETTUCE (*LACTUCA SATIVA L. VAR. LONGIFOLIA*⁴)

5.1. Summary

Leafy vegetables are a rich source of iron and fibers for the human diet, which may become hazardous if exposed to heavy metals contamination. Cadmium (Cd) and lead (Pb) are two highly toxic metals even at trace concentrations. Engineered nanoparticles (ENPs) can alter the uptake of heavy metals and localization of essential minerals such as iron (Fe) through different mechanisms. The goal of this study was to understand the mutual effects of zinc oxide nanoparticles (ZnONPs) and coexisting heavy metals Pb^{2+} and Cd^{2+} on their uptake and accumulation as well as their effects on Fe concentrations in romaine lettuce (*Lactuca sativa L. var. Longifolia*) in a hydroponic system. At termination, shoots were gently separated from the roots, and the concentrations of Pb, Cd, Fe, and Zn in all plant tissues were quantified by inductively coupled plasma-mass spectrometry (ICP-MS). In addition, microbial density analysis in the growth media was performed for each treatment. The results indicated active interactions between ZnONPs and coexisting divalent heavy metals. ZnONPs significantly reduced the accumulation of Cd and Pb in roots by 49% and 81%. In shoots, Cd was reduced by 30%, and Pb elevated by 44%. Fe concentration in shoots was strongly affected by the presence of ZnONPs, and the total Zn in shoots was negatively correlated with the microbial population in the growth media. Exposure to ZnONPs alone increased the total Fe in shoots by 80% compared to controls, and the copresence of ZnONPs and heavy metals increased Fe concentration by about 77%. The results revealed the

⁴Reprinted with permission from (H Sharifan, X Ma, JMC Moore, MR Habib, C Evans., |Zinc oxide nanoparticles alleviated the bioavailability of cadmium and lead and changed the uptake of iron in hydroponically grown lettuce (*Lactuca sativa L. var. Longifolia*). *ACS Sustainable Chemistry & Engineering* **2019**, *7*, 16401-16409.). Copyright (2019) American Chemical Society."

role of ENPs in governing the uptake and translocation of some essential elements and toxic heavy metals in plants.

Keywords: Zinc oxide nanoparticles; Cadmium; Lead; Iron, Lettuce

5.2. Introduction

The applications of engineered metallic oxide nanoparticles in agriculture, and food processing sectors have massively increased ¹⁻³. These engineered nanoparticles (ENPs) can promote the cultivation of dietary plants, including crops and leafy vegetables by reducing the uptake of heavy metals or improving their post harvesting qualities ^{4,5}. ENPs may also increase the shelf life of vegetables by reducing the heavy metal content or act as a strong anti- microbial/fungal agent ^{4,6}.

However, the mechanistic interactions of ENPs with biological systems needs further investigation. For example, several studies have been conducted to elucidate the interactions of ENPs with leguminous plants, but there is a serious lack of studies on ENPs interactions with leafy vegetables that are directly consumed by humans ^{1,7}. Leafy vegetables allegedly accumulate higher concentrations of heavy metals in their edible tissues compared to legumes ⁸. Consumption of leafy vegetables is recommended to pregnant women because of its high iron (Fe) content ⁹. Recent studies showed a significant role of leafy vegetables in the birth weight of newborns by comparing mothers who consumed leafy vegetable and those who did not ^{9,10}. Therefore, controlling the level of microelements in leafy vegetables is of high interest for food scientists and engineers. Production of leafy vegetables has advanced to a fast production track through the application of large urban hydroponic systems ¹¹⁻¹³. Such production systems greatly increase the exposure of leafy vegetables to heavy metals and emerging chemicals such as ENPs through irrigation, atmospheric fallouts or direct applications of nanoagrichemicals ^{14,15}. Co-exposure of

leafy vegetables to ENPs and heavy metals affects plant growth and food safety through their mutual effects on plant uptake and accumulation of these chemicals ¹⁶.

Cadmium (Cd) and lead (Pb) are two ubiquitous carcinogenic contaminants ^{17,18}. Major sources of these metals include mining, emission of fuels, municipal wastes, fertilizers, and pesticide applications ¹⁹. Consumption of contaminated vegetables by Cd and Pb is an important pathway for human exposure ¹⁵. For instance, food consumption corresponds to approximately 90% of Cd and Pb ingestion in non-smoking people around the world ^{20,21}. Pb intake by pregnant women may lead to reduced birth weight, length, and head circumference of new born babies ^{22,23}. Therefore, efforts to alleviate the uptake of heavy metals by dietary plants are of high interest. Potential effects of ENPs interactions with leafy vegetables that are exposed to heavy metals may also alter the bioavailability of essential minerals such as Fe, and the microbial community, which has not been explored as a critical factor in plant ENPs interactions. Microbial communities in hydroponics can be highly beneficial for plant nitrogen fixation, phosphate mobilization, and mediating nutrient uptake ²⁴.

ZnONPs is a frequently used metallic ENPs in a variety of industrial and agricultural products ^{4,6}. For example, ZnONPs have been introduced as an effective nanofertilizer due to its capability to enrich agricultural soils with Zn deficit ²⁵. ZnO is also currently used as a food additive ²⁶. In addition, it acts as an antimicrobial agent, which exhibits strong activity at low concentrations ⁶. Also, it plays a vital role in plant metabolic processes, promoting the synthesis of carotenoids and chlorophylls, resulting in higher photosynthetic performance ²⁵. Some studies reported the toxicity of ZnONPs at high concentrations, and the effects of ZnONPs on the upregulation of Fe in plants is suspected because both ions share the same transporting membrane proteins (Zinc / Iron Regulatory Transporter Proteins family) ²⁷. Therefore, the primary goal of this study was to

investigate the interactions of romaine lettuce (*Lactuca sativa L. var. Longifolia*) with the coexisting ZnONPs, Cd, and Pb and to monitor the translocation of Fe in plant tissues.

Romaine lettuce (*Lactuca sativa L. var. Longifolia*) is a frequently consumed leafy vegetable which is rich in bioactive compounds, essential minerals, and dietary fibers ^{28,29}. The dry or fresh consumption of lettuce through a variety of foods has been extensively increased due to its rich flavor, anti-cancer properties, and high vitamin content ^{28,30}. Therefore, it is formulated in dietary supplements and is a proposed diet for infants ³¹. A hydroponic system was used because mass vegetable productions are obtained through this system. Furthermore, it avoids the interfering effects of soil and the microorganisms in the soil.

5.3. Materials and Methods

5.3.1. Materials

Negatively charged ZnONPs (20% by weight, 10-30 nm) was purchased from the US Research Nanomaterials, Inc. (Houston, TX). High purity Pb ($\text{Pb}(\text{NO}_3)_2$ >99%) was obtained from Alfa Aesar (Ward Hill, MA), and Cd sulfate (CdSO_4) was purchased from Fisher Scientific Inc. (Pittsburgh, PA). Dextrose agar was purchased from Sigma-Aldrich, Merck KGaA, Darmstadt, Germany. All analytical standards of Pb, Cd, Zn, Fe (10000 ppm, %3 nitric acid) were obtained from RICCA Chemical Company, Arlington, TX.

5.3.2. ZnONPs Characterization

The size and shape of the ZnO were fully characterized in our previous study by a Tecnai G2 F20 transmission electron microscope (TEM) ⁷. Briefly, the ZnONPs is primarily spherical, but a small fraction of the particles has triangular or other irregular shapes. The mean diameter of ZnONPs

was around 68.1 nm, within a range of 15 to 137 nm. The hydrodynamic size in 100 mg L⁻¹ water solution was 621.1±7.6 nm determined via dynamic light scattering (DLS). The zeta potential was about -28.8±2.0 mV.

5.3.3. Plant Culture and Exposure Experiments

The lettuce seeds were purchased from Johnny's Selected Seeds (Winslow, ME). The seeds were germinated in moist sand in a greenhouse at a controlled temperature (25°C) under fluorescent light providing 250 μmol m² s⁻¹ photosynthetic photon flux density (16/8 h light/dark cycle). Germinated lettuce seedlings were transferred to clay soil in 12 cm x 10 cm square pots for 14 days. Afterward, the plant seedlings were gently removed from the soil, and roots were thoroughly washed with DI water to remove soil residual, and each plant was immediately transplanted to a 50 mL volume hydroponic system (Becton, Dickinson and Co., Franklin Lakes, NJ, USA) containing one fourth strength Hoagland solution (Phyto Technology Lab, Shawnee Mission, KS). To keep the root area dark, the tubes were covered by aluminum foil.

When the transpiration rate reached 10 mL /day (after 10 days), the plants were transferred from the Hoagland solution to new tubes, which were filled with solutions containing 100 mg L⁻¹ Pb²⁺ + 1.0 mg L⁻¹ Cd²⁺ and/or 100 mg L⁻¹ ZnONPs in DI water. During the exposure period, the Hoagland solution was avoided due to the high ionic strength of the nutrient solution that induces aggregation of the ZnONPs. The hydroponic system was used to prevent sorption of the dosed ZnONPs to soil particles and to ensure that the added ENPs and heavy metals were fully bioavailable¹³. Four replicates for each treatment as well as three replicates of blank controls were grown. To determine water evaporation, two tubes with no plants were placed among the plants. Lettuce seedlings were cultivated in the hydroponic system containing the target solution for an additional 10 days. During the

exposure time, growth media were replenished with DI water two times per day (morning and evening). The plants were randomly rotated and relocated to ensure equal light exposure. After the heavy metal/ENPs exposure, the pH of the growth medium was measured with a pH meter (VWR symphony – SB90M5) at termination.

5.3.4. Growth analyses and biomass partitioning

Immediately after the exposure, plant roots were removed from the hydroponic system and washed with 50 mL CaCl₂ solution (5 mM) five times to remove the Zn, Pb and Cd elements deposited on the root surface²⁰. The growth media were collected for further analysis. Harvested plants were separated into leafy tissues and roots. The fresh weight was measured for three or four replicates of leaves and roots from each treatment. Stem and root lengths were measured with a ruler. To prepare the samples for metal content analysis, fresh samples were dried in an oven at 75°C for 5 days to ensure that the tissues are fully dehydrated. The dry biomass was then determined^{7,20}.

5.3.5. Heavy metals and trace elements of content analyses

An aliquot of 0.15 g of dry leaf and 0.05 g of dry root tissues were homogenized via a household blender (Braun Multiquick MX 2050). Next, the samples were placed into a DigiPREP MS hot block digester (SCP Science, Clark Graham, Canada) and pre-digested with 3 mL of 70% (v/v) nitric acid (Certified ACS Plus) overnight³². Then the samples were heated at 95 °C for 4 hours following the EPA method 3050b^{32,33}. After being cooled down to room temperature, 2 mL of 30% (w/v) H₂O₂ were added to the samples and re-heated in the hot block at 95 °C for an additional 2 hours until fully digested⁷. To quantify Zn, Pb, Cd and Fe, the digest solution was diluted 15 times in ultra-pure water (18.2 MΩ cm, P.LAB Option-Q) containing 1% nitric acid and the element concentrations were quantified by an

inductively coupled plasma-mass spectroscopy (ICP-MS) (Agilent 7500i, Agilent Technologies Co. Ltd, USA) ^{32,33}.

5.3.6. Rhizosphere microbial population assay

Immediately after removing the seedlings from the hydroponic system and pH measurement, 100 μL of the growth medium of each treatment were collected for the microbial analysis. In total, 12 subsamples containing three replicates for each treatment were prepared. Subsequently, the aliquots were ten times diluted (1:10) in ultra-pure water (18.2 M Ω), and strains in 100 μL of the subsamples with no turbidity were loop-inoculated over 100 mm \times 15 mm sterile Petri-dishes containing potato dextrose agar. Next, agar plates were incubated for two days at 37 °C ³⁴. Finally, the colony-forming unit (CFU) was counted ³⁵.

5.3.7. Statistical Analysis

Statistical analysis of Zn, Pb, Cd, and Fe in both shoot and root tissues were performed using the Minitab 18 Statistical Software (Minitab Inc., State College, PA, USA). The One-Way ANOVA followed by Tukey's test at a significance level 5% ($p < 0.05$) was applied to compare the mean values between different treatments of dry weight, pH, CFU and metal concentrations.

5.4. Results

5.4.1. Biomass and Plant Growth

Figure 5.1A, B illustrates the measured dry weight of both roots and shoots under four different treatments. Error bars in each column correspond to the standard deviation. Both the shoot and root dry weight were strongly impacted by ZnONPs. This impact is more profound in shoot dry

weight than root dry weight. ZnONPs alone significantly ($0.05 < P$) reduced the dry shoot biomass by 57%. The co-exposure of Pb and Cd with ZnONPs lowered the dry shoot biomass by 46%. There were no statistically significant impacts of ZnONPs on the dry biomass of roots, but the average root dry biomass was reduced by 50% in the sole presence of ZnONPs compared to the control. The dry biomass data showed strong correlations with the stem and root lengths.

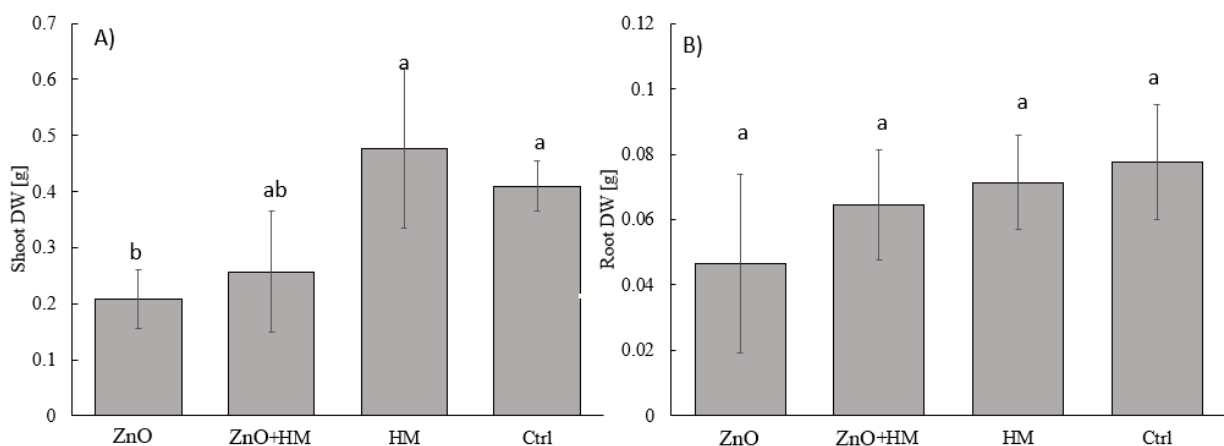


Fig.5.1.1. Dry biomass of lettuce tissues under different treatments including combinations of 1 mg/L of Cd, 100 mg/L Pb and/or 100 mg/L ZnONPs. A) Shoot dry biomass of lettuce treated with different treatments and B) Root dry biomass of lettuce exposed to different combinations of heavy metals and ZnONPs. The column represents the mean value. The error bars indicate standard deviation ($n = 3$ or 4). Different letters designate significant differences ($p \leq 0.05$) analyzed via one-way ANOVA followed by Tukey's test. HM: heavy metals.

Figure 5 A shows images of lettuce from different treatments. Figure 5 B reports the root and shoot length of lettuce from four different treatments. Similar to what was observed for the dry biomass, shoot length was strongly impacted by the presence of the ZnONPs. Heavy metals alone reduced

the shoot length insignificantly by 7%. When (co)-exposed to ZnONPs, the shoot length was significantly reduced by approximately 30% compared to control, with and without the heavy metals ($p < 0.05$)

A similar pattern of root elongation was observed. Introduction of ZnONPs significantly ($0.05 < p$) reduced the length of the roots by 28% in the co-presence of heavy metals and 36% in its sole exposure. The impact of heavy metals on root elongation was insignificant.

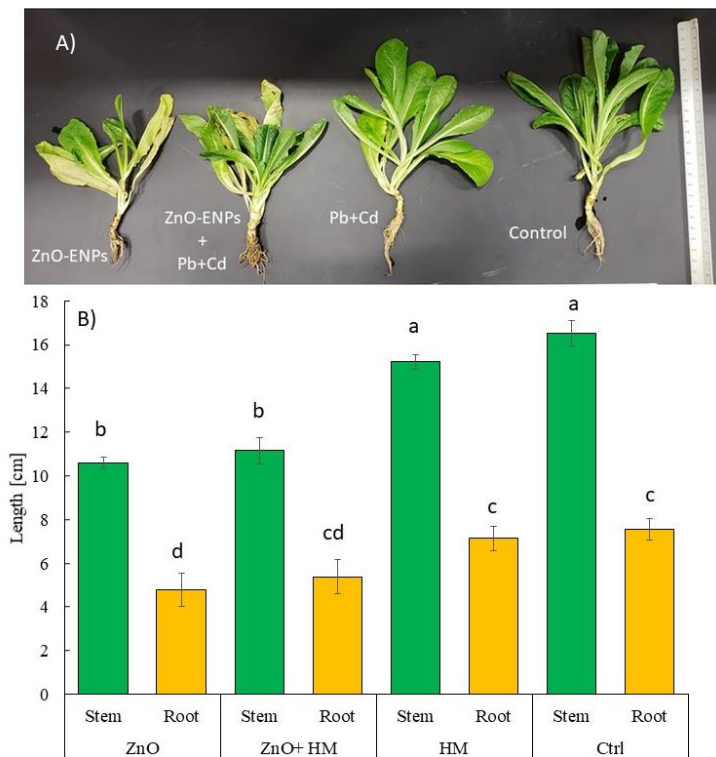


Fig. 5.2. (A) Phenotype of *Lactuca sativa* L. var. *Longifolia* plants grown in hydroponic systems after exposure to different combinations of 1 mg/L of Cd+100 mg/L Pb and 100 mg/L ZnONPs, ; (B) Illustrates the impacts of the four different treatments on plant root and shoot length. Error bars represent standard deviation. Letters above each column differentiate the significance level ($p \leq 0.05$).

5.4.2. Total Heavy Metals and Nanoparticle accumulation

Concentrations of total heavy metals of Cd and Pb in root and shoot tissues of lettuce from different treatments are shown in Figure 5.3. Co-presence of ZnONPs with both Cd and Pb significantly changed the shoot uptake of Cd and Pb. The Cd level in lettuce shoot was significantly reduced by 30% and in contrast, the Pb concentration was increased by 44%. The impact of ZnONPs was significant in the bioaccumulation of heavy metals in lettuce roots, in which both Cd and Pb concentration was significantly reduced by 49% and 81%, respectively.

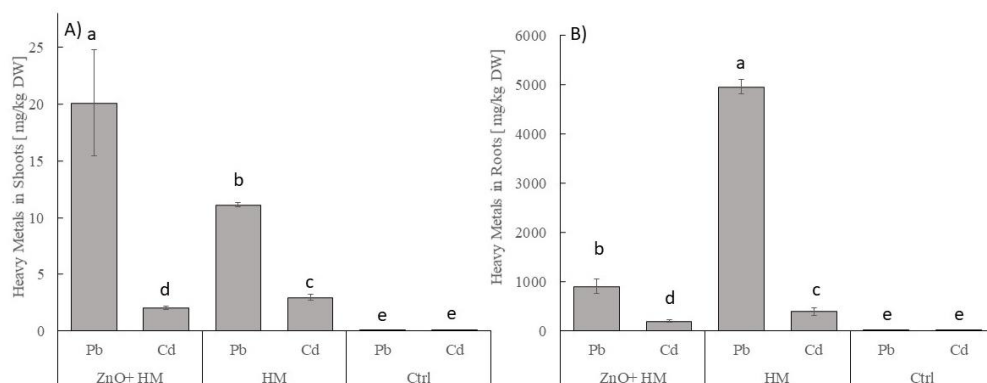


Fig. 5.3. Concentrations of heavy metals (Cd and Pb) in A) lettuce shoot and B) lettuce root tissues from different treatments. Error bars indicate standard deviation, and the alphabetic letters designate the statistical significance of each treatment.

Figure 5.4 shows the total Zn contents in plant tissues. In the co-presence of nanoparticles and both Cd and Pb, the total Zn concentration in shoots was significantly decreased by 73%. The same impact was observed in roots but to a lower extent, in which the total Zn was insignificantly dropped by 7%.

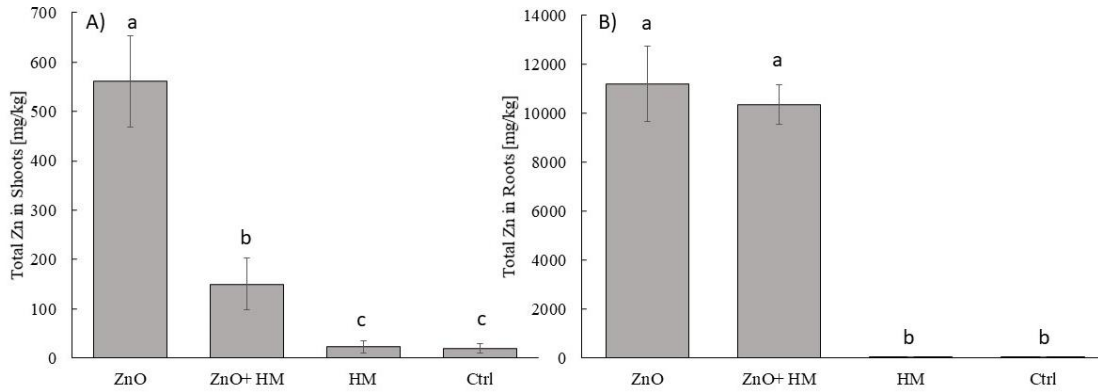


Fig.5.4. The mean concentrations of total Zn in (A) shoots (B) roots of lettuce exposed to four different treatments of heavy metals (Pb and Cd) and nanoparticles (ZnO). Error bars indicate standard deviation (n = 3).

ZnONPs has significantly altered the amount of Fe in shoot tissues. The total Fe concentration in lettuce shoot was elevated as high as 80% when plants were exposed only to ZnONPs compared to the control. In the co-presence of heavy metals and ZnONPs, Fe level in lettuce shoot was about 77% of that in control plants. The Fe concentration in roots responded differently to ZnONPs than that in shoots. All treatments led to significantly higher Fe than in control roots. Combination of heavy metals and ZnONPs reduced the amounts of total Fe by approximately 23% compared to treatments exposed only to ZnO in roots.

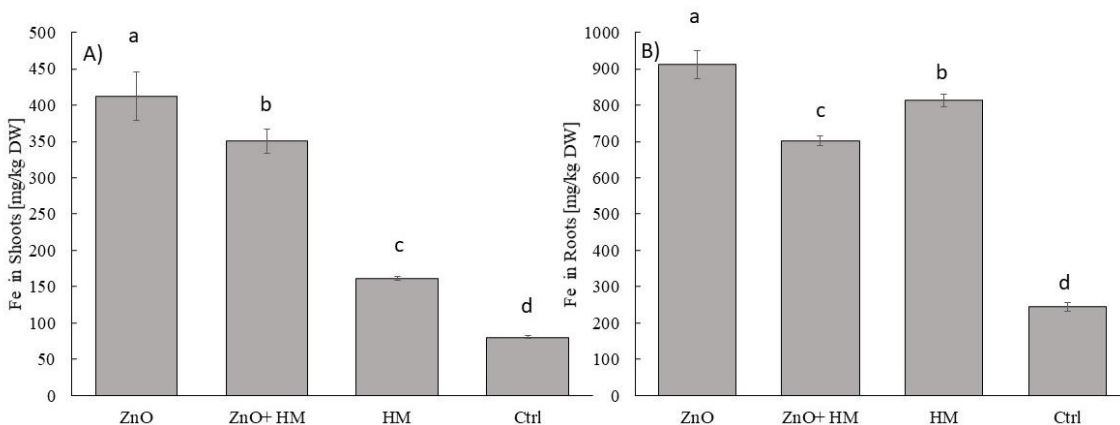


Fig.5.5. Concentrations of Fe in A) lettuce shoots and B) roots exposed to 100 mg/L of ZnONPs alone or in combination with 1 mg/L Cd+ 100 mg/L Pb (. Reported values indicate mean \pm SD (n = 3), and different letters display significant differences ($p \leq 0.05$) conferring to one-way ANOVA post analyzed by Tukey's test.

5.5. Discussion

ZnONPs negatively affected the growth of romaine lettuce at the used concentration as indicated by the lower biomass and short elongation of both roots and shoots, likely due to the phytotoxicity of ZnONPs or/and its dissociated Zn ions. The phytotoxicity of ZnONPs to various crops has been reported in a number of previous studies^{36,37}, but not to leafy vegetables. The phytotoxicity of ZnONPs to romaine lettuce in this study can likely be attributed to the reactive oxidative species (ROS) induced by ZnONPs and their dissociated ions^{36,37}.

ROS can affect plant physiology via the interruption of chlorophyll synthesis, protein denaturation and over-expression of antioxidant enzymes (i.e., superoxide dismutase (SOD), catalase (CAT), peroxidase (POD))^{38,39}. Together they could lead to slower growth; as shown in Figure 5.2. For example, treatment of *C. sativus* with 100 mg/L ZnONPs reduced the plant biomass by about 43%. Some studies hypothesized that the phytotoxicity of ZnONPs is associated with the competition of

the dissociated Zn with Fe ions, leading to the interference of Fe-related physiological processes³⁹⁻⁴¹. The results shown in Figure 5.5 indicate that excessive Zn could mediate the Fe concentration in shoots (shown in Fig 5.6), which can be beneficial to enhance the nutritional values of lettuce. This enhancement may stem from the reduction of the Fe efflux through the root exudate. The results of the translocation pattern of the Fe in relation to Zn concentration provide some evidence that ZnONPs has mitigated the efflux of the Fe. However, the mechanistic interpretation of these results needs further investigations. Figure 5.6 derived from ICP- analysis of four treatments further illustrates the correlation between Fe detected in shoots and available Zn. The results suggest that the physiological impact of ZnONPs can be, at least partially, attributed to its interference on plant Fe uptake. However, the underlying mechanisms for this connection are not well understood.

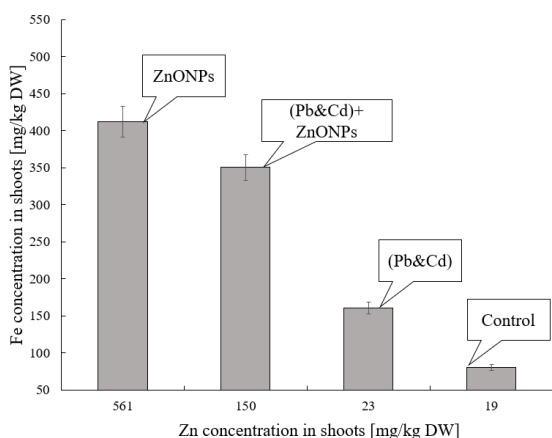


Fig.5.6. Correlation between concentrations of Fe and Zn in *L. sativa* upon exposure to 100 mg/L of ZnONPs alone or in combination with 1 mg/L Cd+ 100 mg/L Pb. Each bar represents the mean (n=3).

The co-presence of Cd and Pb mitigated the impact of ZnONPs. A possible reason for this observation could be the aggregation of ZnONPs in the presence of Cd and Pb. Co-present heavy

metals such as Cd, and metallic ENPs were reported to induce greater excretion of root exudates, which prompted the aggregation of ENPs⁴². Therefore, the bioavailability of ZnONPs might have been significantly reduced when plants were co-contaminated by ZnONPs and heavy metals. This interpretation is consistent with the lower observed Zn concentration of lettuce shoots in the copresence of ZnONPs with heavy metals, compared to plants exposed only to ZnONPs (Fig 5.4). The impact on the microbial community is another very critical consideration to understand the interactions of ZnONPs and heavy metal ions in plant system. Because ZnONPs can act as an antimicrobial agent, and the microbial community affects the Zn uptake, the correlation between Zn accumulation in shoots and numbers of bacterial colonies was investigated, Figure 5.7. A higher concentration of Zn in shoots is negatively correlated to the colony formation units of the microbial community in the rhizosphere area. The results indicate that the microbial community may also play an important role in plant uptake of Zn and other co-contaminants. More comprehensive microbial studies with soil-grown plants are needed to identify and characterize the precise role of the microbial community.

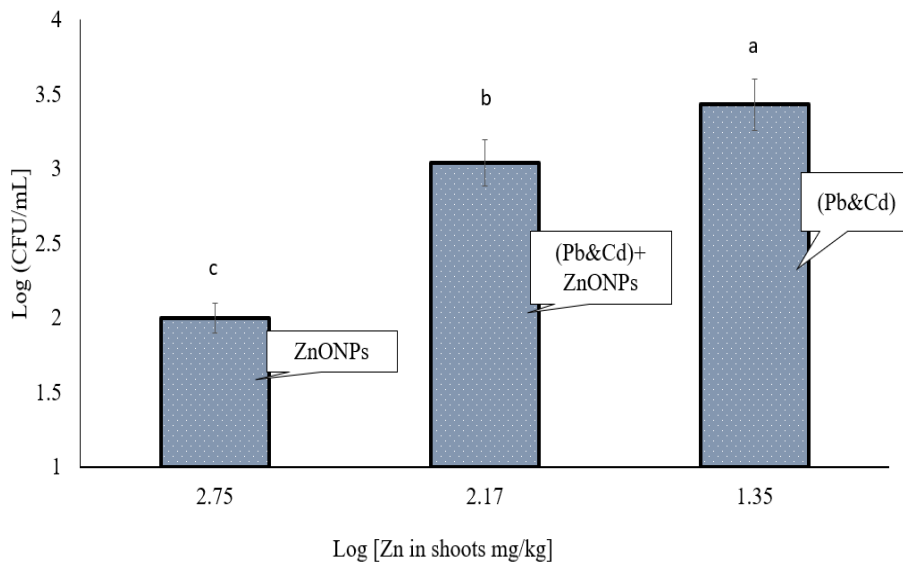


Fig.5.7. A relationship between the log of the colony forming units (CFU) in the growth media and the log of total Zn in shoots. Letters indicate significant differences. Error bars represent the standard deviation between treatments.

One of the interesting findings of this study was the key role of ZnONPs in changing the uptake of Pb and Cd. In an overall biomass analysis, both metals were significantly reduced in the presence of ZnONPs. However, this reduction was more prominent in root tissues. In fact, the concentration of Pb in lettuce shoots was higher in the system with both ZnONPs and heavy metals, compared with plants exposed to heavy metals only. The different accumulation patterns between Cd and Pb suggest that the properties of metals such as their complex chemistry are important factors affecting the interaction of these metals with co-occurring ZnONPs. Different heavy metals also have different adsorption capacity on ZnONPs, and our previous studies suggest that the adsorption of metal ions on metallic ENPs is a significant phenomenon affecting the plant uptake of these metals in a system with both heavy metals and ENPs²⁰.

The overall significant reduction of total Cd and Pb by ZnONPs was attributed to two primary processes. First, higher excretion of root exudates could lead to greater adsorption of heavy metals on ZnONPs and stronger aggregation of ZnONPs. Precipitation of larger particles may reduce the bioavailability of heavy metals. This interpretation was supported by the observation of the lower pH in the solution compared to the control due to greater organic acid secretion from plant roots (Shown in Fig 5.8). In a previous study, higher root exudation was observed in the co-presence of cerium oxide nanoparticle and Cd ²⁰, which was consistent with the lower pH observed in the medium containing coexistence of ZnONPs and heavy metals in this study.

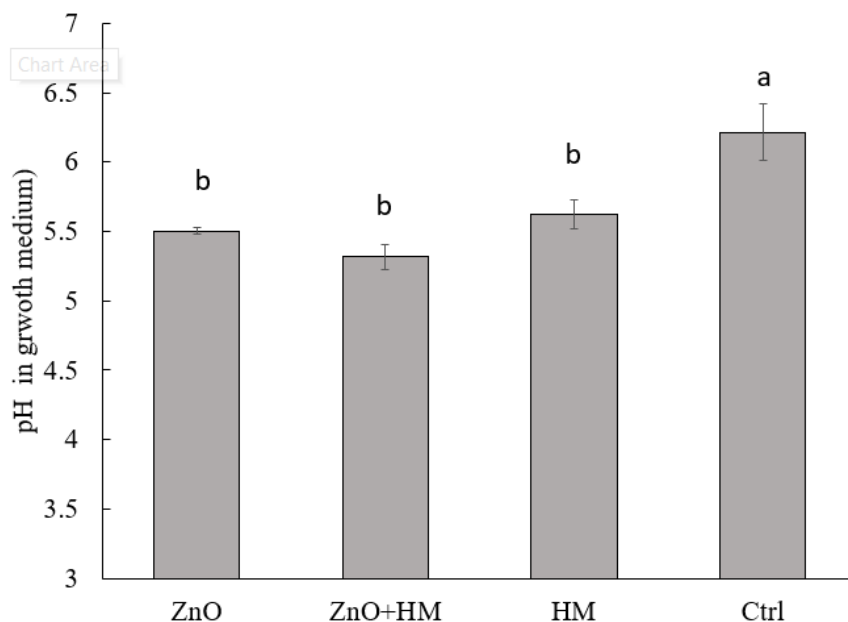


Fig.5.8. pH in the growth media of lettuce grown in the presence of 100 mg/L ZnONPs and/or 1 mg/L Cd +100 mg/L Pb. The reported values are mean ± SD (n = 3). Different letters reflect significant differences as analyzed by ANOVA followed by Tukey's test (p < 0.05).

5.6. Conclusion

In summary, the strong effect of coexisting ZnONPs on the bioavailability of Pb and Cd accumulation and concentration of Fe in lettuce tissues were observed. The explicit effects of ZnONPs on heavy metals uptake depend on the properties of heavy metals. Various biological and chemical processes might be responsible for the altered Fe, Pb and Cd uptake by lettuce in the presence of ZnONPs. Further investigations are necessary to elucidate whether similar uptake pattern in a soil-plant system will occur. Interestingly, Zn is a key biological inorganic compound in the nutritional properties of leafy vegetables, and its concentration was associated with altered Fe accumulation in lettuce. These critical findings suggest that proper concentration of ZnONPs may be applied as an effective agrichemical to simultaneously enhance plant growth and limit Cd and Pb accumulation in the leafy vegetable. Due to the strong dissolution of ZnONPs, a dose-response relationship relating ZnONPs and Zn ions as well as their impacts on plant accumulation of different micronutrients and co-existing environmental pollutants need to be investigated. . Even though underlying mechanisms with regard to the interactions of ZnONPs and coexisting heavy metals, this study highlights the critical role ZnONPs may play in plant accumulation of toxic heavy metals as well as essential micronutrients. Because ZnONPs are receiving increasing acceptance as a novel nanofertilizer, this study shed light on the potential food safety and health impact of nanotechnology applications in agriculture. .

5.7. References

1. Rossi, L.; Fedenia, L. N.; Sharifan, H.; Ma, X.; Lombardini, L., Effects of foliar application of zinc sulfate and zinc nanoparticles in coffee (*Coffea arabica* L.) plants. *Plant Physiology and Biochemistry* **2019**, *135*, 160-166.
2. Rossi, L.; Zhang, W.; Schwab, A. P.; Ma, X., Uptake, Accumulation, and in Planta Distribution of Coexisting Cerium Oxide Nanoparticles and Cadmium in *Glycine max* (L.) Merr. *Environmental Science & Technology* **2017**, *51* (21), 12815-12824.
3. Dasgupta, N.; Ranjan, S.; Ramalingam, C., Applications of nanotechnology in agriculture and water quality management. *Environmental Chemistry Letters* **2017**, *15* (4), 591-605.
4. Donovan, A. R.; Adams, C. D.; Ma, Y.; Stephan, C.; Eichholz, T.; Shi, H., Detection of zinc oxide and cerium dioxide nanoparticles during drinking water treatment by rapid single particle ICP-MS methods. *Analytical and bioanalytical chemistry* **2016**, *408* (19), 5137-5145.
5. Li, J.; Tappero, R. V.; Acerbo, A. S.; Yan, H.; Chu, Y.; Lowry, G. V.; Unrine, J. M., Effect of CeO₂ nanomaterial surface functional groups on tissue and subcellular distribution of Ce in tomato (*Solanum lycopersicum*). *Environmental Science: Nano* **2019**.
6. Londono, N.; Donovan, A. R.; Shi, H.; Geisler, M.; Liang, Y., Impact of TiO₂ and ZnO nanoparticles on an aquatic microbial community: effect at environmentally relevant concentrations. *Nanotoxicology* **2017**, *11* (9-10), 1140-1156.
7. Wang, X.; Sun, W.; Zhang, S.; Sharifan, H.; Ma, X., Elucidating the Effects of Cerium Oxide Nanoparticles and Zinc Oxide Nanoparticles on Arsenic Uptake and Speciation in Rice (*Oryza sativa*) in a Hydroponic System. *Environmental science & technology* **2018**.

8. Bi, C.; Zhou, Y.; Chen, Z.; Jia, J.; Bao, X., Heavy metals and lead isotopes in soils, road dust and leafy vegetables and health risks via vegetable consumption in the industrial areas of Shanghai, China. *Science of the Total Environment* **2018**, *619*, 1349-1357.
9. McCowan, L.; Horgan, R. P., Risk factors for small for gestational age infants. *Best Practice & Research Clinical Obstetrics & Gynaecology* **2009**, *23* (6), 779-793.
10. Ekesa, B.; Nabuuma, D.; Kennedy, G., Content of Iron and Vitamin A in Common Foods Given to Children 12–59 Months Old from North Western Tanzania and Central Uganda. *Nutrients* **2019**, *11* (3), 484.
11. Hosseinzadeh, S.; Liu, Z.; De Graeve, J.; BKheet, M.; Libbrecht, W.; De Clercq, J.; Van Hulle, S., Recirculating Water Treatment in Closed Hydroponic Systems: Assessment of Granular Activated Carbon and Soft Templated Mesoporous Carbon for Adsorptive Removal of Root Exudates. *Environmental Processes* **2019**, 1-23.
12. Moriarty, M. J.; Semmens, K.; Bissonette, G. K.; Jaczynski, J., Internalization assessment of E. coli O157: H7 in hydroponically grown lettuce. *LWT* **2019**, *100*, 183-188.
13. Palermo, M.; Paradiso, R.; De Pascale, S.; Fogliano, V., Hydroponic cultivation improves the nutritional quality of soybean and its products. *Journal of agricultural and food chemistry* **2011**, *60* (1), 250-255.
14. Anarado, C.; Anarado, C.; Okeke, M.; Ezeh, C.; Umedum, N.; Okafor, P., Leafy Vegetables as Potential Pathways to Heavy Metal Hazards. *Journal of Agricultural Chemistry and Environment* **2019**, *8*, 23-32.
15. Massadeh, A. M.; Baker, H. M.; Obeidat, M. M.; Shakatreh, S. K.; Obeidat, B. A.; Abu-Nameh, E. S. J. S.; Contamination, S., Analysis of lead and cadmium in selected leafy and non-leafy edible vegetables using atomic absorption spectrometry. **2011**, *20* (3), 306-314.

16. Ma, X.; Yan, J., Plant uptake and accumulation of engineered metallic nanoparticles from lab to field conditions. *Current Opinion in Environmental Science & Health* **2018**.
17. Grant, C. A., Influence of Phosphate Fertilizer on Cadmium in Agricultural Soils and Crops (Symposium 3.5. 1 Heavy Metal Contaminated Soils,< Special Issue> International Symposium: Soil Degradation Control, Remediation, and Reclamation, Tokyo Metropolitan University Symposium Series No. 2, 2010). *Pedologist* **2011**, 54 (3), 143-155.
18. AYDIN, S. S.; Büyük, İ.; Gündüzer, E. G.; Büyük, B. P.; Kandemir, İ.; Duman, D. C.; Aras, S., Effects of Lead (Pb) and Cadmium (Cd) Elements on Lipid Peroxidation, Catalase Enzyme Activity and Catalase Gene Expression Profile in Tomato Plants. *Tarım Bilimleri Dergisi* **2016**, 22 (4), 539-547.
19. Sung, C. Y.; Park, C.-B., The effect of site- and landscape-scale factors on lead contamination of leafy vegetables grown in urban gardens. *Landscape and Urban Planning* **2018**, 177, 38-46.
20. Rossi, L.; Sharifan, H.; Zhang, W.; Schwab, A. P.; Ma, X., Mutual effects and in planta accumulation of co-existing cerium oxide nanoparticles and cadmium in hydroponically grown soybean (*Glycine max* (L.) Merr.). *Environmental Science: Nano* **2018**, 5 (1), 150-157.
21. Bui, A. T.; Nguyen, H. T.; Nguyen, M. N.; Tran, T.-H. T.; Vu, T. V.; Nguyen, C. H.; Reynolds, H. L., Accumulation and potential health risks of cadmium, lead and arsenic in vegetables grown near mining sites in Northern Vietnam. *Environmental monitoring and assessment* **2016**, 188 (9), 525.
22. Mihaileanu, R. G.; Neamtiu, I. A.; Fleming, M.; Pop, C.; Bloom, M. S.; Roba, C.; Surcel, M.; Stamatian, F.; Gurzau, E., Assessment of heavy metals (total chromium, lead, and manganese) contamination of residential soil and homegrown vegetables near a former chemical

manufacturing facility in Tarnaveni, Romania. *Environmental Monitoring and Assessment* **2018**, *191* (1), 8.

23. Taylor, C. M.; Golding, J.; Emond, A., Adverse effects of maternal lead levels on birth outcomes in the ALSPAC study: a prospective birth cohort study. *BJOG: An International Journal of Obstetrics & Gynaecology* **2015**, *122* (3), 322-328.

24. Sheridan, C.; Depuydt, P.; De Ro, M.; Petit, C.; Van Gysegem, E.; Delaere, P.; Dixon, M.; Stasiak, M.; Aciksöz, S. B.; Frossard, E.; Paradiso, R.; De Pascale, S.; Ventorino, V.; De Meyer, T.; Sas, B.; Geelen, D., Microbial Community Dynamics and Response to Plant Growth-Promoting Microorganisms in the Rhizosphere of Four Common Food Crops Cultivated in Hydroponics. *Microbial Ecology* **2017**, *73* (2), 378-393.

25. Hussain, A.; Ali, S.; Rizwan, M.; Zia ur Rehman, M.; Javed, M. R.; Imran, M.; Chatha, S. A. S.; Nazir, R., Zinc oxide nanoparticles alter the wheat physiological response and reduce the cadmium uptake by plants. *Environmental Pollution* **2018**, *242*, 1518-1526.

26. Espitia, P. J. P.; Soares, N. d. F. F.; dos Reis Coimbra, J. S.; de Andrade, N. J.; Cruz, R. S.; Medeiros, E. A. A., Zinc oxide nanoparticles: synthesis, antimicrobial activity and food packaging applications. *Food and Bioprocess Technology* **2012**, *5* (5), 1447-1464.

27. Ismael, M. A.; Elyamine, A. M.; Moussa, M. G.; Cai, M.; Zhao, X.; Hu, C., Cadmium in plants: uptake, toxicity, and its interactions with selenium fertilizers. *Metallomics* **2019**, *11* (2), 255-277.

28. Kim, M. J.; Moon, Y.; Tou, J. C.; Mou, B.; Waterland, N. L., Nutritional value, bioactive compounds and health benefits of lettuce (*Lactuca sativa* L.). *Journal of Food Composition and Analysis* **2016**, *49*, 19-34.

29. Tamme, T.; Reinik, M.; Roasto, M.; Juhkam, K.; Tenno, T.; Kiis, A., Nitrates and nitrites in vegetables and vegetable-based products and their intakes by the Estonian population. *Food additives and contaminants* **2006**, *23* (4), 355-361.
30. Baliga, M. S.; Shivashankara, A. R.; Venkatesh, S.; Bhat, H. P.; Palatty, P. L.; Bhandari, G.; Rao, S., Phytochemicals in the Prevention of Ethanol-Induced Hepatotoxicity: A Revisit. In *Dietary Interventions in Liver Disease*, Elsevier: 2019; pp 79-89.
31. Garber, A. K.; Binkley, N.; Krueger, D. C.; Suttie, J. J. T. J. o. n., Comparison of phylloquinone bioavailability from food sources or a supplement in human subjects. **1999**, *129* (6), 1201-1203.
32. Zhang, W.; Dan, Y.; Shi, H.; Ma, X., Elucidating the mechanisms for plant uptake and in-planta speciation of cerium in radish (*Raphanus sativus* L.) treated with cerium oxide nanoparticles. *Journal of Environmental Chemical Engineering* **2017**, *5* (1), 572-577.
33. Zhang, W.; Ebbs, S. D.; Musante, C.; White, J. C.; Gao, C.; Ma, X., Uptake and accumulation of bulk and nanosized cerium oxide particles and ionic cerium by radish (*Raphanus sativus* L.). *Journal of agricultural and food chemistry* **2015**, *63* (2), 382-390.
34. Zonaro, E.; Lampis, S.; Turner, R. J.; Qazi, S. J. S.; Vallini, G., Biogenic selenium and tellurium nanoparticles synthesized by environmental microbial isolates efficaciously inhibit bacterial planktonic cultures and biofilms. *Frontiers in microbiology* **2015**, *6*, 584.
35. Angel Villegas, N.; Silvero Compagnucci, M. J.; Sainz Ajá, M.; Rocca, D. M.; Becerra, M. C.; Fabián Molina, G.; Palma, S. D., Novel Antibacterial Resin-Based Filling Material Containing Nanoparticles for the Potential One-Step Treatment of Caries. *Journal of Healthcare Engineering* **2019**, 2019.

36. Lee, S.; Chung, H.; Kim, S.; Lee, I., The genotoxic effect of ZnO and CuO nanoparticles on early growth of buckwheat, *Fagopyrum esculentum*. *Water, Air, & Soil Pollution* **2013**, *224* (9), 1668.
37. Ivask, A.; Bondarenko, O.; Jepihina, N.; Kahru, A., Profiling of the reactive oxygen species-related ecotoxicity of CuO, ZnO, TiO₂, silver and fullerene nanoparticles using a set of recombinant luminescent *Escherichia coli* strains: differentiating the impact of particles and solubilised metals. *Analytical and Bioanalytical Chemistry* **2010**, *398* (2), 701-716.
38. Singh, A.; Singh, N.; Afzal, S.; Singh, T.; Hussain, I. J. J. o. M. S., Zinc oxide nanoparticles: a review of their biological synthesis, antimicrobial activity, uptake, translocation and biotransformation in plants. **2018**, *53* (1), 185-201.
39. Sturikova, H.; Krystofova, O.; Huska, D.; Adam, V., Zinc, zinc nanoparticles and plants. *Journal of Hazardous Materials* **2018**, *349*, 101-110.
40. Ren, F. C.; Liu, T. C.; Liu, H. Q.; Hu, B. Y., Influence of zinc on the growth, distribution of elements, and metabolism of one-year old American ginseng plants. *Journal of plant nutrition* **1993**, *16* (2), 393-405.
41. Krämer, U., Metal hyperaccumulation in plants. *Annual review of plant biology* **2010**, *61*, 517-534.
42. Sharifan, H.; Wang, X.; Guo, B.; Ma, X., Investigation on the Modification of Physicochemical Properties of Cerium Oxide Nanoparticles through Adsorption of Cd and As(III)/As(V). *ACS Sustainable Chemistry & Engineering* **2018**, *6* (10), 13454-13461.

CHAPTER VI

IMPACTS OF ZNO NANOPARTICLES ON THE MOBILIZATION OF ESSENTIAL MICRONUTRIENT (IRON AND COPPER) AND BIOAVAILABILITY OF HEAVY METALS (LEAD AND CADMIUM) IN VEGETABLES

6.1. Summary

The advances in large hydroponic production systems, easy adoption to urban agriculture and higher hydrophobic surface area of leafy greens, highly expose them to atmospheric fallout of heavy metals and nanoparticles. Cadmium (Cd) and lead (Pb) are extremely toxic metallic contaminants, which at trace level threaten humans and livestock health through consumption of edible plant tissues. The uptake of both Cd and Pb may occur through the same protein transporters of essential minerals such as iron (Fe^{2+}) and copper (Cu^{2+}). This study aims to understand the role of zinc oxide nanoparticles (ZnONPs) in uptake pattern of both Cd and Pb and their impacts on re-localization of the iron and copper as the key micronutrient in edible tissues of three species; spinach (*Spinacia oleracea*), parsley (*Petroselinum sativum*) and cilantro (*Coriandrum sativum*). Pre-grown plant seedlings were exposed to four hydroponic treatments (1.0 mg L⁻¹ Cd²⁺+100.0 mg L⁻¹ Pb²⁺, 1.0 mg L⁻¹ Cd²⁺+100.0 mg L⁻¹ Pb²⁺ + 100 mg L⁻¹ ZnONPs, 100 mg L⁻¹ ZnO-ENPs and a control with no chemical exposure) for two weeks. At termination, shoots were gently separated from the roots, and the concentrations of Pb, Cd, and Fe in all plant tissues were quantified by ICP-MS. The results revealed the mitigation of heavy metal root uptake in coexposure to ZnONPs. The response of each plant was different in relocalization of the Cu and Pb in edible tissues. The translocation trend of heavy metals was identical in edible tissues of three species. Fe concentration in edible tissues exposed to ZnONPs compared to control was evaluated as follow spinach(+10%)> cilantro(+9%)>

parsley(-8%). The trend of re-localization of the Cu was different from the Fe contents, and the Cu level in edible tissues of three species were affected in copresence of both heavy metals as follow cilantro (+8%)> spinach (+4%)> parsley (+1.5%).

6.2. Introduction

With the rapid advancement of nanotechnology and release of engineering nanoparticles, the production of healthy food products became a critical concern for many scientists and engineers^{1, 2}. Leafy greens with a wide variety of vegetables are the main ingredients of healthy diets for humans, which are at high risk of contamination by heavy metals and nanoparticles. The large hydroponic production systems^{3, 4}, easy adoption to urban agriculture and higher leaf surface area of leafy greens, highly expose them to atmospheric fallout of heavy metals and nanoparticles⁵. In addition, their growth in hydroponic systems mediates the bioavailability of organic and inorganic elements for the plants^{6, 7}.

Copresence of the heavy metals and nanoparticles is an inevitable event that impacts the physiological and biological systems of the plants⁸. Through these interactions, the localization of essential minerals in dietary tissues may change, leading to varying the nutritional values of the plants. A number of studies have investigated the influence of the nanoparticles, heavy metals or their coexistence on the physiological characteristics of the plants^{9, 10}. For example, the root elongation of corn roots was observed a 17% reduction at a high level of ZnO nanoparticle (ZnONPs)1000 mg L⁻¹¹¹. However, at lower concentration (100-500 mgL⁻¹), positive impacts of the ZnONPs on seed germination, growth, and height of roots and shoots have reported^{12, 13}. The change of plant physiological properties in exposure to ENPs or heavy metals may stem from delocalization and alteration of the essential minerals dynamics inside the plant tissues. Rossi et al. 2018 found that the coexistence of CeO₂NPs was associated with mitigating the bioavailability

of Cd and positive impacts of the chlorophylls contents^{6, 9}. On the contrary, De la Rosa et al. 2013 observed signs of the ZnONPs toxicity in alfalfa and tomato at a concentration greater than 800 mg L⁻¹ in hydroponic system¹⁰.

Cadmium (Cd) and lead (Pb) are the second and third major metallic contaminants of high risk to the environment, which at generally not phytotoxic level threaten humans and livestock health through consumption of edible plant tissue. The uptake of both Cd and Pb ions may occur via the same protein transporters, which are involved in the transport of the essential minerals including Fe²⁺, Cu²⁺, and Zn²⁺. Therefore, the copresence of heavy metals and nanoparticles is of high importance to elucidate their mutual impacts on the mobilization of essential minerals in edible tissues of the plants.

Zinc Oxide nanoparticle (ZnONPs) has a wide application range, including sunscreen products, paint additive, and nano-fertilizers. Due to their specific physicochemical properties, low toxicity, and fungicides properties^{1, 14}, their application have progressively advanced into the agriculture and food processing sectors. ZnONPs represent substantial stimulating impacts on the dietary plant's growth, such as chlorophyll content. It also contains 80% of the essential nutrient of Zn for leafy greens, and possess a high adsorption capacity for heavy metals intrusion^{2, 6}. Bringing all the potential agricultural benefits, the US Food and Drug Administration (FDA) has been recognized as a safe food additive¹⁵.

Therefore, it is very imperative to understand the underlying mechanism of ZnONPs interaction with leafy greens and their behavior in the coexistence of the heavy metals. Type of plant species in such nano-effects studies is a key factor that influences the interaction of heavy metals or nanoparticles with the plants as well as their mutual impacts on the mobilization of the essential minerals¹⁶. Plants have developed various strategies against the intrusion of heavy metals or

nanoparticles to sustain their homeostasis system. Rossi et al. 2018 found the different response of soybean plant through the release of root exudate in exposure to Cd, ENPs, or their coexistence⁶. Such dynamic response will change the uptake and translocation patterns of heavy metals and micronutrients for the plants. This study aims to understand the mutual interaction of leafy greens with the coexistence of ZnONPs and two heavy metals (Cd and Pb) and their impacts on the mobilization of the three essential minerals of Zn, Fe, and Cu. Three frequently consumed vegetables in the human diet, including spinach (*Spinaciae oleracea*), parsley (*Petroselinum sativum*) and cilantro (*Coriandrum sativum*) were selected as study models.

6.3. Materials and Methods

6.3.1. Materials

Zinc oxide nanoparticle with an average size range of 10-30 nm and negative surface charge (ZnO NPs, 20% by weight) was obtained from the US Research Nanomaterials, Inc. (Houston, TX). Lead nitrate ($\text{Pb}(\text{NO}_3)_2$ >99%) and cadmium sulfate (CdSO_4) in high purity were purchased respectively from Alfa Aesar (Ward Hill, MA) and Fisher Scientific Inc. (Pittsburgh, PA). ICP-MS standard solutions (Pb, Cd, Zn, Fe, and Cu) at a concentration of 10000 ppm, in 3% nitric acid were supplied by RICCA Chemical Company (Arlington, TX).

6.3.2. ZnO Characterization

ZnO physiochemical properties (size, zeta potential, and surface structure) were fully characterized through our previous study⁷. Briefly, the image analysis of the Tecnai G2 F20 transmission electron microscope (TEM) showed; a recorded mean diameter of 68.1 nm (15- 137 nm), dominant

spherical shape at high density, as well existence of the triangular or irregular shapes at low density. The average hydrodynamic size of dispersed ZnO NPs in ultra-pure water (18.3 M Ω) was recorded by 621.08 ± 7.63 nm through the dynamic light scattering (Delsa Nano C, Beckman Coulter Inc. Miami, FL) at a concentration of 100 mg L⁻¹. Respectively, the surface charge (zeta potential) was measured -28.80 ± 2.04 mV.

6.3.3. Plant Culture and Exposure Experiments.

The seeds of parsley, cilantro, and spinach were obtained from Johnny's Selected Seeds (Winslow, ME). Before germination, seeds surface were sterilized for about 20 min applying 30% H₂O₂ then carefully rinsed with ultra-pure water¹⁷. Germination took place in moist sand. All cultivation and transplantation steps were performed in a controlled temperature greenhouse (25°C), supplied by a fluorescent light (250 $\mu\text{mol m}^2 \text{s}^{-1}$ photosynthetic photon flux density) cycle of 16/8.

Germinated seedlings were transplanted to a clay-soil square pot (12 cm x 10 cm) for two weeks to naturally regulate the essential mineral uptake from the soil. Next, the plant species were carefully detached from the soil using a smooth flow of DI water, roots were fully cleared off from the soil residual, and each plant was immediately transferred to a hydroponic system: a series of 50 mL tubes (Becton, Dickinson and Co., Franklin Lakes, NJ, USA), covered by aluminum foil. Each tube contained 1/4th strength of the Hoagland solution (Phyto Technology Lab, Shawnee Mission, KS).

Through the hydroponic system's potential interaction of soil compartments with the applied doses of nanoparticle and heavy metals were avoided, and heavy metals and nanoparticles became fully

bioavailable to plant roots. Also, this system has been extensively applied for the production of leafy greens in greenhouses¹⁸.

Once the rate of transpiration was about 10 mL/day (after 10-15 days), plant species were separated into four groups. Each group was assigned to treatments with four replicates. Treatment solutions were prepared in DI water containing i) only heavy metals ($100 \text{ mg L}^{-1} \text{ Pb}^{2+} + 1.0 \text{ mg L}^{-1} \text{ Cd}^{2+}$) ii) heavy metals and $100 \text{ mg L}^{-1} \text{ ZnO-ENPs}$, iii) solution only with $100 \text{ mg L}^{-1} \text{ ZnO-ENPs}$ and iv) control with no external elements. At the exposure step, the Hoagland solution was not applied to avoid aggregation of the nanoparticles as results of its high ionic strength.

To differentiate water evaporation from evapotranspiration, three tubes were filled only with water and monitored among the other plants. During the uptake experiment time, water loss was supplied with the DI water twice a day (morning and evening). To homogenize the effects of light intensity, plants were randomly relocated and rotated. The pH of the growth medium was recorded before and after the uptake experiment using a pH meter (VWR symphony – SB90M5).

6.3.4. Growth analyses and biomass partitioning

Immediately following the uptake experiment, plants were gently isolated from the hydroponic system and submerged in DI water for 30 min, then washed with 50 mL CaCl_2 solution (5 mM) five times to possibly eliminate outer root surface deposition of the Zn, Pb and Cd elements⁶. Each plant species was cut into 1) roots and 2) leafy tissues (shoots). The fresh biomass was measured for both roots and shoots of all species. For the element analysis by ICP-MS, fresh biomasses were dried at 80°C for four days to ensure the biomasses were fully dehydrated through the analytical procedure, and respectively, the dry biomass weight was recorded^{6,7}.

6.3.5. Quantification of the heavy metals and trace elements in plant tissues

Dry biomass of each species (shoot and root) were carefully crushed and homogenized using a household blender (Braun Multiquick MX 2050), then a subsample aliquot of the dry shoot tissues (0.15 g) and dry root tissues (0.05 g) were transferred into a digestion tube placed on DigiPREP MS hot block digester (SCP Science, Clark Graham, Canada). Pre-digestion was performed within 8 hours of preparation by applying 3 mL of 70% (v/v) nitric acid (Certified ACS Plus)¹⁹. Next, predigested samples were heated up to fully digestion stage and reheated using additional 2 mL of 30% (w/v) H₂O₂ (95 °C / 6 hours) following the EPA method 3050b.^{8, 19 7}. Next, 15 mL volume of digested samples were prepared at the level of 1% nitric acid to detect the Zn, Pb, Cd, Cu by an inductively coupled plasma–mass spectrometry ICP-MS (Agilent 7500i, Agilent Technologies Co. Ltd, USA).^{8, 19}.

6.3.6. Relocation rate of the Cu and Fe

The relocation rate of essential minerals (Cu and Fe rate) in response to the presence of the ZnONPs was developed by Xiong et al. 2017 as a function of roots exposure time²⁰. This rate is an indicator of efflux of Cu and Fe from root pores that was primarily articulated as a transferred dose per day. The higher relocation rate in this experimental design indicates a faster interaction in biosystem of the plant and slower efflux of the essential minerals through root exudates. The Cu and Fe relocation rates (milligrams per day) values during the uptake time were calculated with eq 1:

Eq3.1

$$[EM]_{Relocation\ rate} = \frac{([EM]_{Shoot} \times DW_{Shoot}) + ([EM]_{Root} \times DW_{Root})}{Exposure\ Time\ (days)}$$

Where the [EM] represents the essential mineral (Cu or Fe) concentrations (milligrams per kilogram), quantified by ICP-MS analysis, and DW indicates the dry weights of the tissues (mg).

6.3.7. Statistical Analysis

Statistical analysis of the five elements concentration data (Zn, Pb, Cd, Cu and Fe) in both shoot and root tissues of three species (3 or 4 n), as well as data pertaining to their dry and fresh biomass were performed via the Minitab 18 Statistical Software (Minitab Inc., State College, PA, USA). All data were processed through the One-Way ANOVA, to compare the mean of each data set, followed by Tukey's data processing with a significance level of 5% ($p < 0.05$).

6.4. Results

6.4.1. Growth analysis and plant uptake of Pb and Cd

As shown in Fig 6.1, A and B, the biomass of edible tissues of cilantro and parsley in treatments subjected to ENPs were insignificantly reduced by 1.5% compared to control. The sole exposure of the ENPs to the spinach species has shown a significant reduction ($P < 0.05$) in dry shoot biomass by 20% (Fig 6.1 C), while the copresence of ENPs and heavy metals showed positive impacts on the growth (15% increase in shoot yield) compared to control. Regarding the non-edible tissues, as shown in Fig 6.2, the impacts of sole ENPs on dry biomass of the roots were insignificant in all three species. However, in the copresence of heavy metals, a slight increase in dry biomass of roots in all species has been observed.

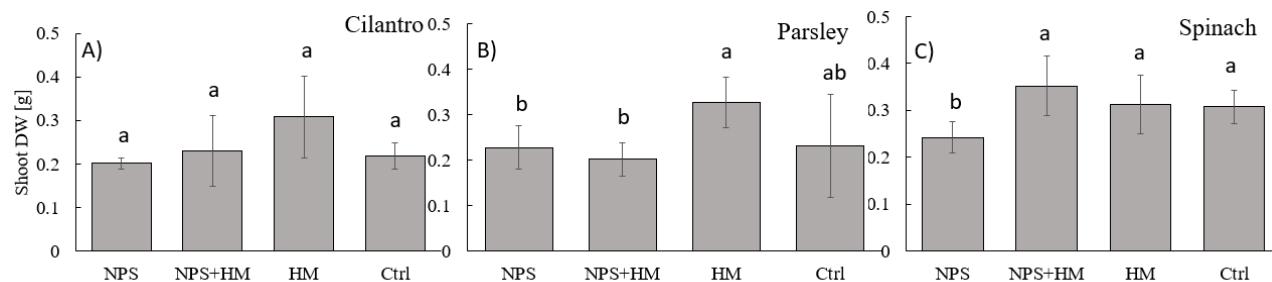


Fig.6.1. Impact of dry biomass of shoot tissues in three species in response to four treatments (ZnONPs, Cd&Pb+ZnONPs, Cd&Pb, Control) A) cilantro (*Coriandrum sativum*) B) parsley (*Petroselinum sativum*), and C) spinach (*Spinaciae oleracea*). Each column indicates the mean of the dataset and the error bars represent standard deviation (n = 3 or 4). Different letters differentiate the significance level ($p \leq 0.05$). HM: heavy metals.

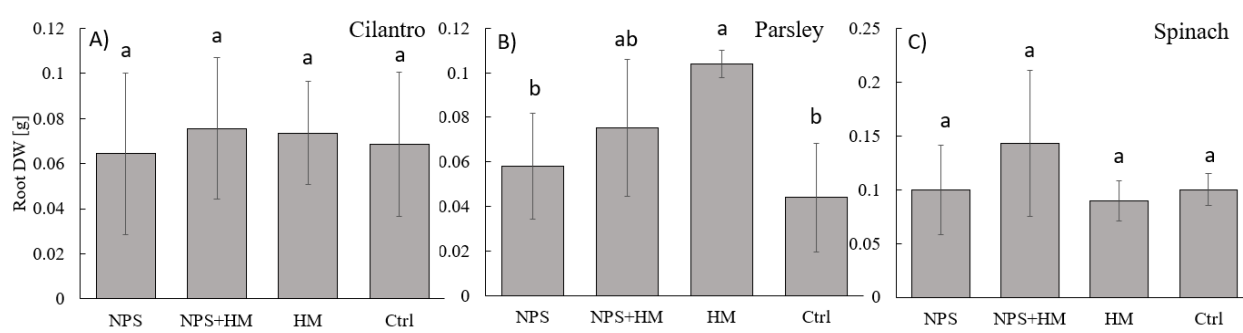


Fig.6.2. Dry biomass of root tissues in three leafy greens under different treatments on the mean basis (ZnONPs, Cd&Pb+ZnONPs, Cd&Pb, Control) A) cilantro (*Coriandrum sativum*) B) parsley (*Petroselinum sativum*), and C) spinach (*Spinaciae oleracea*). The error bars above each column bar indicate standard deviation (n = 3 or 4) and each letter defines the statistical significance ($p \leq 0.05$). HM: heavy metals.

Fig. 6 depicts the uptake pattern of both Cd and Pb in shoot tissues of all three species under three different treatments. A similar pattern was observed in shoot response to uptake of Pb in all three species. However, the extent of uptake in parsley shoots was at least 10 folds greater than cilantro

and spinach. Copresence of the heavy metals and ENPs have mediated the uptake of Pb in shoot tissues of all three species by approximately 54%, 44%, and 58% respectively for cilantro, parsley and spinach compared to the treatments exposed to only heavy metals. In copresence of ENPs, the Cd level was reduced in edible tissues of all three species compared to treatments subjected to the sole presence of heavy metals. However, this reduction was significant only in cilantro by 27%, and statistically insignificant in both parsley and spinach by approximately 5% and 2%, respectively.

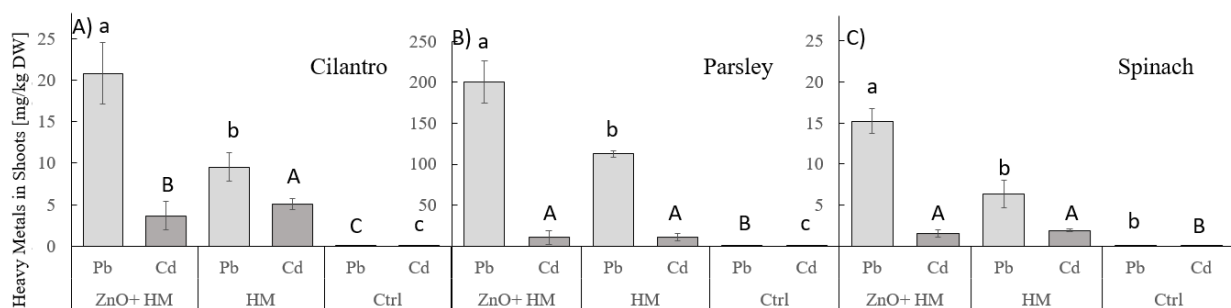


Fig. 6.3. Detected level of heavy metals (Cd and Pb) in shoot tissues A) cilantro (*Coriandrum sativum*) B) parsley (*Petroselinum sativum*), and C) spinach (*Spinaciae oleracea*) exposed to different treatments. Error bars designate standard deviation (n = 3), and the letters indicate the significant difference processed by ANOVA-Tukey.

Figure 6.4 illustrates the uptake of both Cd and Pb in non-edible tissues (roots) of the three species under the three treatments. A similar trend of uptake to the shoots was observed for both heavy metals in all plant's roots. Interestingly, the presence of ENPs was associated with a reduction of both Cd and Pb in all species roots, in which, the concentration of Pb in roots was significantly dropped by 39%, 83% and 85% for cilantro, parsley, and spinach, respectively. Cadmium level was mitigated insignificantly in root cells of cilantro coexposed to ENPs by 11%

(Fig 6.4 A), and significantly reduced in parsley and spinach respectively by 30% and 52% (Fig 6.4 B&C).

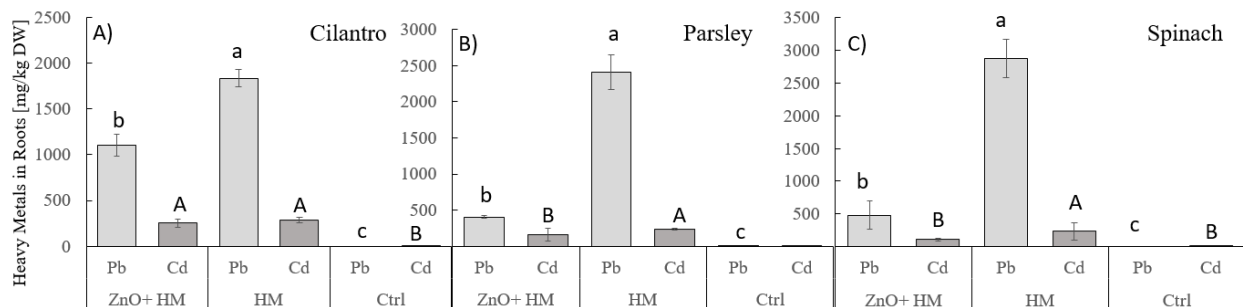


Fig. 6.4. Concentration of cadmium and lead in roots of three species A) cilantro (*Coriandrum sativum*) B) parsley (*Petroselinum sativum*), and C) spinach (*Spinaciae oleracea*) exposed to different treatments (combinations of 1 mg/L of Cd+100 mg/L Pb and 100 mg/L ZnONPs). Error bars designate standard deviations (n = 3), and the letters indicate the significant difference processed by ANOVA-Tukey.

6.4.2. Dynamics of plant localization of Fe and Cu and Zn

Described in Fig 6.5 A, the presence of ZnONPs was associated with elevation of Fe in edible tissues of cilantro compared to control. However, the increase of Fe level was not significant in cilantro shoots, in which the ENPs approximately 10% elevated the Fe levels in both treatments. In comparison to cilantro, a slightly different pattern of Fe levels in shoots of parsley was observed (Fig 6.5B). Though the change of Fe in parsley shoots with copresence of heavy metals and ENPs were insignificant, the presence of ENPs lowered the levels of Fe by 8%, and in the sole presence of ENPs, Fe was reduced significantly by 36% compared to control.

The dynamics of Fe in shoot cells of spinach was very identical to cilantro behavior. Presence of ENPs in either treatment has shown an increase in the shoots Fe concentration of spinach at

insignificant level (Fig 6.5 C), in which, Fe was elevated by 13% and 10%, respectively in the sole presence of ENPs and their copresence with heavy metals.

The Cu content in shoots of cilantro was elevated significantly in both treatments exposed to ENPs by approximately 71% on an average basis (shown in Fig 6.5A). However, in the copresence of ENPs and heavy metals, this elevation was at a lower extent by 31% compared to sole ENPs presence. There was no significant change of Cu in parsley shoots compared to control treatment (Fig 6.5 B). Similar to the uptake pattern of Fe in both cilantro and spinach, the levels of Cu in the shoot tissues were also identical. As shown in Fig 6.5 C, exposure to ENPs was associated with significant elevation of Cu content in edible tissues of spinach (37% on an average basis) but at far lower extent compared to what was observed in cilantro.

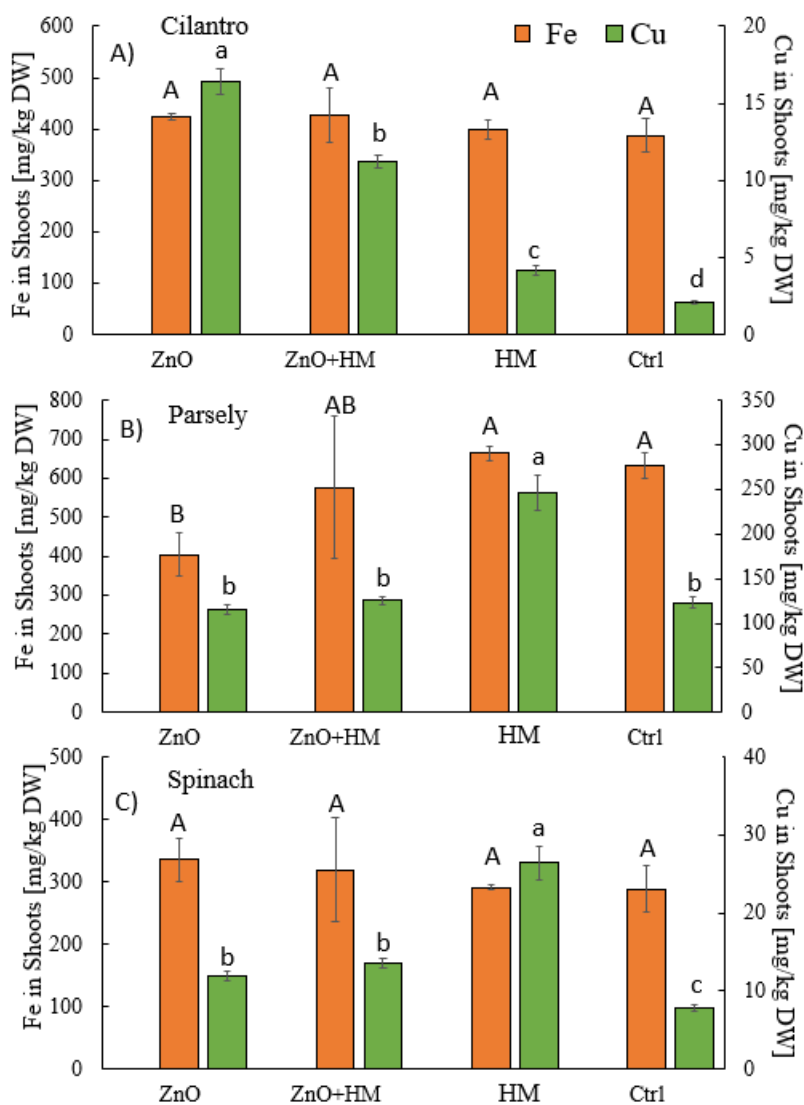


Fig. 6.5. Concentrations of essential minerals (Fe and Cu) in edible biomass (shoots) of A) cilantro (*Coriandrum sativum*) B) parsely (*Petroselinum sativum*), and C) spinach (*Spinaciae oleracea*) subjected to different treatments (100 mg/L of ZnONPs alone or in combination with 1 mg/L Cd+ 100 mg/L Pb). Detected values represent mean \pm SD (n = 3), and different letters differentiate statistical significance ($p \leq 0.05$) conferring to one-way ANOVA post analyzed by Tukey's test.

Figure 6.6 represents the interaction of ZnONPs and heavy metals on the total Zn uptake in both roots and shoots of the plants. The concentration of total Zn in both roots and shoot tissues of all

species which exposed to ENPs were higher than control. However, the detected levels of Zn in spinach shoots (Fig 6.6 C) was relatively higher than two other species.

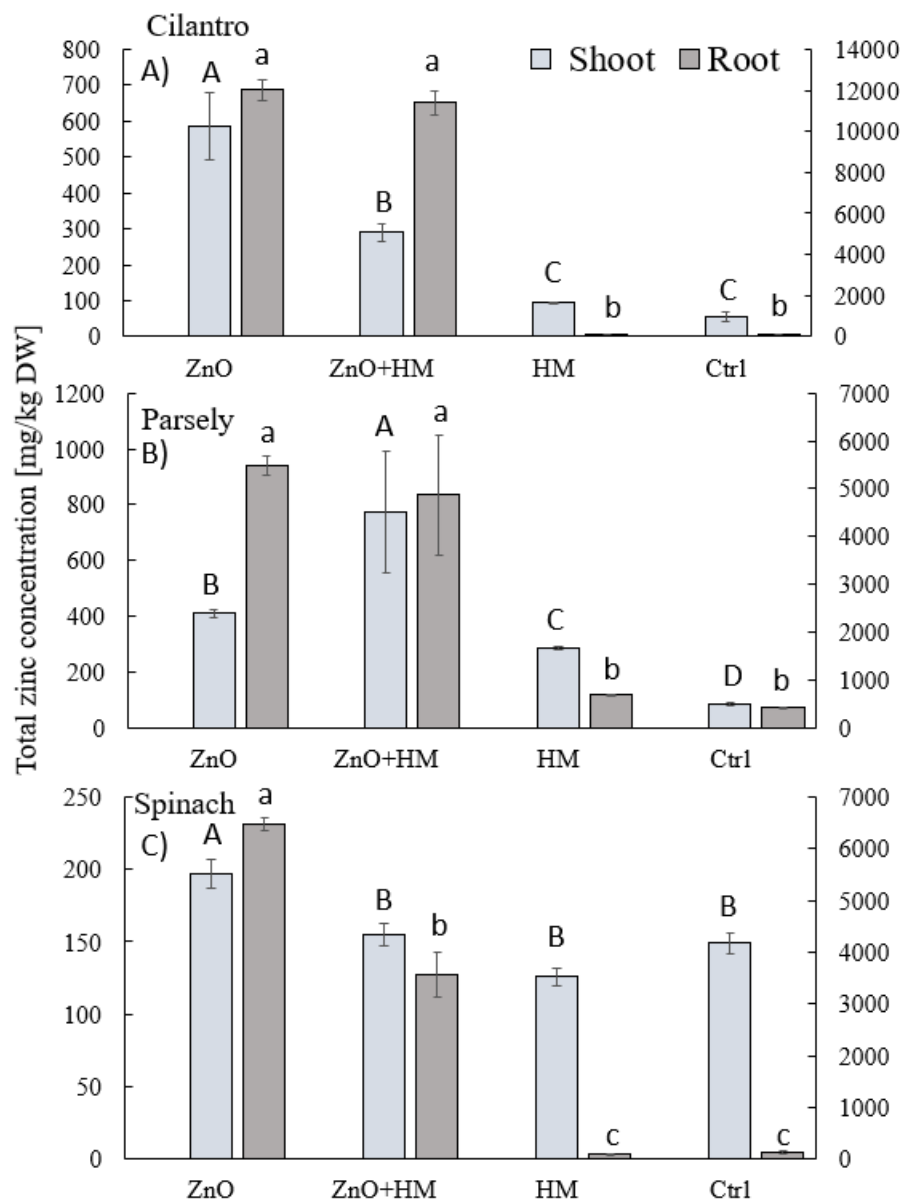


Fig. 6.6. Total Zn concentration on a mean basis in roots and shoots A) cilantro (*Coriandrum sativum*) B) parsely (*Petroselinum sativum*), and C) spinach (*Spinaciae oleracea*) exposed to four different treatments of heavy metals (Pb and Cd) and nanoparticles (ZnO). Error bars specify standard deviation (n = 3).

6.5. Discussion

Considerably increased the biomass of edible tissues in cilantro and spinach at copresence of the ENPs and heavy metals may have resulted from their mutual impacts on the elevation of the Fe levels. Iron plays a fundamental role in photosynthesis, and enzymatic process of the plants, the dynamics of Fe levels can substantially impact the plant's health, and their physiological performance²¹. Slightly reduction of the biomass of edible tissues of all species when exposed to only ZnONPs (Fig 6.1), likely stem from the minor ZnONPs phytotoxicity through their dissociated Zn ions. This interpretation was consistent with total detected levels of Zn in edible tissues, shown in Fig 6.6.

The phytotoxicity impacts of ZnONPs on the biomass production to a variety of the grains and fruits at concentration $\gg 100 \text{ mg L}^{-1}$ have been reported via soil production system^{36, 37}, but few studies concentrated in hydroponics production of leafy vegetables. For example, $1,000 \text{ mg L}^{-1}$ ZnO NPs reduced root elongation of cucumber (*Cucumis sativus L.*) and corn (*Zea mays L.*) by 51 % and 17 %²² and at 500 mg L^{-1} reduced the roots and shoots elongation in wheat (*Triticum aestivum*)²³. Some studies hypothesized that the phytotoxicity of ZnONPs is associated with the competition of the dissociated Zn with Fe ions, leading to the interference of Fe-related physiological processes³⁹⁻⁴¹.

The sole existence of ENPs on the non-edible biomass in all three species was negligible, while by the heavy metal stress, the root biomass was noticeably increased. This difference may be explained by the increasing level of Zn. Our previous study indicated in the presence of heavy metals the release of root exudates may intensify, leading to dissociation of the ZnONPs. Therefore, it mediates the bio-accessibility of the Zn^{2+} supplement that could improve plant growth. This interpretation was consistent with the measurement of the pH values from the

hydroponic system after the uptake experiment. Table 1 represents the change of the pH after adding the heavy metals and in the coexistence of the heavy metals and ZnONPs.

Table 6.1. Measured pH values from the hydroponic system after the uptake experiment

Treatments	pH values		
	Cilantro	Parsley	Spinach
Ctrl	6.19	6.21	6.35
Cd + Pb	6.14	6.1	6.07
Cd+ Pb + ZnONPs	6.06	5.59	6.01

Adequate amounts of the essential minerals, particularly Cu, Fe and Zn is a crucial factor in food quality evaluation of the leafy greens. Unlike many metallic oxide nanoparticles that found to reduce the essential mineral levels^{24, 25}, the overall impacts of 100 mg L⁻¹ in this study on two species of spinach, cilantro were positively evaluated, while its impact slightly lowered the Fe levels in parsley. The order of the positive impacts of ZnONPs in coexistence with Cd and Pb on affecting the Fe concentration in edible tissues was evaluated as follow spinach(+10%)> cilantro(+9%)> parsley(-8%). The trend of re-localization of the Cu was different from the Fe contents, and the Cu level in edible tissues of three species were affected in copresence of both heavy metals as follow cilantro (+8%)> spinach (+4%)> parsley (+1.5%).

Dynamic translocation, uptake, and efflux of essential minerals is very imperative issues that affected by ZnONPs. The efflux of essential minerals through the root pores can be altered by the

presence of either heavy metals or with the coexistence of the ENPs^{6,9}. The obtained results from the detected levels of Cu and Fe suggested the impacts of the ZnONPs on the Cu mobilization is lower than the Fe localizations. Therefore, it was crucial to elucidate the rate of impacts and interaction of ENPs with plant relocation of the essential minerals of Cu and Fe.

Our calculated results of the mobilization rate (shown in Fig 6.7) represent an indication of the efflux between the roots and hydroponic media. Higher transfer rates suggest the less efflux of the elements. The higher transfer rate in parsley was consistent with the observed concentration of the Cu and Fe in their edible tissues. In a general trend, the mobilization of Cu in copresence of heavy metals is at a far lower rate compared to Fe. For example, in the coexistence of Cd and Pb with ZnONPs exposed to the parsley species, the mobilization of the Cu compared to its control and Fe to the control is 3% and 11%, respectively. However, further investigations of the elemental release into the hydroponic system are needed to elucidate the rate of micronutrient loss in exposure to heavy metals and nanoparticles.

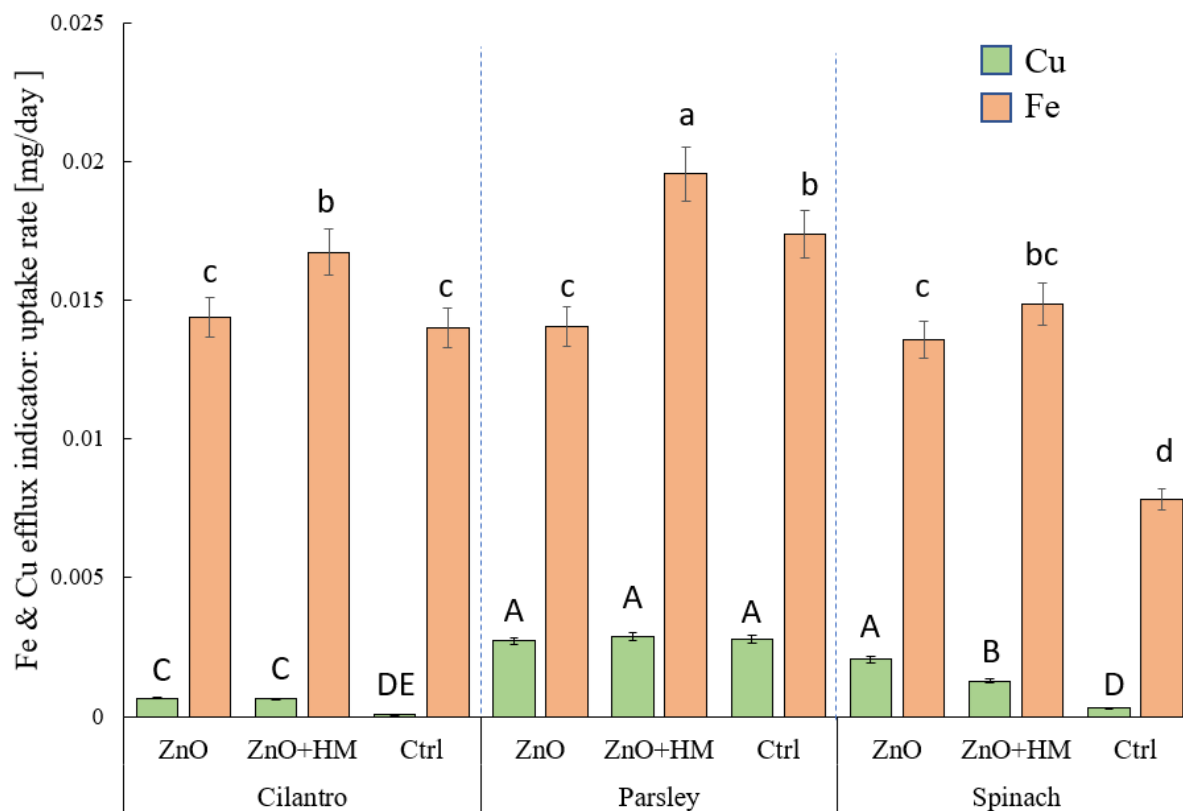


Fig. 6.7. The relocation rate of the essential minerals Fe and Cu on a mean basis in three species of cilantro (*Coriandrum sativum*), parsley (*Petroselinum sativum*), and spinach (*Spinaciae oleracea*) during two weeks of exposure time. The results were calculated by Eq.2. Error bars indicate the standard deviation (n = 3).

The co-presence of Cd and Pb limited the overall uptake of ZnONPs in all three species. This phenomenon will impact the dynamics of another essential mineral of Zn as the main component of the ZnONPs. The underlying mechanism for this limitation may be caused by aggregation of ZnONPs in the coexistence with both Cd and Pb. As discussed earlier (Table.1) the stress of heavy metals co-present induce the higher root exudate leading to the aggregation of ZnONPs²⁶. Consequently, the bioactive surface of the ZnONPs might be shielded with organic materials, while the simultaneous adsorption of the heavy metals on its surface will occur. Our previous study

revealed the root exudate will limit the bioavailability of metallic oxide nanoparticles and will reduce the extent of heavy metal adsorption²⁶.

Heavy metals interactions

The most prominent results were the response of ZnONPs that significantly reduced the Cd at low concentration in edible tissues. The higher concentration of Pb in edible tissues suggests that at high contamination levels ZnONPs will not be effective in the reduction of heavy metals. The different uptake patterns between Cd and Pb in shoots of the three species suggest that the properties of each metal and their concentration are the governing factors in their complex chemical interaction with co-occurring ZnONPs.

Heavy metals represent different adsorption capacity on ZnONPs, and our previous studies revealed that the adsorption of metal ions on metallic oxide ENPs is a significant phenomenon altering the plant metals uptake in a system with both heavy metals and ENPs^{6,27}. In the copresence of ZnONPs, lower level of Cd and elevated level of Pb strengthen a scenario in which the Cd represents higher adsorption tendency compared to Pb towards ZnONPs. Another plausible interpretation on higher Pb level in copresence of ZnONPs is attributed to the reactive oxidative species (ROS) generated by ZnONPs and their dissociated ions. ROS can affect plant homeostasis system via the interruption of photosynthesis, protein denaturation and up-regulation of antioxidant enzymes (i.e., superoxide dismutase (SOD), catalase (CAT), peroxidase (POD)).

One of the interesting findings of this study was the key role of ZnONPs in changing the root uptake of Pb and Cd. In an overall biomass analysis, both metals were significantly reduced in the presence of ZnONPs. However, this reduction was more prominent in root tissues.

The overall significant impacts of ZnONPs in mitigation of total Cd and Pb was attributed to a primary mechanism; it is highly possible that the surface charge of nanoparticles will be partially or entirely affected by the presence of root exudate and associated amino acids in rhizosphere zones of the plants before their uptake ²⁶. Because the pathways of the nanoparticle to the root cells are entrapped by high concentration of amino acids and low molecular chains. As results, amino acids in the rhizosphere are able to indirectly change the enthalpy of certain protein interaction with nanoparticles ²⁸.

The agglomeration of the nanoparticle is a critical phenomenon that occurs upon entrance of nanoparticle in a biological system which may be affected by the particle shape, size, surface area, and charge, as well as their adsorption properties ²⁹. Furthermore, key factors including pH, ionic strength, water quality, and the presence of organic/inorganic matter potentially modify nanoparticle aggregation, which govern the toxicity and reactivity of the nanoparticles ³⁰.

In the plant root zone (the rhizosphere), amino acids are the second most significant component of the root exudates. The release of such molecules has been reported in numbers of plants by 50% ($w v^{-1}$) through the root exudates ³¹. Representative amino acids hold distinctive charges at a pH range (5.5–8.5) characterizing the natural environment. For example, four frequently reported amino acids in rhizosphere include positively charged (Histidine), neutral (Glycine), and negative charges (Aspartic acid and Glutamate) ³¹.

The ZnONPs colloidal stability in exposure to amino acids solution and their tendency to agglomerate corresponds to the surface charge of the nanoparticles as well as functional groups of the amino acids which their overall interaction can be measured in the framework of multiple forces of electrostatic, steric, and van der Waals ³¹.

In copresence of Cd and b and ZnONPs, several processes can lessen the potential adsorption of Pb and Cd onto ZnONPs surface such as competitive adsorption of root exudates that occupy part of the adsorption sites for Pb or Cd; the formation of root exudate and heavy metals complexes which display lower adsorption on ZnONPs than free Pb^{2+} or Cd^{2+} or less available adsorption sites caused by ZnONPs aggregation.

In the presence of root exudates, if the adsorption density of Cd^{2+} is greater than Pb^{2+} or other available organic ions induced by amino acids and charged organic ligands, the imbalance of adsorbed ions will contribute a net positive charge to the surface. Therefore, the charge imbalance might be described either in terms of unequal adsorption of the Pb^{2+} or nonstoichiometric dissolution of the ZnONPs. The higher feasibility of Cd^{2+} adsorption in a substitution mechanism with ZnONPs with respect to higher dissolution of ZnONPs in co-presence of root exudates will be further investigated by measuring the trend of zeta potential at different levels of root exudates²⁶. Above all, the precipitation of larger particles can reduce the bioavailability of Cd and Pb. This interpretation was consistent with the change of the pH in the solution compared to the control (Shown in Table.1).

6.6. Conclusion

The overall impacts of ZnONPs at 100 mg L^{-1} level on the growth and yield production of all three species were positively evaluated towards increasing the nutritional values and reduction of the heavy metals. This evaluation was achieved over data interpretation of the Fe, Zn and Cu as essential minerals, total mitigation of the Cd and Pb as well as their impacts on the total biomass of each species.

6.7. References

1. Rossi, L.; Fedenia, L. N.; Sharifan, H.; Ma, X.; Lombardini, L., Effects of foliar application of zinc sulfate and zinc nanoparticles in coffee (*Coffea arabica* L.) plants. *Plant Physiology and Biochemistry* **2019**, *135*, 160-166.
2. Gui, X.; Zhang, Z.; Liu, S.; Ma, Y.; Zhang, P.; He, X.; Li, Y.; Zhang, J.; Li, H.; Rui, Y., Fate and phytotoxicity of CeO₂ nanoparticles on lettuce cultured in the potting soil environment. *PloS one* **2015**, *10*, (8), e0134261.
3. Jones Jr, J. B., *Hydroponics: a practical guide for the soilless grower*. CRC press: 2016.
4. Prazeres, A. R.; Albuquerque, A.; Luz, S.; Jerónimo, E.; Carvalho, F., Hydroponic System: A Promising Biotechnology for Food Production and Wastewater Treatment. In *Food Biosynthesis*, Elsevier: 2017; pp 317-350.
5. Sung, C. Y.; Park, C.-B., The effect of site-and landscape-scale factors on lead contamination of leafy vegetables grown in urban gardens. *Landscape and urban planning* **2018**, *177*, 38-46.
6. Rossi, L.; Sharifan, H.; Zhang, W.; Schwab, A. P.; Ma, X., Mutual effects and in planta accumulation of co-existing cerium oxide nanoparticles and cadmium in hydroponically grown soybean (*Glycine max* (L.) Merr.). *Environmental Science: Nano* **2018**, *5*, (1), 150-157.
7. Wang, X.; Sun, W.; Zhang, S.; Sharifan, H.; Ma, X., Elucidating the Effects of Cerium Oxide Nanoparticles and Zinc Oxide Nanoparticles on Arsenic Uptake and Speciation in Rice (*Oryza sativa*) in a Hydroponic System. *Environmental science & technology* **2018**.

8. Zhang, W.; Ebbs, S. D.; Musante, C.; White, J. C.; Gao, C.; Ma, X., Uptake and accumulation of bulk and nanosized cerium oxide particles and ionic cerium by radish (*Raphanus sativus* L.). *Journal of agricultural and food chemistry* **2015**, *63*, (2), 382-390.
9. Rossi, L.; Zhang, W.; Schwab, A. P.; Ma, X., Uptake, Accumulation, and in Planta Distribution of Coexisting Cerium Oxide Nanoparticles and Cadmium in *Glycine max* (L.) Merr. *Environmental science & technology* **2017**, *51*, (21), 12815-12824.
10. de la Rosa, G.; López-Moreno, M. L.; de Haro, D.; Botez, C. E.; Peralta-Videa, J. R.; Gardea-Torresdey, J. L., Effects of ZnO nanoparticles in alfalfa, tomato, and cucumber at the germination stage: root development and X-ray absorption spectroscopy studies. *Pure and Applied Chemistry* **2013**, *85*, (12), 2161-2174.
11. Zhang, M.; Liu, X.; Yuan, L.; Wu, K.; Duan, J.; Wang, X.; Yang, L., Transcriptional profiling in cadmium-treated rice seedling roots using suppressive subtractive hybridization. *Plant physiology and biochemistry* **2012**, *50*, 79-86.
12. Thorny Chanu, T.; Upadhyaya, H., Chapter 3 - Zinc Oxide Nanoparticle-Induced Responses on Plants: A Physiological Perspective. In *Nanomaterials in Plants, Algae and Microorganisms*, Tripathi, D. K.; Ahmad, P.; Sharma, S.; Chauhan, D. K.; Dubey, N. K., Eds. Academic Press: 2019; pp 43-64.
13. Zhang, W.; Long, J.; Li, J.; Zhang, M.; Xiao, G.; Ye, X.; Chang, W.; Zeng, H., Impact of ZnO nanoparticles on Cd toxicity and bioaccumulation in rice (*Oryza sativa* L.). *Environmental Science and Pollution Research* **2019**, 1-10.
14. da Cruz, T. N.; Savassa, S. M.; Gomes, M. H.; Rodrigues, E. S.; Duran, N. M.; de Almeida, E.; Martinelli, A. P.; de Carvalho, H. W., Shedding light on the mechanisms of

absorption and transport of ZnO nanoparticles by plants via in vivo X-ray spectroscopy.

Environmental Science: Nano **2017**, *4*, (12), 2367-2376.

15. Umamaheswari, A.; Lakshmana Prabu, S.; Puratchikody, A., Biosynthesis of zinc oxide nanoparticle: a review on greener approach. *MOJ Bioequivalence & Bioavailability* **2018**, *5*, 151-154.

16. Du, W.; Tan, W.; Peralta-Videa, J. R.; Gardea-Torresdey, J. L.; Ji, R.; Yin, Y.; Guo, H., Interaction of metal oxide nanoparticles with higher terrestrial plants: physiological and biochemical aspects. *Plant physiology and biochemistry* **2017**, *110*, 210-225.

17. Qiao, J.-t.; Liu, T.-x.; Wang, X.-q.; Li, F.-b.; Lv, Y.-h.; Cui, J.-h.; Zeng, X.-d.; Yuan, Y.-z.; Liu, C.-p., Simultaneous alleviation of cadmium and arsenic accumulation in rice by applying zero-valent iron and biochar to contaminated paddy soils. *Chemosphere* **2018**, *195*, 260-271.

18. Palermo, M.; Paradiso, R.; De Pascale, S.; Fogliano, V., Hydroponic cultivation improves the nutritional quality of soybean and its products. *Journal of agricultural and food chemistry* **2011**, *60*, (1), 250-255.

19. Zhang, W.; Dan, Y.; Shi, H.; Ma, X., Elucidating the mechanisms for plant uptake and in-planta speciation of cerium in radish (*Raphanus sativus* L.) treated with cerium oxide nanoparticles. *Journal of Environmental Chemical Engineering* **2017**, *5*, (1), 572-577.

20. Xiong, T.; Dumat, C.; Dappe, V.; Vezin, H.; Schreck, E.; Shahid, M.; Pierart, A.; Sobanska, S., Copper oxide nanoparticle foliar uptake, phytotoxicity, and consequences for sustainable urban agriculture. *Environmental science & technology* **2017**, *51*, (9), 5242-5251.

21. Krohling, C. A.; Eutrópico, F. J.; Bertolazi, A. A.; Dobbss, L. B.; Campostrini, E.; Dias, T.; Ramos, A. C., Ecophysiology of iron homeostasis in plants. *Soil science and plant nutrition* **2016**, *62*, (1), 39-47.

22. Zhang, R.; Zhang, H.; Tu, C.; Hu, X.; Li, L.; Luo, Y.; Christie, P., Phytotoxicity of ZnO nanoparticles and the released Zn(II) ion to corn (*Zea mays* L.) and cucumber (*Cucumis sativus* L.) during germination. *Environmental Science and Pollution Research* **2015**, *22*, (14), 11109-11117.
23. Dimkpa, C. O.; McLean, J. E.; Latta, D. E.; Manangón, E.; Britt, D. W.; Johnson, W. P.; Boyanov, M. I.; Anderson, A. J., CuO and ZnO nanoparticles: phytotoxicity, metal speciation, and induction of oxidative stress in sand-grown wheat. *Journal of Nanoparticle Research* **2012**, *14*, (9), 1125.
24. Shams, G.; Ranjbar, M.; Amiri, A. A.; Khodarahmpour, Z., The effect of 35 nm silver nanoparticles on antagonistic and synergistic mineral elements in leaves and fruit of tomato (*Lycopersicon esculentum* Mill.). *International Journal of Agriculture and Crop Sciences (IJACS)* **2013**, *5*, (5), 493-500.
25. Zhao, L.; Peralta-Videa, J. R.; Rico, C. M.; Hernandez-Viezcas, J. A.; Sun, Y.; Niu, G.; Servin, A.; Nunez, J. E.; Duarte-Gardea, M.; Gardea-Torresdey, J. L., CeO₂ and ZnO nanoparticles change the nutritional qualities of cucumber (*Cucumis sativus*). *Journal of agricultural and food chemistry* **2014**, *62*, (13), 2752-2759.
26. Sharifan, H.; Wang, X.; Guo, B.; Ma, X., Investigation on the Modification of Physicochemical Properties of Cerium Oxide Nanoparticles through Adsorption of Cd and As(III)/As(V). *ACS Sustainable Chemistry & Engineering* **2018**, *6*, (10), 13454-13461.
27. Wang, X.; Sun, W.; Zhang, S.; Sharifan, H.; Ma, X., Elucidating the Effects of Cerium Oxide Nanoparticles and Zinc Oxide Nanoparticles on Arsenic Uptake and Speciation in Rice (*Oryza sativa*) in a Hydroponic System. *Environmental science & technology* **2018**, *52*, (17), 10040-10047.

28. Lynch, I.; Dawson, K. A., Protein-nanoparticle interactions. *Nano today* **2008**, *3*, (1-2), 40-47.
29. Espitia, P. J. P.; Soares, N. d. F. F.; Coimbra, J. S. d. R.; de Andrade, N. J.; Cruz, R. S.; Medeiros, E. A. A. J. F.; Technology, B., Zinc Oxide Nanoparticles: Synthesis, Antimicrobial Activity and Food Packaging Applications. **2012**, *5*, (5), 1447-1464.
30. Singh, A.; Singh, N.; Afzal, S.; Singh, T.; Hussain, I. J. J. o. M. S., Zinc oxide nanoparticles: a review of their biological synthesis, antimicrobial activity, uptake, translocation and biotransformation in plants. **2018**, *53*, (1), 185-201.
31. Molina, R.; Al-Salama, Y.; Jurkschat, K.; Dobson, P. J.; Thompson, I. P., Potential environmental influence of amino acids on the behavior of ZnO nanoparticles. *Chemosphere* **2011**, *83*, (4), 545-551.

CHAPTER VII

INVESTIGATION OF EXTERNAL APPLICATION OF ZNO-NANOPARTICLES FOR ENHANCING SHELF-LIFE OF TOMATO (*SOLANUM LYCOPERSICUM*)

7.1. Summary

Tomato (*Solanum lycopersicum*) is rich source of vitamins, essential minerals and amino acids, that ranked it as the second most consumed vegetable in the world. Also, it is rich of anti-cancer compound of lycopene that is a main carotenoid in the entire human body. It is very imperative to apply cutting edge technologies to extend the shelf life of tomato. Zinc oxide nanoparticles (ZnO ENPs) are used in wide range of agricultural practice. Though general consensus has been reached that ZnO ENPs possess high anti-microbial properties and UV absorption, but their external application on shelf life of tomato has not been investigated. To authors's knowledge, for the first time, this study extensively investigated the external application of ZnO nanoparticles at 100 mg L⁻¹ on the shelf life of tomato. Main shelf life factors of tomato including the microbial spoilage, dehydration and color change were investigated. Additional analytical experiment was conducted to elucidate the diffusion of Zn into the tissues and water removal efficiency of the Zn after washing the tomato by an inductively coupled plasma–mass spectrometry ICP-MS. Application of ZnO ENPs was associated with 47% inhibition of the microbial growth and significant increase of the lycopene antioxidant ($P < 0.05$). In summary, results highlight the beneficial application of the ZnO ENPs could enhance the tomato shelf life at room temperature.

7.2. Introduction

Nanotechnology advancement into agricultural practice has developed as a revolutionary breakthrough in food science and engineering. Engineered Nanoparticles (ENPs) have found their ways in post-harvesting technologies through different applications, including food packaging, nanosensors and many more. ENPs possess unique properties, such as high surface area and adsorption capacity, easy operation, and cost-effective production. There is high interest in the use of ENPs towards increasing food safety and agricultural resilience. ENPs can change the precarious state of the toxic metal ions into a stable or safe state and reduce the need for the treatment of contaminated water for agriculture. Also, ENPs can prevent the uptake of heavy metals and enhance the delivery of micronutrient into the edible tissues of the crops.

Recently, ENPs has shown a high potential to increase the shelf life of fresh foods through their anti-fungal/microbial properties. For example, Sing et al 2017 found impregnation of cellulosic food package with silver (Ag) -ENPs at minimum level of 15.3 ug/ml can significantly increase the shelf life of tomato and cabbage [1]. Several metallic nanoparticles have shown high potential in retarding the fungal and microbial activities in fresh foods such as CuO and ZnO ENPs [2, 3]. Losses due to spoilage of the postharvest fresh vegetables are imperative issues in food process engineering. Microbial contamination of post-harvested foods are inevitable. From the field collection and packaging until the vegetable are placed at consumer's cold storage, food quality and shelf life are subjected to reduce [1].

However, the growing demand for less processed foods, extended shelf-life and health concerns for the potential toxicity of food preservatives surge food engineers to find alternatives for a better preservation. Nanotechnology as a promising alternative hailed ENPs application throughout the

food chain supply, which tenders a novel food processing; nano-materials in production efficiency (i.e. packaging), agrochemicals minimization (i.e. preservatives); better flavor and textures; sanitary processing and enhancing the nutritional values. During the past decade, a variety of organic and inorganic ENPs have been introduced in food science.[4, 5] Nanomaterials are generally engineered to increase profitability and sustainability from agricultural field production to the post harvesting processes.

Zinc oxide ENPs with the formula of ZnO is an inorganic compound, is currently being used as food additives and has been recognized as safe material by the Food and Drug Administration [2]. It exhibits specific properties which make it favorable for food industries such as decent transparency, high electron mobility as well as strong room temperature luminescence [6]. ZnO nanostructures are also attractive for biological and agricultural application because of their safe properties and large surface area [7, 8]. For example, in biological systems, ZnO enters into a slow reaction with fatty acids and produce carboxylates compounds, such as oleate or stearate[9]. Also, ZnO nanoparticle represents strong antimicrobial characteristics which may stem from the generation of reactive oxygen species (ROS)[10, 11]. Such ROS could be induced on the nanosurface of ZnO [12]. Its application as an antimicrobial agent against various pathogens including *Escherichia coli*, *Campylobacter jejuni*, *Pseudomonas aeruginosa* has been frequently reported [13, 14].

The benefits of using ZnO as antimicrobial agents is that Zn is an essential mineral element for humans and crops, which exhibit strong activity in the form of oxide at very small amounts [11, 15]. For example, Zn is the sole metal formulated in all six enzyme classes (transferases, viz. oxidoreductases, hydrolases and ligases, lyases, isomerases) [13]. Zn plays a vital role in different integral metabolic processes, promotes the synthesis of carotenoids and chlorophylls leading to

higher photosynthetic apparatus of the crops [9]. It has demonstrated to enhance germination rate, pigments synthesis, the contents of carbs and protein as well as activities of antioxidant enzymes [16, 17].

To the authors' knowledge, for the first time this study investigated the external application of ZnO ENPs in shelf life properties of the tomato. Tomato is rich source of vitamins, essential minerals and amino acids, that ranked it as the second most consumed vegetable in the world[18]. Also, it is rich of anti-cancer compound of lycopene that is a main carotenoid in the entire human body [19]. Lycopene possess the highest antioxidant potential among the six major carotenoids of human plasma [19]. Studies have shown the strong correlation between the lycopene level and tomato color [20]. ZnO ENPs with high UV adsorption capacity, may affect the concentration of the concentration of the lycopene in tomato. Through this research, extensive microbiological and analytical analysis was used to study the potential effects of the ZnO ENPs on the shelf life of tomato.

7.3. Materials and Methods

7.3.1. Materials and characterization

Negatively surface charged ZnO ENPs (20% by weight, 10-30 nm) was purchased from the US Research Nanomaterials, Inc. (Houston, TX). Zinc sulfate heptahydrate ($\text{ZnSO}_4 \cdot 7\text{H}_2\text{O}$ >99%) was provided from Acros Organics (Geel, Belgium). Potato dextrose agar was purchased from Sigma Aldrich Inc. (Merck KGaA, Darmstadt, Germany). Peptone water was purchased from Sigma Aldrich (St. Louis, MO). ZnO ENPs was fully characterized for the size and shape in our previous study by a Tecnai G2 F20 transmission electron microscope (TEM); spherical shape at high density was primarily dominant, with less density of triangular or other irregular shapes at the images [21]. The diameter varied between 15 to 137 nm with a recorded mean size of 68.1 nm. Dynamic light

scattering applied to quantify the hydrodynamic ENPs size at dispersed level of 100 mg L⁻¹ in DI water (621.08±7.63 nm) and zeta potential (-28.80±2.04 mV) [21]. A suspension of ZnO ENPs at concentration of 100 mg L⁻¹ was prepared in ultrapure water and sonicated for one minute at Branson B2510 ultrasonic bath (Branson, Danbury, CT) [15].

7.3.2. External applications and water loss

The fresh ripped tomatoes *Solanum lycopersicum* were purchased from local farmers in College Station, Texas. Before any treatments, tomatoes were disinfected with 3% sodium hypochlorite solution for 15 min, washed with deionized water (DI) three times [1]. Tomatoes were grouped in three treatments, 100 mg L⁻¹ ZnO ENPs, 100 mg L⁻¹ ZnSO₄ and control with no chemical exposure. Each treatment series were exposed at three different temperatures, room temperature 25 °C, average summer temperature of Texas 33 °C and refrigerator temperature of 4 °C. tomatoes were hold in climate chambers under a 16/8 h fluorescent illumination cycle (250 μmol m² s⁻¹) and were randomly rotated every other day during the storage stage to reduce possible differences in light reception [22]. All samples were subjected to weight on a daily basis to determine the water loss factor.

7.3.3. Color measurement

To evaluate the color of tomato under different treatments, HunterLab LabScan XE spectrophotometer (Hunter Associates, USA) was used with a port size of 10.1 mm and a view area of 6.35 mm. The CIE illuminant C applied for the color characterization [20, 23]. The colorimeter was calibrated before each measurement, using a black, red and white standard tiles. Three color dimensions of the L, a and b values were read from the processed colors [23, 24]. In each treatment, the final color values were quantified by mean of three replicates. Each measurement was recorded within at 8 am and the treatments were kept under constant climatic

condition at room temperature (16/8 h fluorescent illumination cycle ($250 \mu\text{mol m}^{-2} \text{s}^{-1}$)). The quantity of lycopene was simulated based on the linear model developed by Barret and Anton 2008[20].

7.3.4. Natural microflora analyses of fresh-cut tomato

Before any treatments, intact tomatoes in three replicates were homogenized in 250 mL 3% sterile peptone water (Sigma–Aldrich, Louis, MO) using a sterile Blender bag (VWR, Randor, PA, USA)[25]. Next, triplicates of tomatoes were classified in three treatments groups, 100 mg L ZnOENPs, 100 mg L ZnSO₄ and control with no chemical exposure. After the external treatments, tomatoes were subjected to air dry for 24 h at room temperature. At day 4, tomatoes were prepared for microbial analysis on the outer skin. Approximately 1 Cm² of the outer skin of each tomato (<1 mm depth) were cut and plated on Potato Dextrose Agar (PDA, Difco) petri dish (15 x 5 mm) [1]. The plates in triplicates were incubated at 30 °C for 72 h.

7.3.5. Microbial growth of existing tomato spoilage agents

A spoiled tomato was collected from the shelf of the control treatments at 25 °C. The tomato was submerged and shaken into a sterile Blender bag for 15 min to retrieve homogenate aliquot of the microbial communities for further analysis [26]. On the side, agar plates in three replicate of three treatments were prepared; two were inoculated with 20 μL of either (100 mgL) ZnO ENPs or 100 (mgL) ZnSO₄, and a control with no Zn exposure. A 100 μL of the tomato filtrate were spread on agar plates for the enumeration of microbial communities. Plates were kept in incubation chamber at 35 °C for 48 h and colony forming units (CFU) were counted respectively with an automated plate counter (ProtoCOL, Synoptics, Cambridge, UK).

7.3.6. Zn Diffusion Analysis

At day four of the exposure, three tomatoes from each treatment were randomly selected and fully washed with DI water three times. Each tomato was chopped and dried in an oven at 75 °C for 5 days and acid digested following published protocols [4, 27, 28]. Briefly, 5 mL of 70% (w/w) nitric acid (Certified ACS Plus) was added to a 50 mL digestion tube containing 0.5 g of homogenized dry biomass of tomato and heated at 95 °C for 5 h on a DigiPREP MS hot block digester (SCP Science, Clark Graham, Canada). After being cooled down to room temperature, 2 mL of hydrogen peroxide (30%, Certified ACS) was added to each tube and re-heated on the hot block to 95 °C until the biomass was fully digested [28, 29]. The amount of Zn in each sample was then quantified by an inductively coupled plasma–mass spectrometry (ICP-MS) (Agilent 7500i, Agilent Technologies Co. Ltd, USA). Detailed information on the operational parameters of ICP-MS and sample quality control can be found from our previous publications [30].

7.3.7. Statistical Analysis

Statistical analysis of cerium and cadmium concentration in dry plant tissues was performed using the Minitab 18 Statistical Software (Minitab Inc., State College, PA, USA). The comparison between mean values of different treatments was carried out using One-Way ANOVA, followed by Tukey's test at significance level 5% ($p < 0.05$).

6.4. Results and Discussion

6.4.1. Biological analysis

Figure 1 illustrate the impacts of the 100 mg L⁻¹ ZnO ENPs on the microbial growth of tomato. The ZNO ENPs significantly reduced the microbial growth compared to control by approximately

47%, which indicate its high potential for hindering the spoilage of the tomato. However, the impacts of the Zn^{2+} ions were also statistically significant ($P < 0.05$) in reduction of the microbial community in comparison to control (14%) but to less extent in comparison to ENPs. These results provide strong evidence upon anti-microbial/fungal properties of the ZnO NPs, leading to further experimental investigation. It is noteworthy to mention that the anti-microbial properties of the ZnO ENPs may stem from the release of Zn^{2+} on the outer skin of the tomato because of the significant reduction of microbial activities over applying the Zn ions instead of ENPs in this experiment. Several studies have shown strong antimicrobial properties of ZnO ENPs at a very low level on retarding the growth of both gram negative and gram-positive bacteria, in which in some cases reach up to 99.9% efficiency [31]. Figure 2 displays the qualitative analysis of the microbial growth of the outer skin of the tomato within 24 and 72 incubation hours. The qualitative results in Figure 2 provides a very critical information upon the growth rate of the microbial community that has been substantially limited with the presence of the ZnO ENPs compared to control and Zn^{2+} ions. One of the responsive mechanisms can be the inducing of the ROS by ENPs that strongly interrupt the function of the microbial cell wall [5] and prohibits their further development of the bio-surface of tomato. Studies have proposed that Zn^{2+} at low level might behave as a nutrient supplement for microbial communities leading to enhance the metabolic process of microbial community [32], developing their footprint.

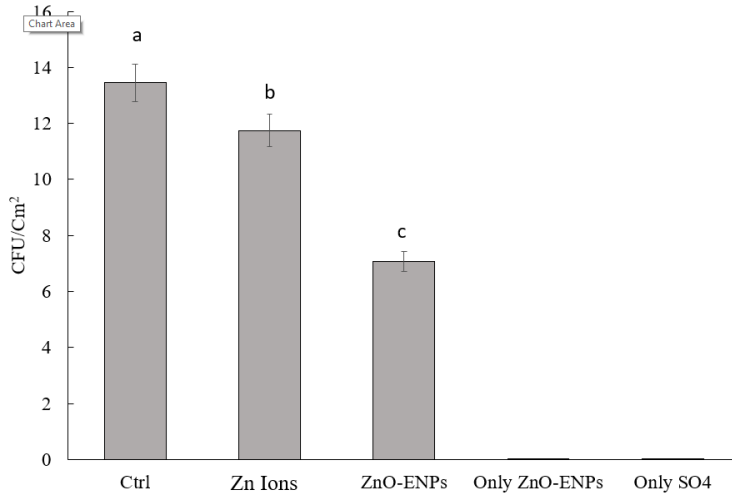


Figure 7.1. The Colony Forming Units (CFU) formed after 100 mg L⁻¹ external application of ZnO ENPs in potato dextrose agar medium to monitor the susceptibility of existing microbial community on tomato skins to presence of ENPs.

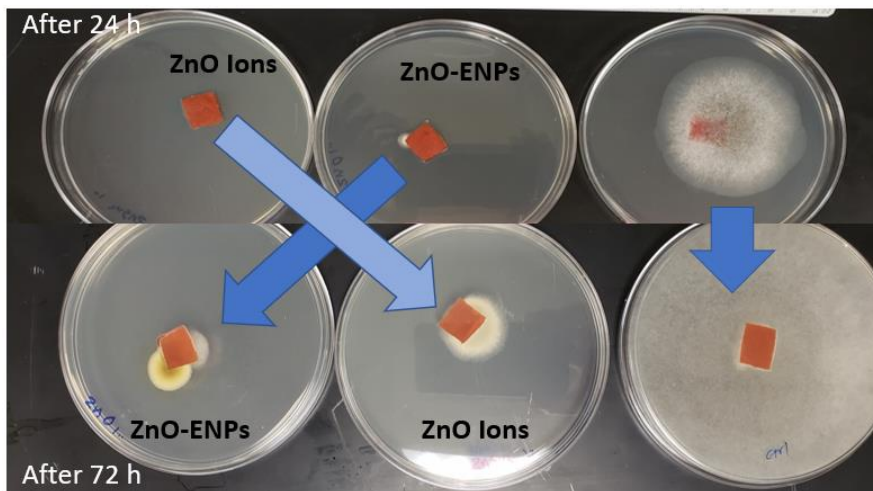


Figure 7.2. Inhibition of microbial growth in presence of the 100 mg L⁻¹ external application of ZnO ENPs or Zn²⁺ on outer surface of tomato. Plates on the top indicate the response of microbial community and 24 hours of incubation at 35 C and the lower plates display their response after 72 hours.

7.4.2. Water loss and color change in shelf life experiment

Figure 3 shows the key parameter in shelf life of tomato as a customer perception factor and indicator of the microbial activities within the bio-surface. Water loss is directly related to the storage temperature of the tomato; however, it can be impacted by applying the ZnO ENPs. The applied ZnO ENPs have shown strong UV absorber that increased its content in formulation of the several sunscreen products [33]. Also, it has shown that increase the photosynthesis of the several of crops [2, 15]. In case of tomato, the higher UV absorption may change the color and reduce the water contents of tomato. The observation of tomato treated with 100 mg L⁻¹ ZnO ENPs under the higher temperature of 33 °C compared to the room temperature in Figure 3 shows stronger relation between the tomato water loss and presence of the ZnO ENPs at higher temperature. ENPs elevated the water loss significantly by 60 % compared to control at 33 °C. This reduction was 50% less at room temperature (25 °C) compared to treatments at higher temperature. However, in case of the room temperature this relation was not significant compared to control. The key point of this observation was the factor of temperature than the presence of the ENPs. Future investigation may be conducted to optimize the temperature and ENPs application regarding the water loss factor. The reaction response of treatments by the Zn²⁺ ion and increasing the water loss is not clear yet. One reason can be the energy absorption of the metallic ions and promoting the surface evaporation from the tomato skin.

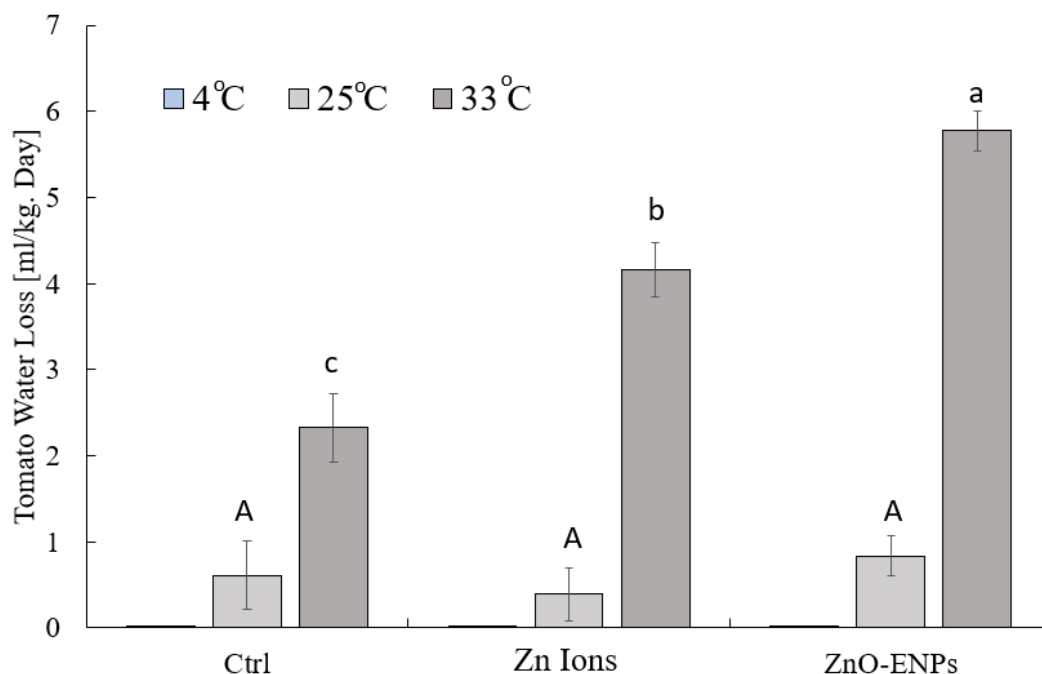


Figure 7.3. Water loss profile of tomato: the mean data set of control, ZnO ENPs and Zn²⁺ treatments under three storage temperatures were examined by measuring the biomass change over five days of exposure. All treatments were kept under a 16/8 h fluorescent illumination cycle (250 $\mu\text{mol m}^{-2} \text{s}^{-1}$). The letters indicate the statistical significance ($p < 0.05$, $n = 3$).

Shelf life results based on water loss measurements have been further coupled with colorimetric analysis of the pigments. Using LabScan XE spectrophotometer technique reduces the complexity of the shelf life data-set under ZnO ENPs treatments. The characteristic structure of the data-set is a strong indicator as ZnO ENPs UV absorption and promotional factor in ripening the tomato. As shown in Figure 4, exposure to ENPs significantly increased the redness of the tomato as time proceeds. The scores obtained from the instrument, further indicates nearly neutral impacts of the Zn²⁺ on the color properties of the tomato. Combination of all treatments dictates the beneficial application of ZnO ENPs in enhancing the red color of tomato while the water loss may offset

this factor. A very important protein of tomato known as lycopene is indicator of nutritional value of tomato shelf life was respectively simulated. As it can be seen from the Figure 4 the contents of lycopene may closely relate to the presence of ENPs. For example, within four days of the storage time, the lycopene content may increase by at least 5 mg/kg compared to control. However, these results call for further investigations of the change of antioxidant level in tomato exposed to external application of ZnO ENPs.

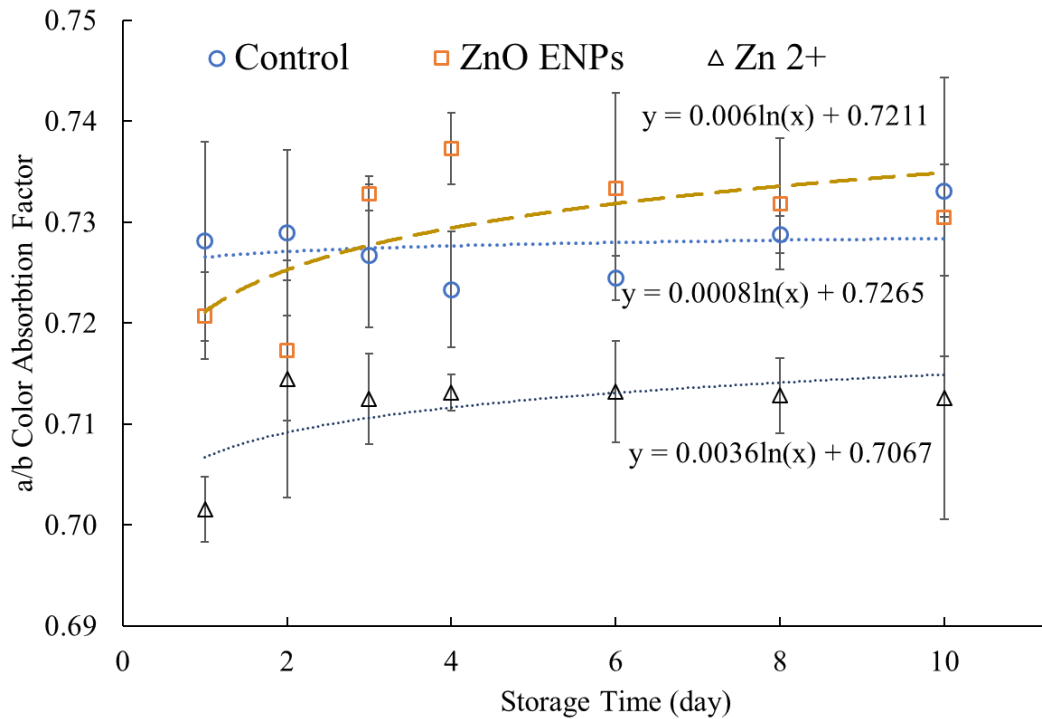


Figure 7.4. The black curves represent the relationship between the a/b color factor of tomatoes under each treatment (control, 100 mg L⁻¹ external application of ZnO ENPs or Zn²⁺) and storage time. Each curve is representative of a simulated value of the final experiment.

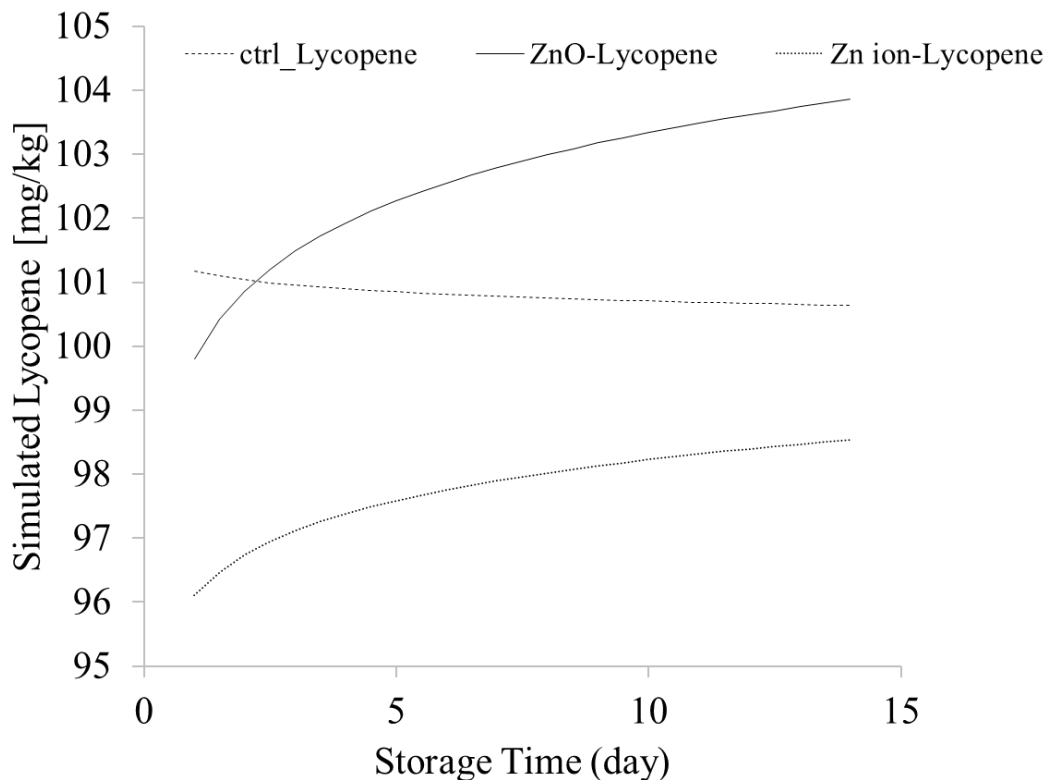


Figure 7.5. Projected concentration of lycopene antioxidant under three different treatments. The colorimetric experimental data were applied through the suggested linear developed model of Barret and Anthon, 2008.

7.4.3. Zn enrichment

Figure 6 illustrate imperative results regarding the essential element enrichment of tomato after the exposure time to ENPs. The amounts of the ZnO ENPs has been remarkably washed off from the tomato surface. The high efficiency of the water removal of this nanoparticle cleared the concerns regarding over dose concentration of Zn after uptake experiment. In addition, the Zn level was enhanced towards the enrichment of the nutritional values, in which treatments exposed to ENPs the total Zn content was increased by 16% and those exposed to only Zn ions, it was increased by 13%. Surface absorption and diffusion of ZnO from the hydrophobic surface of tomato into the edible tissues may strongly relate to the coating material of the ENPs. For example,

there are several ZnO ENPs in the market coated materials with a variety of organic substances such as amino acids which can be further investigate towards enhancing the shelf life of tomato.

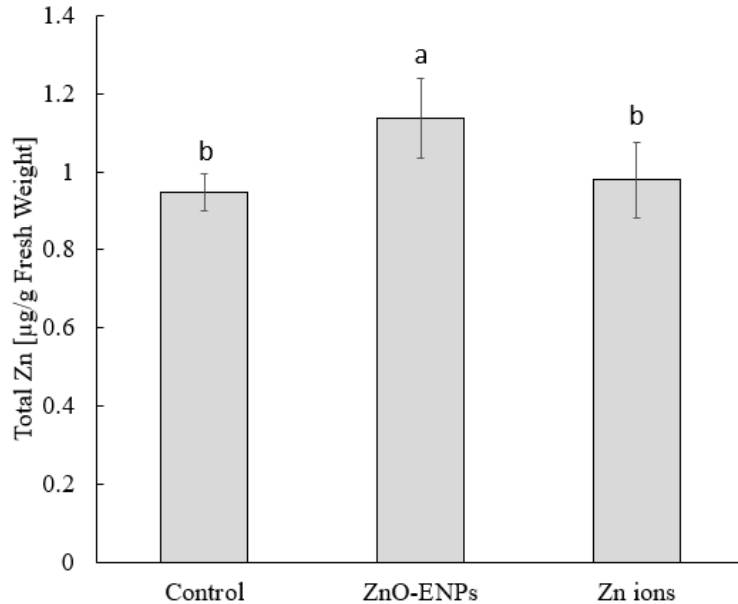


Figure 7.6. illustration of the total Zn contents after washing the tomato at termination stage. The letters indicate the significance level using one-way ANNOVA ($p < 0.05$, $n = 3$).

7.5. Conclusion

Despite the importance of external application of ZnO ENPs for improving crop nutrition and extending the shelf life, the underlying mechanisms by which external-applied ZnO ENPs move across the outer surface or stays on the surface remain unclear. Using XE spectrophotometer, revealed the role of ZnO ENPs in ripening and color improvement can be further investigated. The microbial analysis indicated the anti-microbial properties of the ZnO ENPs can be main governing factor in extending the tomato shelf life. Finding from the impact of the ZnO on the dehydration may be further investigated under different climatic set up. Enhancing the nutritional value of the tomato by increasing 16% of total Zn content was one of the key finding in this study. This study established a baseline for more investigation on external applications of a variety of metallic oxide

nanoparticles with anti-microbial/fungal properties such as CuO on a variety of susceptible vegetables to spoilage. Overall, this suggests the potential application of ZnO to extend of shelf life. However, further studies are needed to extend and safely apply this ENPs in extending the shelf life.

7.6. References

1. Singh, M. and T.J.L. Sahareen, Investigation of cellulosic packets impregnated with silver nanoparticles for enhancing shelf-life of vegetables. 2017. 86: p. 116-122.
2. Rossi, L., et al., Effects of foliar application of zinc sulfate and zinc nanoparticles in coffee (*Coffea arabica* L.) plants. 2019. 135: p. 160-166.
3. Safaei, M., et al., Preparation, structural characterization, thermal properties and antifungal activity of alginate-CuO bionanocomposite. 2019. 101: p. 323-329.
4. Wang, X., et al., Elucidating the Effects of Cerium Oxide Nanoparticles and Zinc Oxide Nanoparticles on Arsenic Uptake and Speciation in Rice (*Oryza sativa*) in a Hydroponic System. *Environmental science & technology*, 2018. 52(17): p. 10040-10047.
5. Kumar, R., et al., Antimicrobial properties of ZnO nanomaterials: A review. 2017. 43(5): p. 3940-3961.
6. Makino, T., et al., Room-temperature luminescence of excitons in ZnO/(Mg, Zn) O multiple quantum wells on lattice-matched substrates. *Applied Physics Letters*, 2000. 77(7): p. 975-977.
7. McNeil, S.E., Nanotechnology for the biologist. *Journal of Leukocyte Biology*, 2005. 78(3): p. 585-594.

8. Wang, Z.L., ZnO nanowire and nanobelt platform for nanotechnology. *Materials Science and Engineering: R: Reports*, 2009. 64(3-4): p. 33-71.
9. Hussain, A., et al., Zinc oxide nanoparticles alter the wheat physiological response and reduce the cadmium uptake by plants. *Environmental Pollution*, 2018. 242: p. 1518-1526.
10. Sirelkhatim, A., et al., Review on zinc oxide nanoparticles: antibacterial activity and toxicity mechanism. *Nano-Micro Letters*, 2015. 7(3): p. 219-242.
11. Zhang, L., et al., Investigation into the antibacterial behaviour of suspensions of ZnO nanoparticles (ZnO nanofluids). *Journal of Nanoparticle Research*, 2007. 9(3): p. 479-489.
12. Espitia, P.J.P., et al., Zinc Oxide Nanoparticles: Synthesis, Antimicrobial Activity and Food Packaging Applications. 2012. 5(5): p. 1447-1464.
13. Singh, A., et al., Zinc oxide nanoparticles: a review of their biological synthesis, antimicrobial activity, uptake, translocation and biotransformation in plants. 2018. 53(1): p. 185-201.
14. Wang, L., et al., Removing *Escherichia coli* from water using zinc oxide-coated zeolite. *Water research*, 2018. 141: p. 145-151.
15. Kouhi, S.M.M., et al., Long-term exposure of rapeseed (*Brassica napus* L.) to ZnO nanoparticles: anatomical and ultrastructural responses. 2015. 22(14): p. 10733-10743.
16. Scott, N.R., H. Chen, and H. Cui, *Nanotechnology applications and implications of agrochemicals toward sustainable agriculture and food systems*. 2018, ACS Publications.
17. Medina-Velo, I.A., et al., Minimal transgenerational effect of ZnO nanomaterials on the physiology and nutrient profile of *Phaseolus vulgaris*. *ACS Sustainable Chemistry & Engineering*, 2018.

18. Onyia, V., et al., Evaluation of Tomato Genotypes Growth, Yield, and Shelf Life Enhancement in Nigeria. 2019. 21(1): p. 143-152.
19. Wang, Y., et al., Lycopene, tomato products and prostate cancer-specific mortality among men diagnosed with nonmetastatic prostate cancer in the Cancer Prevention Study II Nutrition Cohort. 2016. 138(12): p. 2846-2855.
20. Barrett, D.M., G.E.J.C.q.o.f. Anthon, and W. processed foods. American Chemical Society, DC, USA, Color quality of tomato products. 2008: p. 131-139.
21. Wang, X., et al., Elucidating the effects of cerium oxide nanoparticles and zinc oxide nanoparticles on arsenic uptake and speciation in rice (*oryza sativa*) in a hydroponic system. 2018. 52(17): p. 10040-10047.
22. Sharifan, H., X. Wang, and X.J.I.J.o.P. Ma, Impact of nanoparticle surface charge and phosphate on the uptake of coexisting cerium oxide nanoparticles and cadmium by soybean (*Glycine max.*(L.) merr.). 2019: p. 1-8.
23. Sandei, L., et al. Processing tomato by-products re-use, secondary raw material for tomato product with new functionality. in XV International Symposium on Processing Tomato 1233. 2018.
24. Kaur, C., et al., Functional quality and antioxidant composition of selected tomato (*Solanum lycopersicon L*) cultivars grown in Northern India. 2013. 50(1): p. 139-145.
25. Chitarra, W., et al., Potential uptake of *Escherichia coli* O157: H7 and *Listeria monocytogenes* from growth substrate into leaves of salad plants and basil grown in soil irrigated with contaminated water. 2014. 189: p. 139-145.

26. Allende, A., et al., Antimicrobial effect of acidified sodium chlorite, sodium chlorite, sodium hypochlorite, and citric acid on *Escherichia coli* O157:H7 and natural microflora of fresh-cut cilantro. 2009. 20(3): p. 230-234.
27. Cao, Z., et al., Physiological effects of cerium oxide nanoparticles on the photosynthesis and water use efficiency of soybean (*Glycine max* (L.) Merr.). *Environmental Science: Nano*, 2017. 4(5): p. 1086-1094.
28. Zhang, W., et al., Elucidating the mechanisms for plant uptake and in-planta speciation of cerium in radish (*Raphanus sativus* L.) treated with cerium oxide nanoparticles. *Journal of Environmental Chemical Engineering*, 2017. 5(1): p. 572-577.
29. Zhang, W., et al., Uptake and accumulation of bulk and nanosized cerium oxide particles and ionic cerium by radish (*Raphanus sativus* L.). *Journal of agricultural and food chemistry*, 2015. 63(2): p. 382-390.
30. Sharifan, H., et al., Investigation on the Modification of Physicochemical Properties of Cerium Oxide Nanoparticles through Adsorption of Cd and As(III)/As(V). *ACS Sustainable Chemistry & Engineering*, 2018. 6(10): p. 13454-13461.
31. Agarwal, H., S.V. Kumar, and S.J.R.-E.T. Rajeshkumar, A review on green synthesis of zinc oxide nanoparticles—an eco-friendly approach. 2017. 3(4): p. 406-413.
32. Guo, B.-L., et al., The antibacterial activity of Ta-doped ZnO nanoparticles. 2015. 10(1): p. 336.
33. Sharifan, H. and X.J.M.-R.i.O.C. Ma, Potential Photochemical Interactions of UV Filter Molecules with Multichlorinated Structure of Pymnesins in Harmful Algal Bloom Events. 2017. 14(5): p. 391-399.

CHAPTER VIII

CONCLUSION AND RESEARCH PERSPECTIVE

This dissertation work aimed *to elucidate the underlying mechanisms of interaction between engineering metallic oxide nanoparticles and biosystem of different plant species and possibly finding their potential phytoremediation application*. With embracement of nanotechnology into agrichemicals, the presence of engineered nanoparticles (ENPs) can strongly affect the modulating factors and changing the bioavailability of heavy metals and essential minerals to plants. Exposure of edible plants with the coexistence of ENPs and heavy metals can alter their uptake and localization of essential minerals such as iron (Fe) and copper (Cu) through different mechanisms. Agricultural commodities such as legumes, grains, leafy vegetables, and herbs are a rich source of proteins, essential minerals, and fibers for the human diet and livestock. Heavy metals and metalloids including cadmium (Cd), lead (Pb), and arsenic (III/V) are extremely toxic elements to humans even at trace concentrations that their accumulation in edible plants turns them to phytotoxic foods. Several factors can modulate the availability of such metals and other essential minerals to plants, such as pH, the rhizosphere microbiome, and the presence of organic acids. Characterizing these factors and revealing this role can substantially add to the advancement of nanotechnology. My research area is very interesting for students; it is an interdisciplinary research and can be supported by different source of funding.

In addition, as has been shown in my publication list the *environmental fate of organic and inorganic contaminants in various environmental compartments* has been among my top research interests. I have three peer-reviewed publication regarding the environmental fate of organic Ultraviolet (UV) filters and five printed publications as the outcome of my Ph.D. progress on underlying mechanisms of the interaction of coexisting metallic oxide nanoparticles (CuO, ZnO, and CeO₂) with different crops including rice and soybean.

8.1. The Challenge and Research Needs

Due to different size-specific properties, surface charge, and phytotoxicity potential, the risk of bioaccumulation of ENPs in dietary plants and edible crop tissues is increasing. In addition, different plant species have developed different defense mechanisms towards the intrusion of organic and inorganic contaminants. Coexistence of ENPs and organic and inorganic contaminants change the physiochemistry of ENPs and response of the plants.

For organic chemicals, hydrophobicity is a key parameter which mediates the entrance of compounds into the plant and dictates the primary mechanism for ENPs when they co-exist with the organic compounds¹. This pathway is known as the “Trojan horse effect” in which adsorption of the organic compounds onto the ENPs surface leads to concomitantly uptake by plants². For inorganic elements including heavy metals and metalloids, sophisticated plant root systems can regulate their transport into root cytoplasm. Two pathways are well known. First, actively regulating the shuttle of heavy metals through various ion and protein channel embedded in the cell membrane. Second, passively transporting via passive diffusion which occurs through the cell membranes³. Passive transport of ENPs into plants could occur through cells via Van der Waals forces, steric interactions and electrostatic charges without stimulus on vesicles formation⁴. Taking advantage of advanced analytical techniques, a previous study using confocal microscopic images of fluorescein isothiocyanate-stained (FITC)-labeled CeO₂NPs showed the presence of CeO₂NPs in the intercellular spaces, suggesting a passive apoplastic pathway of CeO₂NPs uptake⁵. Active transport, including signaling from calcium channels and the regulation of plasma membranes are also likely important mechanisms for ENPs uptake⁶. The possibility of active

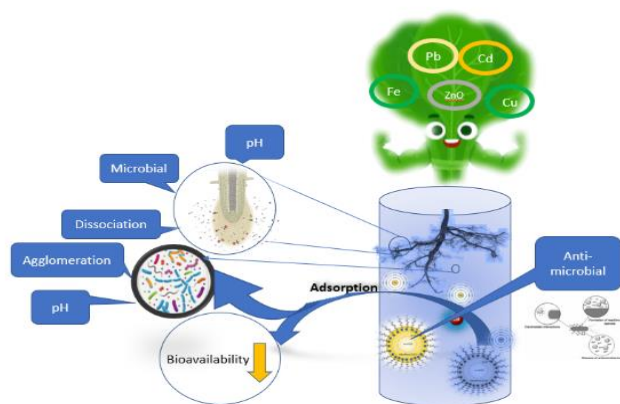


Fig. 8.1. potential interaction of between plant and nanoparticles and heavy metals in a hydroponic system.

transport of ENPs through different ion and protein channels into plant roots was also proposed by other researchers ⁷. However, no conclusive evidence has been reported up to now to substantiate the assumption that ENPs are actively transported into plant roots through proteinous channels.

ENPs surface charge also plays a distinctive role in their fate and transport. For example, after wheat seedlings were treated with CeO₂NPs possessing different surface charges for 34 h, positively charged CeO₂NPs were mostly retained on the root surface while the neutral and negatively charged CeO₂NPs showed much higher accumulation in wheat shoots⁸. Similarly, positively charged gold nanoparticles (AuNPs) were readily retained by plant roots while negatively charged AuNPs were more efficiently translocated from roots to shoots ⁹. Different surface charge of ENPs also leads to different subcellular localization in plant roots ¹⁰. Overall, the underlying mechanisms for plant uptake of ENPs are still poorly understood.

Therefore, the interactions between ENPs and co-existing heavy metals and metalloids can be different from plants interactions with organic compounds. In addition, ENPs have been observed to alter the gene expressions, interrupt the bilayer membrane of the cell, adsorb on the cell wall,

and interact with root exudate¹¹. As a result, exposure to ENPs expected to alter plant uptake and accumulation of co-existing heavy metal and metalloid ions. ENPs can be taken up by crops roots and translocated into edible parts of plants including leaf and fruits¹². However, uptake and accumulation of ENPs in co-existence with heavy metals as well as the physiological effects of this co-exposure on plants are affected by the interference of various abiotic stresses¹³

Potential effects of ENPs interactions with leafy vegetables that are exposed to heavy metals may also alter the bioavailability of essential minerals such as Fe, and the microbial community, which have not been explored as a critical factor in plant ENPs interactions. Microbial communities in hydroponics can be highly beneficial for plant nitrogen fixation, phosphate mobilization, and mediating nutrient uptake¹⁴. Fig.1 illustrates some of the possible interaction of heavy metals and ENPs in a hydroponic system.

Therefore, there is a need to elucidate the impacts of ENPs on plants, their uptake pathways, and underlying mechanisms in plant tissues. In this regard, most ongoing research is centered on the potentially detrimental effects of ENPs¹⁵; while, the effects of ENPs on dietary plant uptake in exposure to a group of highly toxic contaminants, heavy metals, and metalloids, have not been adequately addressed.

8.2. Research Perspective

Understanding the interfacial chemistry of nanostructures in a biosystem which extends their application in environmental remediation efforts and other preventive protocols defines my research perspective. Elucidating the underlying mechanism of the altered uptake pattern by ENPs is a novel approach and a very critical research for the leafy greens (vegetables) compared to legumes and grains, because of their direct consumption by humans and, hydrophobic cuticle surface, higher leaf surface area and large hydroponic production systems, which highly expose them to risk of contamination by atmospheric

industrial fallout. My research plan is to start my initial research on this area that is very cost-effective research, and I have strong expertise, knowledge, and collaborative contacts to develop it through the funding and collaboration opportunities.

Due to the multi-disciplinary nature of my research, research funding through different financial sources is highly expected. The governmental organizations; USDA and EPA funding opportunities are directly related to my research benefit. In addition, NSF (BIO, ENG), NIH (NIBIB, NIHS), and DOE are major source of research funding in the area of my research. Private chemical companies such as BASF that provide research support are a great supplemental source to apply for a grant.

8.3. References

1. Dan, Y.; Zhang, W.; Xue, R.; Ma, X.; Stephan, C.; Shi, H., Characterization of gold nanoparticle uptake by tomato plants using enzymatic extraction followed by single-particle inductively coupled plasma–mass spectrometry analysis. *Environmental science & technology* 2015, 49, (5), 3007-3014.
2. Ma, C.; White, J. C.; Zhao, J.; Zhao, Q.; Xing, B., Uptake of Engineered Nanoparticles by Food Crops: Characterization, Mechanisms, and Implications. *Annual review of food science and technology* 2018, 9, 129-153.
3. Sharifan, H.; Wang, X.; Guo, B.; Ma, X., Investigation on the Modification of Physicochemical Properties of Cerium Oxide Nanoparticles through Adsorption of Cd and As (III)/As (V). *ACS Sustainable Chemistry & Engineering* 2018, 6, (10), 13454-13461.
4. Anjum, N. A.; Rodrigo, M. A. M.; Moulick, A.; Heger, Z.; Kopel, P.; Zítka, O.; Adam, V.; Lukatkin, A. S.; Duarte, A. C.; Pereira, E., Transport phenomena of nanoparticles in plants and animals/humans. *Environmental Research* 2016, 151, 233-243.

5. Zhao, L.; Peralta-Videa, J. R.; Varela-Ramirez, A.; Castillo-Michel, H.; Li, C.; Zhang, J.; Aguilera, R. J.; Keller, A. A.; Gardea-Torresdey, J. L., Effect of surface coating and organic matter on the uptake of CeO₂ NPs by corn plants grown in soil: Insight into the uptake mechanism. *Journal of Hazardous Materials* 2012, 225, 131-138.
6. Tripathi, D. K.; Shweta; Singh, S.; Singh, S.; Pandey, R.; Singh, V. P.; Sharma, N. C.; Prasad, S. M.; Dubey, N. K.; Chauhan, D. K., An overview on manufactured nanoparticles in plants: Uptake, translocation, accumulation and phytotoxicity. *Plant Physiology and Biochemistry* 2017, 110, 2-12.
7. Zuverza-Mena, N.; Martínez-Fernández, D.; Du, W.; Hernandez-Viezcas, J. A.; Bonilla-Bird, N.; López-Moreno, M. L.; Komárek, M.; Peralta-Videa, J. R.; Gardea-Torresdey, J. L., Exposure of engineered nanomaterials to plants: Insights into the physiological and biochemical responses-A review. *Plant Physiology and Biochemistry* 2017, 110, 236-264.
8. Spielman-Sun, E.; Lombi, E.; Donner, E.; Howard, D.; Unrine, J. M.; Lowry, G. V., Impact of surface charge on cerium oxide nanoparticle uptake and translocation by wheat (*Triticum aestivum*). *Environmental Science & Technology* 2017, 51, (13), 7361-7368.
9. Zhu, Z.-J.; Wang, H.; Yan, B.; Zheng, H.; Jiang, Y.; Miranda, O. R.; Rotello, V. M.; Xing, B.; Vachet, R. W., Effect of surface charge on the uptake and distribution of gold nanoparticles in four plant species. *Environmental science & technology* 2012, 46, (22), 12391-12398.
10. Ma, X.; Quah, B., Effects of Surface Charge on the Fate and Phytotoxicity of Gold Nanoparticles to *Phaseolus vulgaris*. *Food Chem. Nanotechnol* 2016, 2, (1), 57-65.
11. Shang, L.; Nienhaus, K.; Nienhaus, G. U., Engineered nanoparticles interacting with cells: size matters. *Journal of nanobiotechnology* 2014, 12, (1), 5.

12. Rossi, L.; Sharifan, H.; Zhang, W.; Schwab, A. P.; Ma, X., Mutual effects and in planta accumulation of co-existing cerium oxide nanoparticles and cadmium in hydroponically grown soybean (*Glycine max* (L.) Merr.). *Environmental Science: Nano* 2018, 5, (1), 150-157.
13. Li, J.; Tappero, R. V.; Acerbo, A. S.; Yan, H.; Chu, Y.; Lowry, G. V.; Unrine, J. M., Effect of CeO₂ nanomaterial surface functional groups on tissue and subcellular distribution of Ce in tomato (*Solanum lycopersicum*). *Environmental Science: Nano* 2019.
14. Sheridan, C.; Depuydt, P.; De Ro, M.; Petit, C.; Van Gysegem, E.; Delaere, P.; Dixon, M.; Stasiak, M.; Aciksöz, S. B.; Frossard, E.; Paradiso, R.; De Pascale, S.; Ventorino, V.; De Meyer, T.; Sas, B.; Geelen, D., Microbial Community Dynamics and Response to Plant Growth-Promoting Microorganisms in the Rhizosphere of Four Common Food Crops Cultivated in Hydroponics. *Microbial Ecology* 2017, 73, (2), 378-393.
15. Liu, R.; Lal, R., Potentials of engineered nanoparticles as fertilizers for increasing agronomic productions. *Science of the total environment* 2015, 514, 131-139.